TNO report
PML 1998-C53

Application of correlations to quantify the source strength of vapour cloud explosions in realistic situations. Final report for the project: 'GAMES'

TNO Prins Maurits Laboratory

Lange Kleiweg 137
P.O. Box 45
2280 AA Rijswijk
The Netherlands

Phone +31 15 284 28 42
Fax +31 15 284 39 58

Date
October 1998

Author(s)
W.P.M. Mercx
A.C. van den Berg
D. van Leeuwen

Assignor : Air Liquide, France
BP International Ltd, United Kingdom
ENEL Spa CRIS, Italy
Elf Atochem, France
Gaz de France, France
Health and Safety Executive, United Kingdom
ICI, United Kingdom
INERIS, France
Norsk Hydro, Norway
RIVM, The Netherlands
Snamprogetti SpA, Italy

Title : Ongerubriceerd
Abstract : Ongerubriceerd
Report text : Company Confidential
Annexes A - G : Company Confidential

No. of pages : 156 (incl. annexes, excl. documentation page)
No. of annexes : 7

All information which is classified according to Dutch regulations shall be treated by the recipient in the same way as classified information of corresponding value in his own country. No part of this information will be disclosed to any party.

The classification designation Ongerubriceerd is equivalent to Unclassified.

TNO Prins Maurits Laboratory is part of
TNO Defence Research which further consists of:

TNO Physics and Electronics Laboratory
TNO Human Factors Research Institute

Netherlands Organization for
Applied Scientific Research (TNO)

1 Summary

Correlations were derived in the preceding GAME project to quantify the source strength of a vapour cloud explosion required to apply the Multi-Energy Method for the determination of blast characteristics. The correlations relate a set of parameters describing the obstacle configuration in which the flammable cloud is present and the fuel, to a single value for the overpressure in the exploding vapour cloud.
This project investigates the difficulties and problems encountered while applying the correlations to a number of realistic scenarios. The objective is to provide guidance and recommendations on how to overcome these difficulties and to decide on the actual values to be chosen for the parameters of the correlations in specific situations. The emphasis is on the determination of the parameters: ‘Volume Blockage Ratio’ and ‘Average Obstacle Diameter’.

The main finding is that a safe approach in most situations is to apply the procedure of the new Yellow Book for the determination of the volume of the obstructed region in combination with the hydraulic average obstacle diameter and a flame path length equal to the radius of a hemisphere with a volume equal to the volume of the obstructed region.
Lack of experimental data on specific items prevents the generation of more detailed guidance. Some guidance is developed based on a theoretical approach, to assess the influence of the aspect ratio of the obstructed region and to quantify the separation distance between multiple explosion sources. It is recommended to perform an experimental research programme to generate the required data to improve and validate the suggested procedures.

2 Samenvatting

In het voorafgaande GAME project zijn correlaties afgeleid waarmee de bronsterkte van een gasexplosie kan worden bepaald. Deze is nodig bij het toepassen van de Multi-Energie methode voor het bepalen van de blast-karakteristieken. De correlaties relateren een aantal parameters dat de obstakelconfiguratie waarin de gaswolk zich bevindt en de brandstof beschrijft, met een enkele waarde voor de overdruk in de exploderende gaswolk.
In het onderhavige project wordt onderzocht welke moeilijkheden en problemen zich voordoen bij het toepassen van de correlaties op een aantal realistische situaties. Het doel is te komen tot adviezen en aanbevelingen om deze moeilijkheden aan te pakken en de parameters van de correlaties te kunnen quantificeren in specifieke situaties.

Het belangrijkste resultaat is dat voor de meeste situaties een veilige aanpak bestaat uit het toepassen van de procedure uit het nieuwe Gele Boek voor het bepalen van het volume van ruimte waarin de obstakels zich bevinden in combinatie met de gemiddelde hydraulische obstakeldiameter en een vlampadlengte gelijk aan de straal van een halfbol die een volume heeft gelijk aan dat van de ruimte waarin zich de obstakels bevinden.
Een gebrek aan experimentele gegevens betreffende enkele specifieke aspecten is de oorzaak voor het niet kunnen geven van meer gedetaileerde adviezen. Enkele adviezen zijn gegeven op basis van een theoretische beschouwing, voor het bepalen van de invloed lengte/breedte-verhouding van het volume waarin zich de obstakels bevinden en voor het bepalen van de scheidingsafstand tussen meerdere explosiebronnen. Aanbevolen wordt om een experimenteel onderzoeksprogramma uit te voeren waarmee de vereiste gegevens worden verkregen zodat de adviezen verbeterd en gevalideerd kunnen worden.

Contents

Summary 3

Samenvatting 4

1 Introduction 7

2 Background and objectives 9
2.1 Characterisation of source strength 9
2.2 Objectives and approach 11

3 Considerations on the application of the GAME correlation to realistic situations 13
3.1 Choice of a correlation 13
3.2 Determination of V_{or} 14
3.3 Determination of D 16
3.4 Determination of L_p 17
3.5 Determination of S_L 19

4 AutoReaGas calculations 21
4.1 REAGAS 21
4.2 BLAST 22
4.3 Adopted approach 22

5 Application to the Chemical Plant case 23
5.1 Description of case 23
5.2 Reduction of problem size 28
5.3 Application to reduced problem 28
5.4 Application to another reduced problem 32
5.5 Combination of two obstructed regions 35
5.6 Application to whole case 37
5.7 Influence of detail of obstacle description 41
5.8 Overall evaluation of the Chemical Plant case 43

6 Application to the LNG Terminal case 47
6.1 Description of case 47
6.2 First impression of potential explosion severity 50
6.3 Application of correlation to obstructed subregion 1 51
6.4 Application of correlation to obstructed subregion 2 57
6.5 Application of the correlation to a combination of obstructed subregion 1, 2 and 5 61
6.6 Application of the correlation to a combination of obstructed subregions 1, 3, 6, 7, and 8 63

6.7 Blast outside obstructed regions 66
6.8 Overall evaluation of the LNG Terminal case 70

7 Application to the Gas Processing case 75
7.1 Description of case 75
7.2 Test performed 75
7.3 AutoReaGas calculation 80
7.4 Application of correlation to obstructed region 81
7.5 Blast outside obstructed region 82
7.6 Evaluation and conclusion 82

8 Application to the Hydrogen case 85
8.1 Description of case 85
8.2 Application of correlation and ARG simulations 85
8.3 Evaluation and conclusion 89

9 Overall evaluation and guidance obtained 91
9.1 General 91
9.2 The correlation and parameters 92
9.3 Guidance and remaining white spots 94
9.4 Possible extensions of the blast charts 98

10 Conclusions and recommendations 99

11 References 101

12 Acknowledgement 103

13 Authentication 105

Annexes:
A Procedure for the determination of the boundaries of the obstructed region according to the Yellow Book
B Procedure for the application of the Multi-Energy Method according to the Yellow Book
C Application of procedure to determine obstructed region boundaries
D Critical separation distances between obstructed areas
E Application of GAME correlation to obstacle configurations of high aspect ratio
F AutoReaGas pressure histories for the various situations simulated with the Chemical Plant case
G AutoReaGas pressure histories for the various situations simulated with the LNG Terminal case

3 1 Introduction

The Multi-Energy Method (MEM) is a rather simple and practical method of determining the blast parameters from a vapour cloud explosion. It is generally accepted that the concept of the MEM better represents the specific character of a vapour cloud explosion. MEM-like methods should therefore be preferred above practical methods based on TNT equivalency.
The application of the MEM is hindered by a lack of guidance concerning the choice of the source strength. The GAME project: 'Guidance for the Application of the Multi-Energy Method' was performed to provide this additional guidance (Eggen, 1995). Very specific guidance was given in the form of correlations. A relation was derived for a set of parameters describing the obstacle configuration and the fuel, and the overpressure in the vapour cloud explosion.

The follow-up GAMES project: 'Guidance for the Application of the Multi-Energy Method, Second phase' was initiated to investigate the applicability of the derived guidance to realistic cases.

This report is the final report of the GAMES project.

First, the background and objectives of the project are presented in Chapter 2. While applying the correlations to determine the source overpressure to be used in the Multi-Energy Method, values for the parameters of the correlation have to be chosen. This introduces a number of specific questions. Considerations with respect to the quantification of the parameters is the subject of Chapter 3. Also, a number of white spots are identified. Initial thoughts on approaches to deal with these deficiencies are presented in the same chapter.

No realistic cases are available for which accurate enough data on overpressure occurring in a vapour cloud explosion exist. In order to be able to evaluate and to compare the results of the application of the correlations to realistic cases, a reference was requested. This reference was obtained by applying a numerical code to generate data on overpressures. Chapter 4 briefly describes how that reference set of data was obtained.

The correlations were applied to four realistic cases. The exercises that were performed for each case are described in the successive chapters, 5, 6, 7 and 8.
In two of the cases, the Chemical Plant case in Chapter 5 and the LNG Terminal in Chapter 6, a number of exercises were performed on interesting subsets of the obstacle configuration.
Chapter 7 deals with a large-scale experiment on a realistic obstacle configuration typical of a gas-processing site for which some data is available. Chapter 8 deals with a specific part of the LNG Terminal case, but filled with a flammable hydrogen mixture in order to investigate the influence of reactivity.

Each of the Chapters 5, 6, 7 and 8 contains a final paragraph on the evaluation and conclusions for that specific case.
Chapter 9 contains an overall evaluation of the exercises performed and provides guidance to determine values for the parameters of the correlations. Also the identified white spots are discussed and guidance to deal with these white spots is presented and discussed.
Finally, Chapter 10 summarises the conclusions. Recommendations are given to generate specific experimental data in order to be able to develop models to take into account the influence of the aspect ratio of the obstacle configuration and of the separation distance between obstacle configurations.

4 2 Background and objectives

4.1 2.1 Characterisation of source strength

In order to apply the blast charts of MEM, one requires values for two parameters characterising the source, namely the overpressure P_0 and the total combustion energy E which contributes to the explosion.

Figure 1 shows the blast chart of the MEM. In order to determine the peak blast overpressure P_s at a distance r from the centre of the explosion, a scaled distance r' has to be calculated according to:

$$r' = \frac{r}{(E / p_0)^{1/3}} \tag{1}$$

in which p_0 is the ambient overpressure.

The blast chart provides a value for the scaled blast overpressure P_s'. The blast overpressure P_s is obtained by multiplying P_s' by p_0.

The overpressure in the explosion P_0, the pressure for scaled distance values smaller than r_0', determines which line to follow to choose the correct overpressure at the required scaled distance.

4.1.1 Overpressure

Two correlations were derived in the GAME project to determine a value for the overpressure in a vapour cloud explosion. The overpressure is correlated to a set of parameters characterising the environment in which the vapour cloud is located and the vapour cloud itself. The difference between the two correlations is due to the type of confinement of the vapour cloud.

For low ignition energy and no confinement (open, 3D), the expression is:

$$P_0 = 0.84 \cdot (VBR \cdot L_p / D)^{2.75} \cdot S_L^{2.7} \cdot D^{0.7} \tag{2}$$

with:

P_0	the maximum explosion overpressure (bar)
VBR	the volume blockage ratio (-)
L_p	length of the flame path (m)
D	typical diameter (m)
S_L	laminar burning velocity of flammable mixture (m/s)

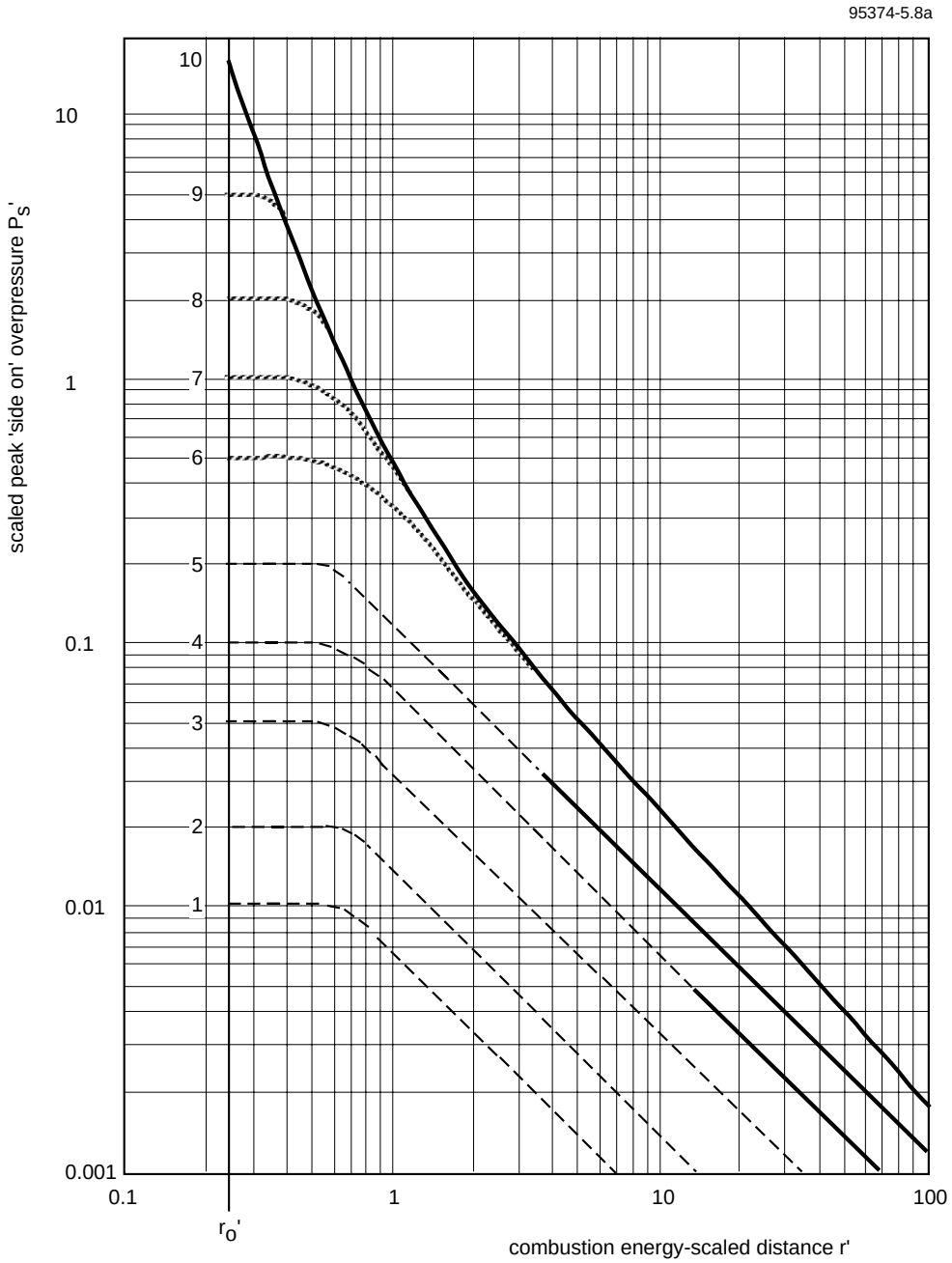

Figure 1: Blast chart MEM for overpressure.

For low ignition energy and confinement between parallel plates (2D):

$$P_0 = 3.38 \cdot (VBR \cdot L_p / D)^{2.25} \cdot S_L^{2.7} \cdot D^{0.7} \quad (3)$$

4.1.2 Combustion energy

The recommendation to obtain a value for the combustion energy is to calculate the combustion energy of those parts of the flammable mixture which are located in obstructed regions. An evaluation of experimental data performed in GAME reve-

aled that the recommendation of taking 100% of the energy of the obstructed part of the cloud is conservative for low overpressures. The term ‘efficiency’ was introduced, defined as the percentage of the energy of the obstructed part of the cloud which contributes to the generation of blast. It appeared that the efficiency is lower than 20% for overpressures below 0.5 bar.

4.2 2.2 Objectives and approach

The objective of the GAMES project is to apply the correlations to three realistic cases in order to investigate which problems are encountered while doing so.

The correlations were derived from experiments in which the parameters in the correlation were well-defined. This is not the case in realistic situations.
The purpose of the GAMES work programme is especially to investigate which values to choose for the total volume of the obstructed region, V_{or} (which determines VBR), and for the diameter D.

The cases were selected based on availability of appropriate information and the level of detail available on the plant lay-out. The plant lay-out constitutes the so-called obstacle configuration which is used to determine the V_{or} and D and which is used as part of the input of a numerical model to simulate explosions inside the obstacle configuration.

A numerical model is necessary to create a reference for the results of the correlations. In general, accidental explosions are not monitored. The overpressure and blast from an accidental vapour cloud explosion can only be estimated from damage analysis.
In the selection procedure for the three cases, it was investigated whether the information of the well-known explosions at DSM in Beek (1975) and in Flixborough (1974) could serve as a reference. This was not the case. The information on the exact plant lay-out was too coarse to be used.

An important practical issue in the selection of the cases was the availability of the plant lay-out in digital format. Creating such a digital lay-out from scratch would absorb too much of the available budget.

The next three cases were selected:
- the *Chemical Plant case*, because the plant lay-out was available in digital format, which could be used directly as an input to the numerical code and because of its compact lay-out;
- the *LNG Terminal case*, because of its complicated and stretched lay-out and because of the relative ease of creating a suitable digital file;
- the *Gas Processing case*, because of the availability of the digital file and because of the availability of experimental data on overpressure and blast.

An additional fourth case was added to the programme in order to investigate a high reactive fuel. It was decided to select a part of the LNG Terminal case as the obstacle configuration for the fourth case and to fill it with hydrogen. The fourth case is referred to as:

- the *Hydrogen case*.

During the execution of the project it was decided to put effort into two additional items that were considered important.

4.2.1 1 Detail of obstacle description

In important issue in numerical simulations of gas explosions is the level of detail with which the obstacle configuration is described. The results of the JIP project (Selby and Burgan, 1998) demonstrate that calculated pressures increase if the level of detail increase. In order to investigate the influence small obstacles have on the results of the simulations, additional runs were made using adapted obstacle databases for the Chemical Plant case.

4.2.2 2 Blast overpressure

The objective of the project was to investigate especially the determination of an average obstacle diameter and the volume of the obstructed region in order to obtain a good prediction for the source overpressure.
As the main purpose of the MEM is to correctly predict blast outside the gas explosion, the influence of the correlation parameters on blast characteristics is of importance. This influence will be investigated in the LNG Terminal case.

5 3 Considerations on the application of the GAME correlation to realistic situations

While applying the correlation in a realistic situation, some basic questions arise. In trying to find an answer to these questions, other, more detailed, questions come to one's mind. The intention is to go through this procedure and try to find answers to all those questions. Some answers may be obvious or can be derived from current knowledge; others may need a more practical solution. Some answers may not be found due to lack of knowledge.

The basic questions with which to start are:
- which correlation do I have to apply?
- which value for VBR do I have to take, or better, which value for V_{or}?
- which value for D do I have to take?
- which value for L_p do I have to take?
- which value for S_L do I have to take?

The remainder of this chapter consists of separate sections for some considerations on each of these questions.

5.1 3.1 Choice of a correlation

The adopted approach in GAME to relate explosion overpressure to the explosion parameters resulted in a need for six correlations; one correlation for each combination of low and high ignition energy with 1D, 2D and 3D expansion (for instance, jet ignition was considered a high ignition energy source). Within GAME, only two correlations could be derived.

White spot 1: the missing correlations could not be derived due to a lack of sufficient experimental data.
Proposed approach: although there are only two correlations, these are expected to cover most situations. By applying the available ones to the cases to be considered, an impression may be obtained about the necessity to develop the remaining four.

In many realistic situations the expansion will be partially 2D or 3D. For instance, part of the gas cloud will be underneath a roof or floor. An important ratio to consider then is the ratio of the horizontal dimensions of the cover and the height underneath. If this ratio approaches unity then the main part of the expansion process is three-dimensional. Also, the shape of the flame will be spherical rather than cylindrical during most of the explosion process.

White spot 2: a criterion to choose for the 2D or 3D correlation is lacking.

Proposed approach: An exact value for the height over length ratio in order to have a criterion to separate the application of the two correlations cannot be given. One might expect though that the ratio should be between 5 and 10.

5.2 3.2 Determination of V_{or}

A formal procedure for the determination of the volume of the obstructed region is given in the third edition of the 'Yellow Book' (CPR 14E,1997). The completely revised Yellow Book now contains the MEM for determination of blast from vapour cloud explosion.

5.2.1 Yellow Book procedure

The Yellow Book contains a procedure to apply the MEM step-by-step. One of the steps to be taken is the determination of the volume of the so-called obstructed region. The obstructed region is the region where obstacles are located, so the region is to be considered as a potential source for overpressure generation in a vapour cloud explosion. There are two ways to define an obstructed region, either to estimate its boundaries or to follow an alternative procedure.
The procedure for the MEM according to the Yellow Book is given in Annex B. The procedure for determination of the obstructed region is given in Annex A.

The procedure attempts to describe in a formal way a number of subsequent rather obvious steps one would probably take by intuition.
The procedure to determine the obstructed region starts with an initial obstructed region containing the obstacles located near an assumed ignition point. Depending on the distance to obstacles further away in relation to the size of the obstacles near the ignition location, the initial obstructed region is extended to include those obstacles further away.

White spot 3: the criteria given in the Yellow Book to decide whether an obstacle belongs to an obstructed region cannot be motivated objectively.
Proposed approach: in most situations however it will be more or less obvious and the rough boundaries of an obstructed region can be estimated.

It is explicitly stated in the Yellow Book that the criteria to decide whether or not a specific obstacle belongs to the obstructed region are questionable and further research is required to better define them. Also, the Yellow Book procedure does not distinguish multiple explosion sources. If the procedure results in multiple obstructed regions, one has to add all the volumes together to get one large explosion source.

White spot 4: the separation into multiple explosion sources, often referred to as the donor-acceptor problem, cannot be solved yet.

Proposed approach: the new Yellow Book offers a procedure to reduce the combustion energy in situations where one expects multiple explosion sources. More consideration on separation distances is given in Annex D. A first attempt to quantify a separation distance is given. A separation distance between two obstructed regions should be at least half the linear dimension of the donor-obstructed region to consider the donor and acceptor obstructed region as separate potential blast sources.

The procedure to determine the volume of the obstructed region starts with the definition of a box containing all obstacles in the obstructed region. The volume of that box is the initial volume of the obstructed region. As this box probably contains a lot of free space without obstacles, the volume can be reduced by excluding this free space. The initial box is then replaced by a number of adjacent boxes, the total volume of which is smaller than the initial box. This optimisation can be repeated until all free space is eliminated; however, the time involved for the optimisation may not be worthwhile.

Annex C contains an example of the application of the procedure to determine the volume of the obstructed region.

5.2.2 Application of procedure in GAMES

For GAMES, the volume of the obstructed region is specifically required in the determination of the VBR.
VBR is defined as the ratio of the total volume of the obstacles inside an obstructed region V_{ob} and the volume of that obstructed region V_{or}.
If the value of V_{or} is chosen too large, VBR will be too low and the correlation provides a too low overpressure P_0 and vice versa.

The correlations provide a possibility to derive a criterion for the optimisation of V_{or} according to the Yellow Book procedure: given two values for V_{ob}: $V_{or,1}$ and $V_{or,2}$ the ratio of the overpressures according to the correlation (1) is (it is assumed that L_p does not change):

$$\frac{P_{0,2}}{P_{0,1}} = \left(\frac{V_{or,1}}{V_{or,2}} \right)^{2.75} \tag{4}$$

If, for instance, $V_{or,2}$ equals $0.86V_{or,1}$, the overpressure $P_{0,2}$ is 50% higher than $P_{0,1}$. An increase of 10% in overpressure is obtained when the volume of the obstructed region is reduced by 3%.

The accuracy of the correlation is about ±30%. With this value in mind, it is not profitable to take the next step in the reduction of V_{or} if it cannot be reduced more than 10%.

The volume of the obstructed region influences the value of the energy E to be used in MEM. This influence is of less importance than its influence on VBR. A variation of ΔE implies an influence of $\Delta E^{1/3}$ on the distance at which a certain blast overpressure will occur.

5.3 3.3 Determination of D

The determination of D in a realistic case is not obvious. Various definitions for the average obstacle size are possible.

To facilitate the definition of various means, we limit ourselves to obstacle configurations consisting solely of tubes of various diameters and lengths.

- Arithmetic mean weighted by the tube length L_i

$$D_{arm} = \frac{\sum L_i \cdot D_i}{\sum L_i} \tag{5}$$

  Harmonic mean weighted by the tube length L_i. Relative to the arithmetic mean, the harmonic mean overweighs the smaller diameters.

$$\frac{1}{D_{ham}} = \frac{\sum L_i \cdot \frac{1}{D_i}}{\sum L_i} \tag{6}$$

- Many other formulations are imaginable, for instance a mean on the basis of the concept of hydraulic diameter, which is defined as 4 times the ratio between the summed volumes and the summed surface areas of an object distribution.

$$D_{hym} = 4\frac{\sum V_i}{\sum A_i} \tag{7}$$

  This definition overweighs the larger objects in the collection.

The expressions to determine D give a single average value for the whole obstructed region under consideration, assuming a homogeneous distribution of obstacle types and obstacle diameters. In many cases the obstructed region will consist of a number of subregions, each with a typical obstacle distribution. In those cases it may be more appropriate to calculate D (and VBR) for each subregion and combine these to a single value for the whole obstructed region.
An attempt to describe the framework of such a procedure was given by Eggen in the GAME project (Eggen, 1995).

An issue not discussed yet is how to model non-cylindrical obstacles. The experiments underlying the correlations were all with cylindrical obstacles. Non-

cylindrical obstacles will produce another turbulence field than that of cylindrical obstacles. It is yet not clear to what extent the shape of an obstacle will influence the explosion progress.

White spot 5: influence of non-cylindrical obstacles.
Proposed approach: non-cylindrical obstacles like boxes and plates will be represented by cylinders having a length equal to the largest dimension of the obstacle and a cross-section area equal to the cross-section area of the obstacle.

5.4 3.4 Determination of L_p

The ignition location in the experiments used to derive the correlations was always in the centre of the symmetrical obstacle configuration. A value for L_p is then easy to determine. In other situations, this may not be the case. Three situations were identified:

- an obstacle configuration with an aspect ratio other than 1;
- an ignition location outside the centre of the obstacle configuration;
- an obstacle configuration partially filled with a flammable mixture.

5.4.1 Aspect ratio

The aspect ratio of an obstructed region can be defined as its length/width or length/height ratio. In the case of central ignition, there are three values to choose for L_p: half the length, half the width or half the height. This issue is discussed in Annex E.

White spot 6: which L_p to choose in the case of non-point symmetrical situations.
Proposed approach: a practical, though not validated solution is proposed in Annex E. In case there are more Lp's possible, it is stated that the overpressure at the moment the flame travelled L_p should be higher than a specific threshold in order to further increase. If the overpressure is lower than this threshold, side venting will prevent further flame acceleration and increase in overpressure. The value proposed for the threshold is 30 kPa. Note that there is no information available to support that choice.

5.4.2 Ignition location

The discussion for non-central ignition is similar to the discussion on the aspect ratio. An extreme situation is present if the ignition location is at an edge or corner a of the obstructed region; then side (back) venting starts immediately after ignition, possibly preventing any flame acceleration. The conclusion then is that edge or corner ignition always results in lower overpressures than central ignition.
On the other hand, the available flame path length for edge ignition is greater than for central ignition. So although flame acceleration is slow initially in the case of an edge ignition, higher overpressures may be obtained due to the longer flame

path. Flame acceleration may still occur later in the process when the flame front is inside the obstacle configuration where back venting has less influence.

5.4.3 Large V_{or} relative to volume of flammable cloud

Until now, we considered situations were the flammable cloud was larger than the obstructed region. The correlations were based also on tests simulating that situation.
In most realistic situations, the obstructed region (chemical unit, offshore installation) will not be completely filled with a flammable cloud. A heavy gas cloud will have a limited height, say 4 to 10 m, while the height of the obstructed region will be greater. Also, a limited release will result in a small cloud relative to the size of the obstructed region.
It can be argued that the overpressure in a situation with an obstructed region larger than the flammable cloud will be higher than in the situation where the volume of the flammable cloud is the same but the volume of the obstructed region is reduced to the volume of the flammable cloud.

It was demonstrated in GAME (Eggen, 1994) that the amount of combustion energy contributing to blast generation is lower than 100% for low overpressures. At the present wa can only give the following explanation for the existence of an efficiency factor: a fraction of the unburned mixture is pushed outside the obstacle array due to expansion. Therefore, not all the gas that is initially inside the array will burn inside the array. If the flame speed inside the array is high (also high overpressure), the fraction that is pushed outside will have a high turbulence level. If the flame speed is low, the turbulence level outside the array will be low.
The turbulence level outside the array will decrease rapidly. One may expect that when the flame leaves the array and starts to burn through the mixture outside, the turbulence level of that mixture in the case of high overpressure will be higher than in the case of low overpressure. So more of the expelled mixture will burn outside when the overpressure is higher and contribute to the explosion energy.

In the case of an extended obstructed region, the expanded unburned gas will burn inside the obstructed region instead of being expelled outside. The result is that the efficiency will increase, but as the length of the flame path is longer, the overpressure will be greater too.

The combination of L_p/D in the correlation is in fact a measure of the number of obstacles the flame passes while it burns through the mixture.
In situations of a larger obstructed region it may therefore be better to determine L_p from the expanded flammable cloud size rather than from the size of the obstructed region inside the unburned cloud.

White spot 7: influence of obstructed region being larger than the vapour cloud.
Proposed approach: due to the lack of any experimental back-up, any influence is neglected.

5.5 3.5 Determination of S_L

It is common use to assume a homogeneous stoichiometric flammable cloud in all assessments. Also most available experimental data on explosion overpressures are based on experiments using homogenous mixtures. The laminar burning velocities of these mixtures is known. A huge benefit using the correlation is that now various gases can be compared for their explosion overpressure potential.
Using homogeneous mixtures will result in high overpressures, which may be non-realistic. There is, however, no guidance available on how to treat non-homogeneous (so more realistic) mixtures.

6 4 AutoReaGas calculations

In order to create a reference with which the results of the application of the correlations can be compared, numerical simulations have to be performed for three of the four cases. The code AutoReaGas is used as the numerical simulator (van den Berg et al., 1995). Actually the code AutoReaGas consists of two numerical solvers. The solver REAGAS is for modelling the combustion, expansion and turbulence phenomena inside the exploding vapour cloud. The solver BLAST is for modelling the propagation of the blast wave outside the combustion zone and the interaction of the blast wave with structures.

6.1 4.1 REAGAS

The basic mechanism of a gas explosion consists of the interaction of a premixed combustion process with its self-induced expansion flow field. The development of this process is predominantly controlled by the turbulent structure of the flow field, which is induced by the boundary conditions. Modelling of a gas explosion requires careful modelling of all aspects of this complicated process. The model underlying the AutoReaGas gas explosion simulator can be characterised as follows.

- The gas dynamics is modelled as a perfect gas which expands as a consequence of energy addition. This is mathematically formulated in conservation equations for mass, momentum and energy.
- The energy addition is supplied by combustion which is modelled as a one-step conversion process of flammable mixture into combustion products. This is formulated in conservation equations for the fuel mass fraction and the composition. The combustion rate is a source term in the fuel mass fraction conservation equation.
- Turbulence is modelled by a two parameter model (k-ε) which consists of conservation equations for the turbulence kinetic energy k and its dissipation rate ε.
- Turbulent combustion is modelled by an expression which relates the combustion rate to turbulence. Several options are available varying from theoretical relations such as the Eddy Break Up model and the Eddy Dissipation model to experimental correlations between turbulence and combustion. Because the cell size in many applications is often far too large to fully resolve a turbulent combustion zone, the combustion rate is corrected using a calibration factor Ct.
- The initial stage of combustion upon ignition is modelled by a process of laminar flame propagation whose speed is controlled on the basis of experimental data.
- Objects too small to be represented by solid boundaries in the computational mesh, are modelled by a subgrid formulation. The presence of a subgrid object is modelled by the specification of appropriate flow conditions, i.e. a fluid dynamic drag and a source of turbulence.

- Numerical solution of the set of equations is accomplished by means of the ‘power law’ scheme applied within a finite volume approach.

6.2 4.2 BLAST

As long as objects with large cross-flow dimensions are considered, the interaction of gas explosion blast is predominantly governed by the pressure wave character of a blast wave and the drag component can be neglected. The pressure wave character of blast flow fields is accurately represented by inviscid flow. Often, blast flow fields are characterised by the presence of gas dynamic discontinuities such as shocks. Modelling of blast-object interaction requires careful description of such phenomena. Therefore, the blast simulator models blast-object interaction as follows.

- The gas dynamics is modelled as inviscid compressible flow of a perfect gaseous fluid which can be formulated as the conservation equations for mass, momentum and energy for inviscid flow, i.e. the Euler equations.
- Description of shock phenomena requires a sophisticated numerical technique tailored to proper representation of steep gradients. To this end, the blast simulator utilises Flux-Corrected Transport (FCT). FCT makes an optimised use of numerical diffusion so that steep gradients present in shocks are retained. Numerical diffusion is added only where it is required for numerical stability.

6.3 4.3 Adopted approach

W have chosen to use a single calibration of the code for all simulations.

Large-scale validation has been performed recently in the Joint Industry Project (Selby and Burgan, 1998). We applied the calibration factor for the combustion model Ct = 65 in combination with a cell size of about 1 m and got acceptable results for all tests in JIP. The same combination has been applied for all GAMES simulations with AutoReaGas.
In all cases, we let the code automatically decide whether an obstacle has to be modelled as a ‘solid’ or as a ‘subgrid’.

7 5 Application to the Chemical Plant case

7.1 5.1 Description of case

The digital file containing the chemical plant to be assessed in GAMES, describes a volume of width 32 m (x-direction), length 57 m (y-direction) and height 39 m (z-direction).
Various parts can be distinguished:

1 a two storey concrete structure consisting of columns and floors containing lots of equipment, vessels and pipelines, of various dimensions and orientated in all three perpendicular directions (x: 8.5-25 m, y: 18.5-48.5 m, z: 0-15 m, volume: 7425 m^3); a stack is located on top of this structure with the outlet at z: 33 m;
2 a large three storey pipebridge with numerous pipes running in the y-direction (x: 0.5-8.5 m, y: 0-57 m, z: 0-7.5 m, volume: 3420 m^3);
3 a small two story pipebridge with pipes orientated in the x-direction (x: 8.5-32.5 m, y: 16.5-18.5 m, z: 0-5 m, volume: 240 m^3);
4 a single floor concrete support structure (columns and floor) containing some vessels (x: 8.5-18 m, y: 9-16.5 m, z: 0-12 m, volume: 855 m^3);
5 two stacks with supply equipment; the equipment is bounded by x: 8.5-12.5 m, y: 2-9 m and z: 0-7.5 m, volume: 210 m^3, the outlet of the stacks is at z = 39 m.
6 a single floor concrete structure containing some vessels (x: 8.5-17 m, y: 48.5-56.5 m, z: 0-12 m, volume: 816 m^3).

The numbers given correspond with the numbers in Figure 2. Other numbers in Figure 2 denote ignition locations (IL-i) and pressure sampling locations (P-i) to be used elsewhere in this chapter.

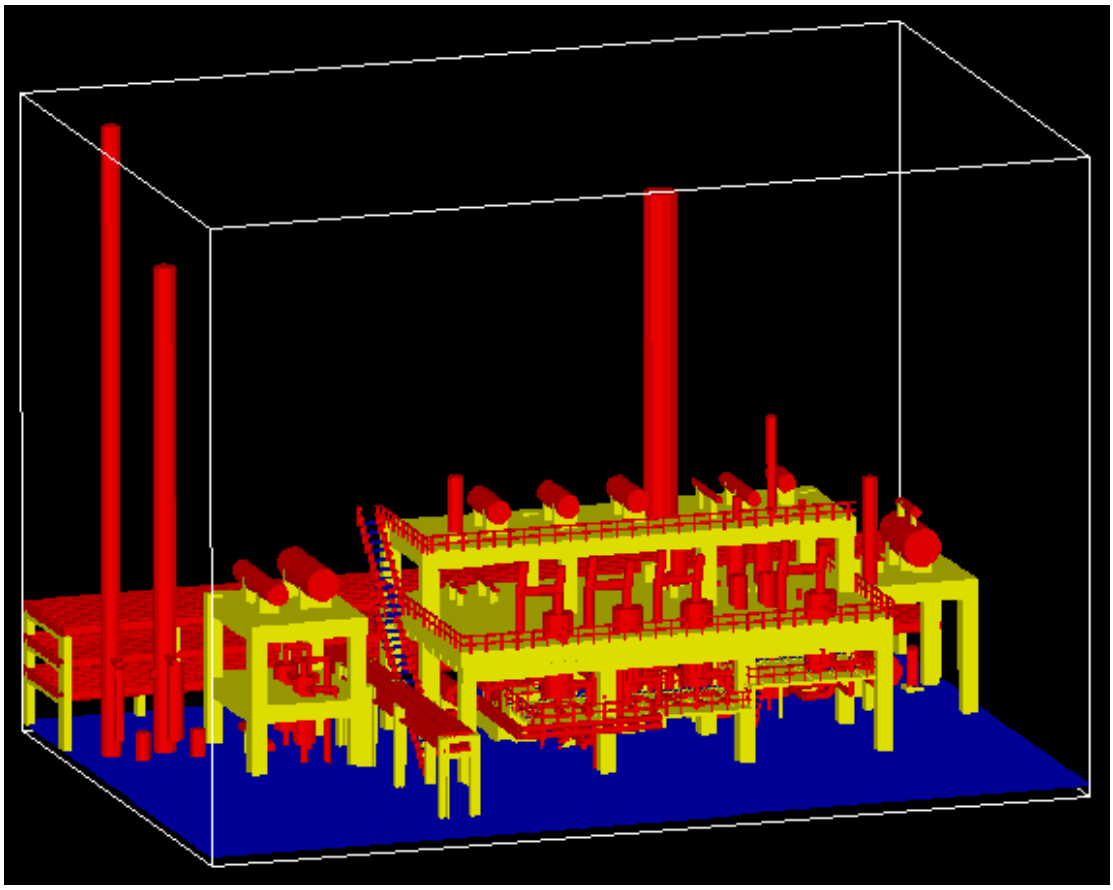

Figure 2.a: View of the Chemical Plant case: overall view.

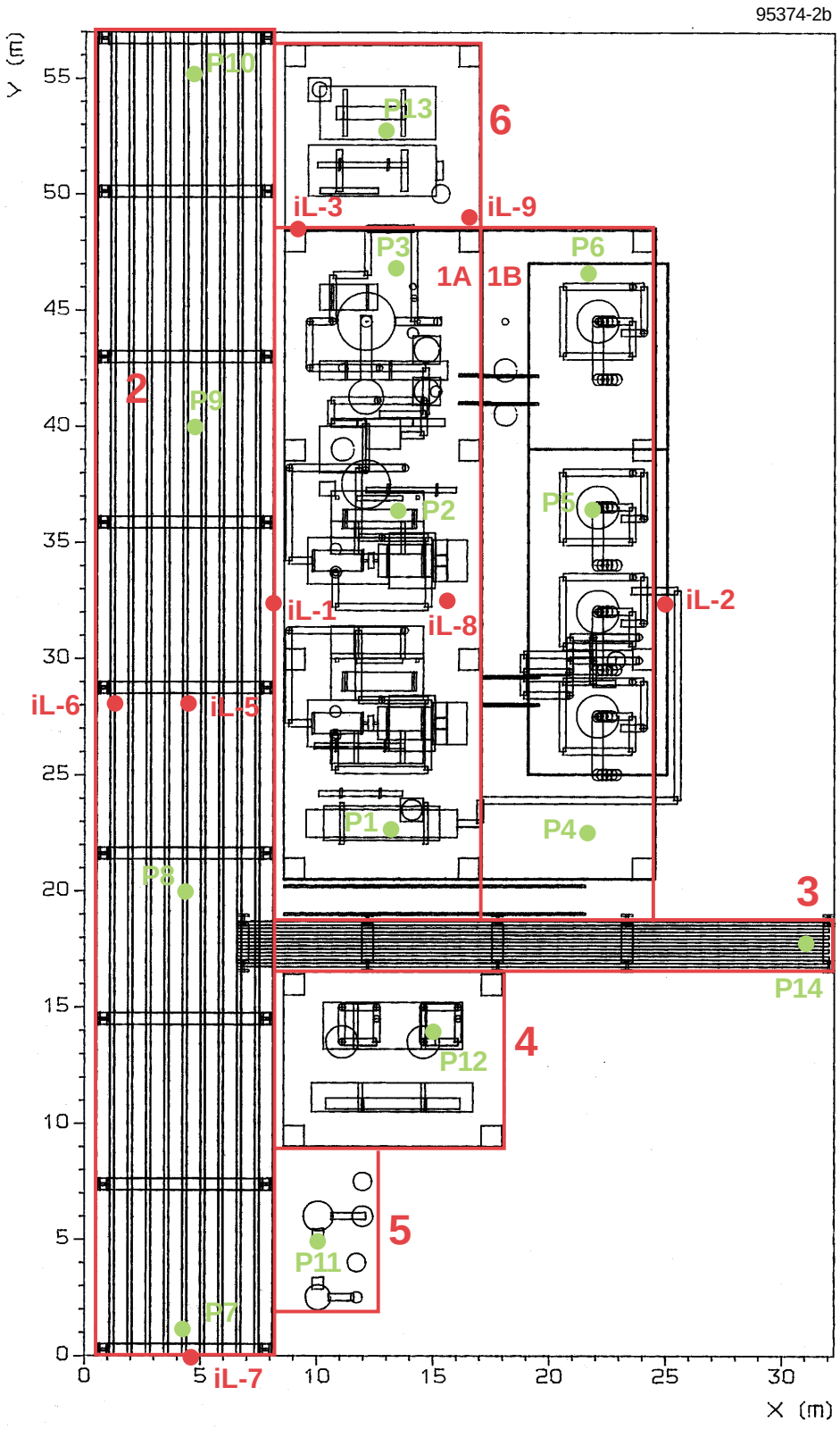

Figure 2.b: View of the Chemical Plant case: horizontal projection on xy-plane.

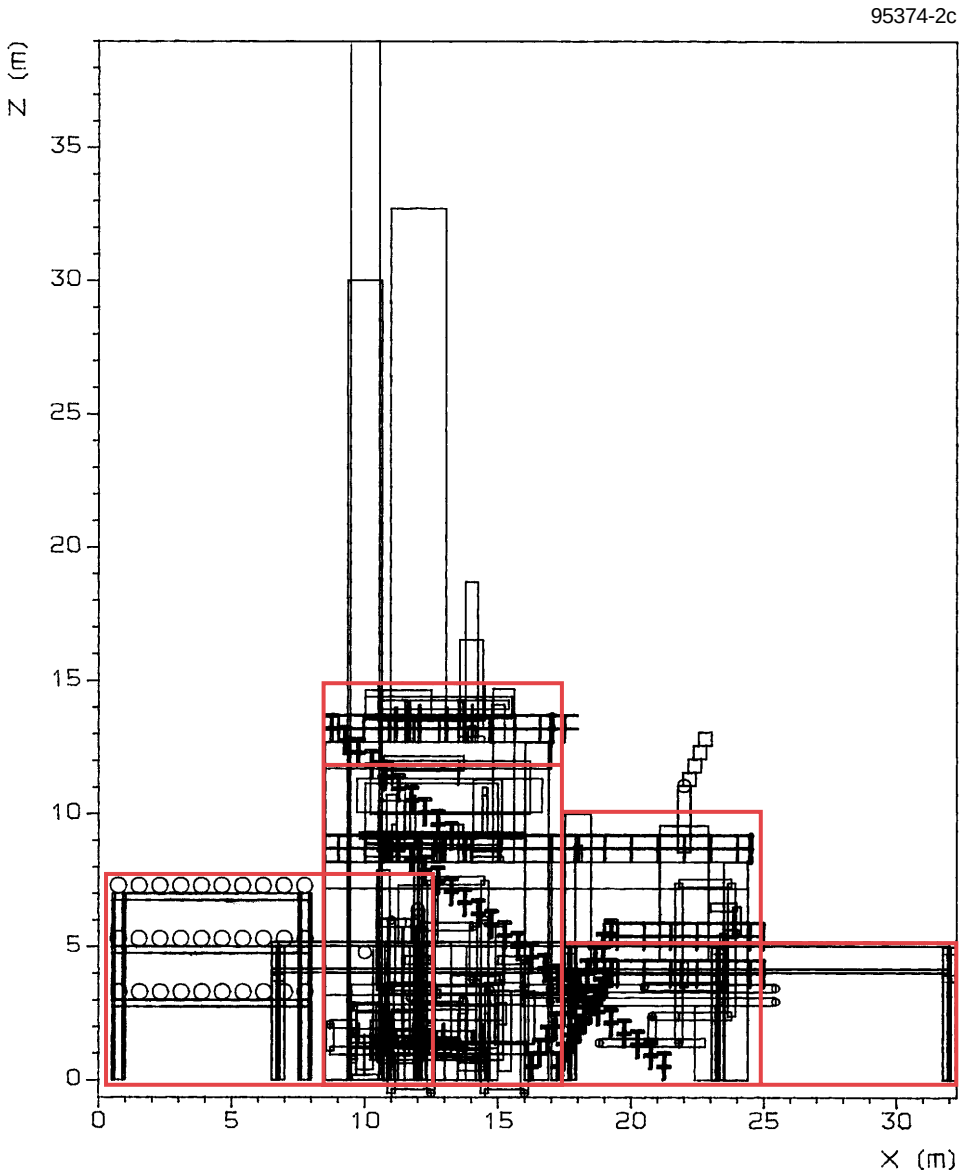

Figure 2.c: View of the Chemical Plant case: vertical projection on xz-plane.

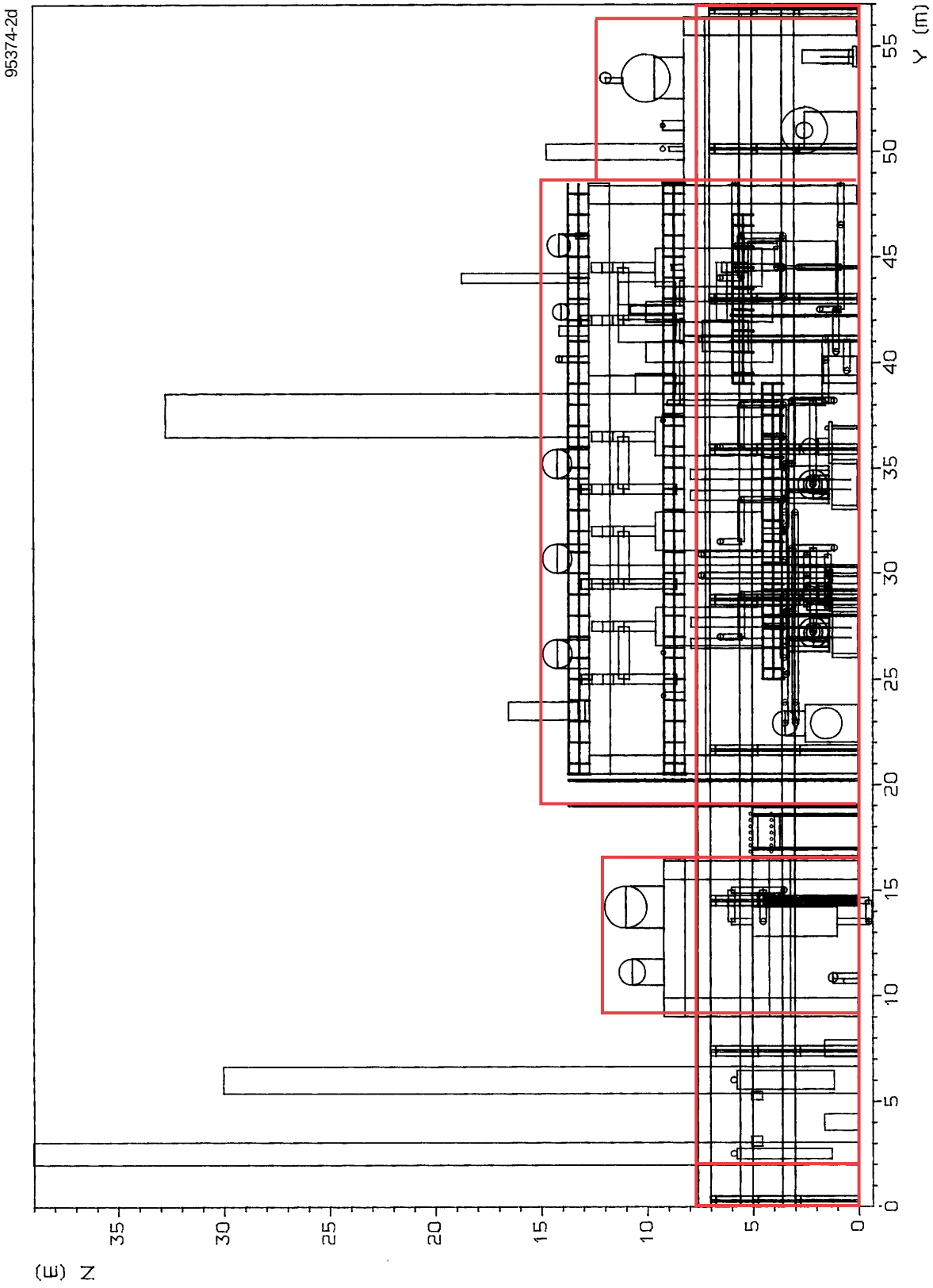

Figure 2.d: View of the Chemical Plant case: vertical projection on xy-plane.

7.2 5.2 Reduction of problem size

As this case is the first case to be considered in GAMES, it should be reduced and simplified.

It was decided to isolate the two storey concrete structure from the rest of the installation and to consider it a separate case for a first assessment in the GAMES exercise because:

- the borders of the obstructed region can be rather well defined;
- it consists of a variety of different sized, shaped and orientated obstacles;
- confinement between two surfaces.

The third value is of importance as one of the two correlations derived in GAME is applicable to the two-dimensional expansion.

The first floor of the obstructed region is only partially covered by the floor of the second storey.
To simplify the problem more, we will assume that the obstructed region is filled with a homogeneous stoichiometric mixture of methane in air. The cloud has a height of 7.5 m, so the ground level is completely filled with the cloud.

The first floor is supported by a large number of stiffeners, which do not have a physical thickness in the submitted database. This large number of stiffeners will largely determine the determination of D. For reasons of simplification, these stiffeners are neglected and the floor is considered smooth in this case.
There are also floors present inside the configuration. These floors are supported by stiffeners also, which are taken into account in this case. They are given a thickness of 0.01 m.
The simplified case, obstructed subregion number 1 (OSR-1), now consists of the volume between:

x: 8.5 - 25 m, width 16.5 m;
y: 18.5 - 48.5 m, length 30 m;
z: 0 - 7.5 m, height 7.5 m.

The volume is filled with a variety of obstacles, and is confined between two surfaces: the ground floor and the first floor.

7.3 5.3 Application to reduced problem

We will now try to come up with a value for the explosion overpressure in the case of ignition of the flammable mixture using the correlations and keeping the considerations of Chapter 2 in mind to answer:

- which correlation do I have to apply?
- which value for VBR do I have to take, or better, which value for V_{or}?
- which value for D do I have to take?

- which value for L_p do I have to take?
- which value for S_L do I have to take?

7.3.1 Correlation?

At first glance, the explosion process will be governed by a 2D expansion. However, the length to height ratio equals 30/7.5= 4 or 16.5/7.5 = 2.2. This implies that a large part of the process is 3D.
At this stage it is not clear which correlation to choose. The AutoReaGas calculation of the case should provide more insight.

7.3.2 VBR?

At this stage we will not go into detail to accurately determine the volume of the obstructed region. It will be obvious that a good estimate for the volume of the obstructed region is the product of its dimensions:

- V_{or} = 16.5 x 30 x 7.5 = 3712.5 m^3.

The obstructed volume contains 760 objects, consisting of 618 cylinders and 142 boxes.
The VBR is calculated to be:

- VBR = 0.10.

7.3.3 D?

The objects in the obstructed region contain cylinders and boxes. To calculate a diameter according to equations 6 and 7, the ‘diameter’ of a box should be calculated. For that, we calculated the diameter of a circle having the same surface area as the surface of the box perpendicular to its longest dimension.
Applying equations 5, 6 and 7 resulted in:

- D_{arm} = 0.23 m;
- D_{ham} = 0.08 m;
- D_{hym} = 0.49 m.

7.3.4 L_p?

There are a number of possibilities for L_p.
The correlations are derived for central ignition. The longest path the flame can travel for central ignition is $L_{p,1}$ = 15 m. Assuming symmetric shape, the flame reaches the boundary of the obstructed region already after $L_{p,2}$ = 8.25 m because of the length over width ratio is not equal to unity. It may be expected that using $L_{p,1}$ will result in a too large overpressure, as venting has already started before the flame reaches the short edge. Using $L_{p,2}$ will result in a too low value for the overpressure, as combustion inside the obstructed region is not completed at the moment the flame reaches the long edge.

Ignition may also occur elsewhere. The longest path for the flame is $L_{p,3}$ = 30 m when ignition occurs in the centre of one of the edges of the obstructed region. As explained in Chapter 2, using the correlations for edge ignition will result in too high overpressures, as venting will start immediately after ignition.

7.3.5 S_L?

The choice of this parameter in the present exercise is straightforward. The correlations were derived with S_L = 0.45 m/s for methane, so

S_L = 0.45 m/s

7.3.6 Overpressure?

Combinations of possible values for the parameters involved result in Table 1.

Table 1: Combination of parameters considered.

	P_0 (kPa)					
	2D			3D		
L_p	8.25 m	15 m	30 m	8.25 m	15 m	30 m
D_{arm} = 0.23 m	250	450	4502	120	600	4060
D_{ham} = 0.08 m	1270	1890	2320	1010	5260	3537
D_{hym} = 0.49 m	80	294	1400	25	128	861

7.3.7 AutoReaGas

Numerical simulations were performed with the CFD code AutoReaGas (ARG) using the obstacle configuration defined in this section. Various ignition locations were used:

Case:	Ignition location:	x(m):	y(m):	z(m):	
NH01	IL1	8.5	33.5	4	centre of large edge
NH02	IL2	25	33.5	4	centre of large edge
NH03	IL3	8.5	48.5	4	corner
NH12	IL8	16.5	33.5	4	centre
NH13	IL9	16.5	48.5	4	centre of small edge

The pressure was sampled in six locations, P1 -P6, equally distributed over the obstructed region. The pressure histories are presented in Annex F. An overview of the maximum overpressures in these locations is given in Table 2; the highest value per case is printed in bold.

Table 2: Maximum overpressures according to ARG simulations.

Case: Sample location (x, y, z)	NH01	NH02	NH03	NH12	NH13
			Pmax (kPa)		
P1 (13, 22, 4)	18	36	13	47	**55**
P2 (13, 36, 4)	24	34	11	41	23
P3 (13, 47, 4)	26	**59**	5	65	9
P4 (22, 22, 4)	36	21	14	51	51
P5 (22, 36, 4)	**40**	19	**22**	42	34
P6 (22, 47, 4)	37	35	8	**73**	10
average	30	34	12	**53**	30

The table shows the highest pressures for central ignition.
Ignition in the centre of an edge results in lower overpressures. In spite of the longer flame path compared to central ignition, the immediate back-venting after ignition prevents flame acceleration into the obstructed region. Maximum overpressures occur in locations farthest away from the ignition location where the flame speed is the fastest.
The surplus of back-venting in the case of corner ignition results in the lowest overpressures.

7.3.8 Evaluation

The first question which arises when comparing the numerical results with the correlation overpressure is how to perform the comparison. The correlation gives a single value, while numerical simulation will obviously result in a distribution of maximum overpressures.
The correlation was derived based on an average of maximum overpressures measured during the experiments. One may wonder how to average, as a localised high overpressure peak may contribute less to the blast than the lower overpressure in a larger subvolume of the obstructed region. A definite answer cannot be given yet. Therefore, the correlation results will be compared with an average value of the maximum overpressures per case (last row of Table 2).

White spot 8: how to conclude on a single value for the overpressure
Proposed approach: an arbitrary number of pressure sampling locations is chosen, homogeneously distributed in the obstructed region. The average value of the maximum of all locations is denoted as ‘the overpressure’.

Table 3: Overpressures for various L_p.

	P_0 (kPa)					
	2D			3D		
L_p	8.25 m	15 m	30 m	8.25 m	15 m	30 m
D_{hym} = 0.49 m	180	294	1400	25	128	861

In comparison with the correlation results, the only reasonable results are predicted with the largest average diameter: $D_{hym.}$ The maximum average AutoReaGas value (53 kPa) is in between the 3D correlation result for L_p = 8.25 and 15 m.
As could be expected based on the considerations in section 2.1, the best result is obtained with the 3D correlation, and this correlation gives too low a value for the smaller L_p and too large a value for the larger L_p.

An optimal value for central ignition may be expected for an averaged L_p. An average value may be obtained by assuming the flammable cloud to be a hemisphere with radius L_p and having the same value. In that case, L_p = 12.1 m. The correlation (1) provides now P_0 = 71 kPa using D_{hym} (P_0 = 330 kPa for D_{arm}, P_0 = 2910 kPa for D_{ham}).

While the AutoReaGas calculation would result in a class 6 for the MEM, the 3D correlation with a conservative estimate for L_p would result in a class 7.5, and an average value for L_p would result in a class 6.5.

7.4 5.4 Application to another reduced problem

Another typical part of the Chemical Plant case is the large pipebridge that runs along the whole length of the total obstructed region.
We will consider the pipebridge a separate and isolated case, as this type of obstructed region is present in many industrial situations.

Obstructed subregion number 2 (OSR-2) occupies the space between x: 0-8 m, y: 0-57 m and z: 0-8 m.

7.4.1 Correlation?

Neither of the two available correlations seems suitable to cover this case. The 2D correlation is not applicable as there are no two confining surfaces. The density of the layers of pipes might give the impression of a confining surface, they also may act as turbulence generators. Although 3D expansion is possible, the obstacle configuration as well as the aspect ratio of the obstructed region differs considerably from those that were used to derive the 3D correlation. Nevertheless, taking the 3D correlation seems to be the best bad choice.

7.4.2 VBR?

The boundaries of the obstructed region are quite clear. An optimisation procedure according to Annex A will therefore not be performed.
The boundaries are x:0.5-8.5 m, y: 0-57 m, z: 0-8 m. The volume V_{or} equals 3648 m^3 resulting in a volume blockage ratio:

VBR = 0.14

7.4.3 D?

The obstructed region contains 505 objects, consisting of 30 cylinders and 475 boxes.

We calculated that:

- D_{arm} = 0.50 m;
- D_{ham} = 0.41 m;
- D_{hym} = 0.53 m.

7.4.4 L_p?

We will consider the following values for the length of the flame path:

- L_p = 28.5 m central ignition, half the length;
- L_p = 4 m central ignition, half the width or height;
- L_p = 12 m central ignition, radius of hemisphere with equal volume;
- L_p = 8 m ignition in centre long edge, width;
- L_p = 57 m ignition in centre short edge, length.

7.4.5 S_L?

Again we will take S_L = 0.45 m/s.

7.4.6 Overpressure?

Combinations of possible values for the parameters involved result in the following table (Table 4).

Table 4: Overpressures for various parameter combinations.

	P_0 (kPa)				
	Central ignition			Long edge ignition	Short edge ignition
L_p	28.5 m	4 m	12 m	8 m	57 m
D_{arm} = 0.50 m	2300	10	213	70	15500
D_{ham} = 0.41 m	3400	15	315	103	22900
D_{hym} = 0.53 m	2080	9	192	63	14000

7.4.7 AutoReaGas

Numerical simulations were performed with the obstacle configuration defined in this section. Three different ignition locations were used:

Case:	Ignition location:	x(m):	y(m):	z(m):	
NH04	IL5	4.5	28.5	4	centre of obstructed region;
NH05	IL6	0.5	28.5	4	centre of long edge;
NH06	IL7	4.5	0	4	centre of short edge.

Pressure were sampled in four locations, P7 -P10, equally distributed over the obstructed region. Pressure histories are presented in Annex F. An overview of the maximum overpressures in these locations is given in Table 5; the highest value per case is printed in bold.

Table 5: Overpressures according to ARG simulations.

Case: Sample location (x, y, z)	NH04	NH05 Pmax (kPa)	NH06
P7 (4, 1, 4)	27	13	**9**
P8 (4, 20, 4)	**62**	**33**	**9**
P9 (4, 40, 4)	50	28	5
P10 (4, 55, 4)	26	13	5

The same trend is visible as in the obstructed region considered in the previous section.
The table shows the highest pressures for central ignition.
Ignition in the centre of an edge results in lower overpressures. In spite of the longer flame path compared to central ignition, the immediate back-venting after ignition prevents flame acceleration into the obstructed region.
The side-, back- and top-venting apparently have a great influence. Maximum overpressures do not occur in locations farthest away from the ignition location but in a region around the ignition location. Initially, the flame accelerates, but because of the large aspect ratio, the expansion is easily vented, resulting in a deceleration of the flame in the later stage.

7.4.8 Evaluation

Table 6 gives values for the average maximum overpressures.

Table 6: Averaged maximum overpressures according to ARG simulations.

Case	Central ignition NH04	Long edge ignition NH05	Short edge ignition NH06
Average P_0 (bar)	41	22	7

Comparing these values with the predictions according to the correlation shows that none of the predictions are acceptable.
The aspect ratio of the obstructed region is too large to obtain a reasonable answer by using an average L_p and central ignition. The aspect ratio here is more than 7. The approach adopted for aspect ratios other than one does not give an acceptable answer here. The correlation gives 9 to 15 kPa for an L_p of 4 m. This is lower than 30 kPa, so the overpressure is not expected to increase. The overpressure according to ARG reaches an average value of 41 kPa instead, more than a factor three higher.

It is not possible to conclude on the diameter to apply. The variation of the various average diameters is too small.

7.5 5.5 Combination of two obstructed regions

The two obstructed regions considered in the two previous paragraphs form together a large part of the total case. It is therefore interesting to investigate the combination of the two before considering the case as a whole.

The volume of the combination of the two obstructed subregions (OSR-1/2) equals: V_{ob} = 7364 m^3. The volume contains 1265 objects, consisting of 648 cylinders and 617 boxes. It can be calculated that:

- VBR = 0.12;
- D_{arm} = 0.37 m;
- D_{ham} = 0.14 m;
- D_{hym} = 0.51 m.

Table 7: L_p values considered per ignition location.

Ignition location	L_p (m)	Description
IL-1		
	4	distance to top of cloud
	8	width of OSR-2
	16.5	width of OSR-1
	33.5	maximum distance to short edge of OSR-2
IL-2		
	4	distance to top of cloud
	24.5	width of OSR-1/2
	41.5	distance to corner (0.5,0,4) of OSR-1/2
IL-5		
	4	distance to top of cloud
	4	distance to long edge of OSR-2
	20.5	distance to long edge of OSR-1
	28.5	distance to short edge of OSR-2
IL-7		
	4	distance to top of cloud
	4	half width of OSR-2
	57	length of OSR-2
IL-8		
	4	distance to top of cloud
	8.5	distance to long edge of OSR-1
	16	distance to long edge of OSR-2
	37	distance to corner (0.5,0,4) of OSR-1/2
	15.2	radius of hemisphere with equal volume

Five ignition locations are considered; all coincide with an ignition location used in the previous assessments. A number of L_p values can be chosen.

With S_L = 0.45 m/s and the value defined above, the 3D correlation results in a set of overpressures which are collected in Table 8.

Table 8: Overpressures according to correlation.

Ignition location	L_p (m)	P_0 (kPa) D_{arm} = 0.37 m	D_{ham} = 0.14 m	D_{hym}= 0.51 m	AutoReaGas average
IL-1					137
	4	10	72	5	
	8	67	490	34	
	16.5	500	358	**253**	
	33.5	3420	25100	1770	
IL-2					142
	4	10	72	5	
	24.5	1450	10620	**350**	
	41.5	6170	45200	3200	
IL-5					109
	4	10	72	5	
	4	10	72	5	
	20.5	890	6510	**460**	
	28.5	2200	16100	1140	
IL-7					17
	4	10	72	5	
	4	10	72	5	
	57	14780	108300	7650	
IL-8					167
	4	10	72	5	
	8.5	79	578	41	
	16	449	3290	**232**	
	37	4500	33000	2330	
	15.2	390	2860	**202**	

AutoReaGas simulations were performed for the various ignition locations. Pressures were sampled at the same locations used in the simulations of OSR-1 and OSR-2. Pressure histories are presented in Annex F. Results are presented in Table 9. The last row of the table shows average maximum overpressures.

The average overpressure is highest in the case of central ignition (IL-8). The difference in average overpressure for the edge ignition locations is striking. Back- and side-venting for IL-7 appears to have a strong influence on flame development. The flame is still so slow when it enters OSR-1 that it cannot accelerate to produce high overpressures inside OSR-1.
The influence of venting in the case of IL-2 is less pronounced. The flame is able to accelerate inside OSR-1, producing pressures above 0.5 bar and accelerates even more inside OSR-2 where the highest overpressures are reached at the edge. The flame speed inside OSR-2 is high enough to reduce the influence of side-venting.

Table 9: ARG results.

Case:	NH07	NH010	NH08	NH09	NH14
Ignition:	IL-1	IL-2	IL-5	IL-7	IL-8
Sample location (x, y, z)			Pmax (kPa)		
P1 (13, 22, 4)	97	74	63	7	99
P2 (13, 36, 4)	114	77	81	16	99
P3 (13, 47, 4)	166	90	166	30	115
P4 (22, 22, 4)	153	42	103	17	84
P5 (22, 36, 4)	143	36	158	**34**	75
P6 (22, 47, 4)	**178**	60	**187**	19	112
P7 (4, 1, 4)	174	**394**	70	8	**380**
P8 (4, 20, 4)	127	154	65	8	238
P9 (4, 40, 4)	61	106	70	11	107
P10 (4, 50, 4)	158	387	125	19	359
Average	137	142	109	17	167

The average overpressure according to ARG does not depend much on the ignition location. Overpressures are in between 1 and 1.7 bar, except for corner ignition, where they are much lower.
The results of the correlation are confusing. The dependence on L_p and D is strong. The best result seems to be a small L_p (for top-venting) in combination with D_{ham} = 0.14 m, the smallest diameter. This result is, however, in contradiction to the adopted approach for the aspect ratio.

A fairly good result is provided by taking the radius of an equivalent hemisphere for L_p = 15.2 m with D_{hym}: P_0 = 202 kPa (MEM class 8), while the maximum of the average ARG maximum overpressures is 167 (MEM class 7.5).

7.6 5.6 Application to whole case

7.6.1 Determination of parameters

Step 1 to step 5 of the procedure in Annex A leads to a box containing the obstructed region. The box has dimensions: length 57 m, width 32.5 m and height 15 m. The height is arbitrary as one has to decide whether some stacks belong to the obstructed region.

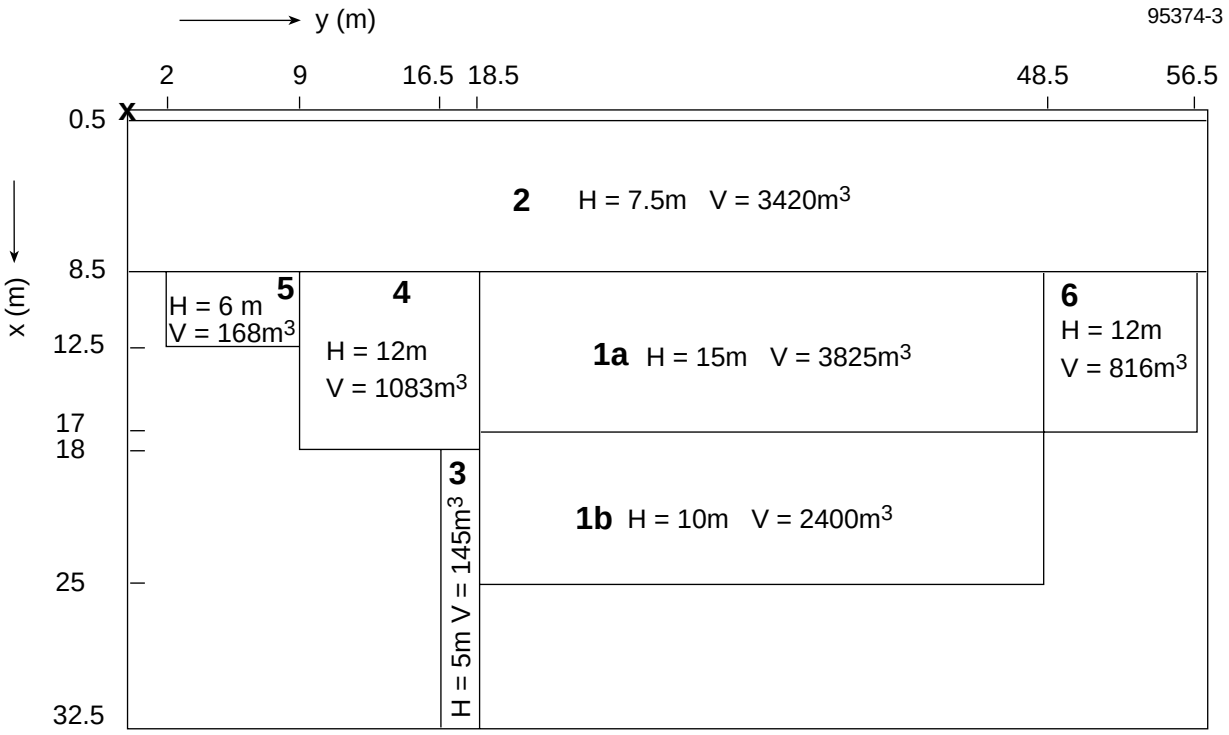

Figure 3: Obstructed region according to Yellow Book (CPR14E, 1997) procedure.

Following step 6 of the procedure in Annex A and the example in Annex C one arrives at the shape of the obstructed region as given in Figure 3. Figure 3 shows the contours of a number of boxes with different heights. The height and volume of each box is given in the figure. The total volume of the obstructed region is:

$V_{or} = 11857\ m^3$

A more accurate determination of V_{or} does not seem worthwhile. A further reduction of 10%, about 1200 m^3, cannot be found.

The formal procedure of the Yellow Book leads to almost the same intuitive subdivision into typical obstructed regions as given in 2.2. The total volume of this intuitive subdivision is V_{or} = 12966 m^3.
According to equation (4), the Yellow Book obstructed volume results in a 28% higher overpressure using the correlation than the intuitive obstructed region.

The procedure of the Yellow Book does not account for typical obstacle configurations within each box defined in the obstructed region. Therefore, the intuitive subdivision is preferred.
The intuitive subdivision can be improved by subdividing subregion 1 (see Figure 2) into two parts, because one part consists of two storeys while the other is a single storey support structure:

1a width 8.5 m (x: 8.5 -17 m), length 30 m (y: 18.5 - 48.5 m) and height 15 m, volume 3825 m^3;

1b width 8 m (x: 17 - 25 m), length 30 m (y: 18.5 - 48.5 m) and height 10 m, volume 2400 m^3.

The volume of the intuitive obstructed region now reduces by 1200 m^3 to 11766 m^3.

The VBR and D can now be calculated for each obstructed subregion and for the obstructed region as a whole (Table 10).

Table 10: Parameters for various obstructed subregions.

Obstructed subregion	x (m)	y (m)	z (m)	VBR	D_{arm} (m)	D_{ham}(m)	D_{hym} (m)
OSR-1a	8.5-17	18.5-48.5	0-15	0.19	0.41	0.10	1.07
OSR-1b	17-25	18.5-48.5	0-10	0.13	0.20	0.07	0.82
OSR-2	0.5-8.5	0-57	0-7.5	0.14	0.49	0.40	0.52
OSR-3	8.5-32.5	16.5-18.5	0-5	0.03	0.16	0.15	0.16
OSR-4	8.5-18	9-16.5	0-12	0.25	1.16	0.61	1.40
OSR-5	8.5-12.5	2-9	0-7.5	0.11	0.91	0.75	1.03
OSR-6	8.5-17	48.5-56.5	0-12	0.16	0.83	0.08	1.45
SR (total)				0.18	0.41	0.14	0.84

We are considering a problem where the obstructed region is filled with a homogeneous and stoichiometric mixture of methane/air up to a height of 7.5 m.
Here, the obstructed region is larger than the flammable cloud. The problem here is which obstacle parameters to use. This problem was identified as a white spot (section 2.4). We choose to work with the obstacle parameters of that part of the obstructed region filled with the cloud. Table 11 contains the obstacle parameters for the obstructed subregions limited to a height of 7.5 m.

The total volume of the obstructed part filled with the cloud is: V_{or} = 8627 m^3. The radius of a hemisphere with equal volume is 16 m.

Table 11: Parameters for various obstructed subregions with height limited to height of cloud.

Obstructed subregion	x (m)	y (m)	z (m)	VBR	D_{arm} (m)	D_{ham} (m)	D_{hym} (m)
OSR-$1a^{7.5}$	8.5-17	18.5-48.5	0-7.5	0.12	0.32	0.11	0.56
OSR-$1b^{7.5}$	17-25	18.5-48.5	0-7.5	0.07	0.17	0.07	0.41
OSR-2	0.5-8.5	0-57	0-7.5	0.15	0.50	0.40	0.52
OSR-$3^{7.5}$	8.5-32.5	16.5-18.5	0-5	0.03	0.16	0.15	0.16
OSR-$4^{7.5}$	8.5-18	9-16.5	0-7.5	0.20	0.95	0.51	1.29
OSR-5	8.5-12.5	2-9	0-7.5	0.11	0.91	0.75	1.03
OSR-$6^{7.5}$	8.5-17	48.5-56.5	0-7.5	0.11	1.01	0.09	0.87
$SR^{7.5}$ (total)				0.13	0.37	0.14	0.55

Ignition location 1 (IL-1) will be considered for the next L_p:

- L_{p1} = 3.5 m, distance to top of cloud;

- L_{p2}= 8.5 m, distance to long edge;
- L_{p3} =16.5 m, distance to opposite long edge;
- L_{p4} = 33.5 m, distance to short edge;
- $L_{p,ave}$ = 16 m, radius of equivalent hemisphere.

Application of the 3D correlation provides the following results.

Table 12: Overpressures (kPa) for various L_p and D.

L_p (m)	D_{arm} = 0.37 m	D_{ham} = 0.14 m	D_{hym} = 0.55 m
3.5	7	63	4
8.5	98	721	44
16.5	609	4460	270
33.5	4260	31300	1890
16	595	4100	248

7.6.2 AutoReaGas simulations

The ARG simulation performed with the total obstructed region (simulation NH11) resulted in an average maximum overpressure of 182 kPa (see Table 13 for details), which equals an MEM class of about 8. As in previous cases, an acceptable result is obtained by using the correlation with D_{hym} and the radius of the equivalent hemisphere (last row of Table 12): 248 kPa, which is equal to an MEM class of about 8.5.

Table 13: Comparison of all ARG results.

						Pmax (kPa)								
Case	NH01	NH02	NH03	NH12	NH13	NH04	NH05	NH06	NH07	NH010	NH08	NH09	NH14	NH11
OSR	1	1	1	1	1	2	2	2	1-2	1-2	1-2	1-2	1-2	all
Ignition:	IL-1	IL-2	IL-3	IL-8	IL-9	IL-5	IL-6	IL-7	IL-1	IL-2	IL-5	IL-7	IL-8	IL-1
Sample location														
P1	18	36	13	47	**55**				97	74	63	7	99	109
P2	24	34	11	41	23				114	77	81	16	99	123
P3	26	**59**	5	65	9				166	90	166	30	115	176
P4	36	21	14	51	51				153	42	103	17	84	158
P5	**40**	19	**22**	42	34				143	36	158	**34**	75	144
P6	37	35	8	**73**	10				**178**	60	**187**	19	112	186
P7						27	13	**9**	174	**394**	70	8	**380**	**374**
P8						**62**	**33**	**9**	127	154	65	8	238	128
P9						50	28	5	61	106	70	11	107	61
P10						26	13	5	158	387	125	19	359	196
P11														239
P12														215
P13														163
P14														270
Average	30.2	34.0	12.0	53.1	30.3	41.3	21.8	7.0	137	142	109	17	167	182

Table 13 shows the details of the ARG simulation in comparison with the other cases, the results of which are given in previous tables. The highest overpressures in NH11 occurred in the corners of the obstructed region. The extension of OSR-1/2 with OSR 3, 4 and 5 appears to promote flame acceleration in the large pipe-bridge (OSR-2).

7.7 5.7 Influence of detail of obstacle description

The numerical simulations for the Chemical Plant case and also for the cases to be presented in the following chapters, were performed using an obstacle database. Such an obstacle database can never exactly match the obstacle configuration as built in reality. There will also be details which are not described in the database. As obstacles play an important role in the gas explosion mechanism, the level of detail with which the obstacles are described may influence the numerical result.

In order to investigate the effect of detail of obstacle description, a number of AutoReaGas simulations were performed using the Chemical Plant obstacle database. In subsequent simulations, obstacles with a diameter smaller than a specified value were omitted.
The first simulation was run using the original database. Subsequent simulations omitted all obstacles with a diameter of less than 0.1, 0.2, 0.25, 0.3, 0.4, 0.5, 0.6 and 0.7 m.

The results of the numerical simulations are visualised in Figure 4. Overpressures were sampled at similar locations as in Table 13 including some locations outside the obstacle configuration. The number of obstacles in each simulations are given in Table 14.
Even if all obstacles smaller than 0.3 m are deleted, there is hardly any effect on the overpressures; the influence being stronger for the higher pressures. Overpressures are lowered by about 20% when only obstacles with a diameter larger than 0.6 m are considered. Overpressures become unacceptable in the last simulation with obstacles larger than 0.7 m only.
Because the overpressure level is rather constant for all simulations with obstacles smaller than 0.3 m, it can be expected that the overpressures will not increase when more detail is included in the obstacle database.

This result is in contradiction to the common opinion that adding more small objects will result in an increase in overpressure. On the other hand, this common opinion is not fully supported by the physical modelling. The consequence of leaving out small objects is a reduction of the fluid dynamic drag. This means a reduction of the fluid dynamic drag leading to a reduction of the turbulence source term At the same time, a reduction in drag means an increase in the expansion velocity and, in this way, an increase in the turbulence source term. Thus, there are competing effects, the balance of which is case dependant.

Table 14 shows how the omission of small obstacles influence the parameters in the correlation.
The reduction in overpressures according to the correlation follow the same trend as the results of the numerical simulations. There is hardly an effect until obstacles with a diameter smaller than 0.4 m are removed. Until that point the removal of obstacles did not result in a significant reduction of the total obstacle volume.

Table 14: Influence of obstacle removal.

Removed obstacles	Number of obstacles left	Total obstacle volume (m^3)	Percentage of initial volume (%)	VBR (-)	D_{hym} (m)	Percentage of initial P_0 according to correlation (%)
None	1923	2080	100.00	0.18	0.84	100
< 0.1 m	1417	2079	99.95	0.18	0.84	98
< 0.2 m	1049	2069	99.51	0.18	0.87	93
< 0.25 m	975	2064	99.25	0.18	0.89	89
< 0.3 m	703	2061	99.08	0.18	0.90	88
< 0.4 m	471	2030	97.62	0.18	0.93	81
< 0.5 m	433	2024	97.33	0.18	1.02	67
< 0.6 m	162	1973	94.88	0.17	1.09	50
< 0.7 m	125	1486	71.46	0.13	1.48	13

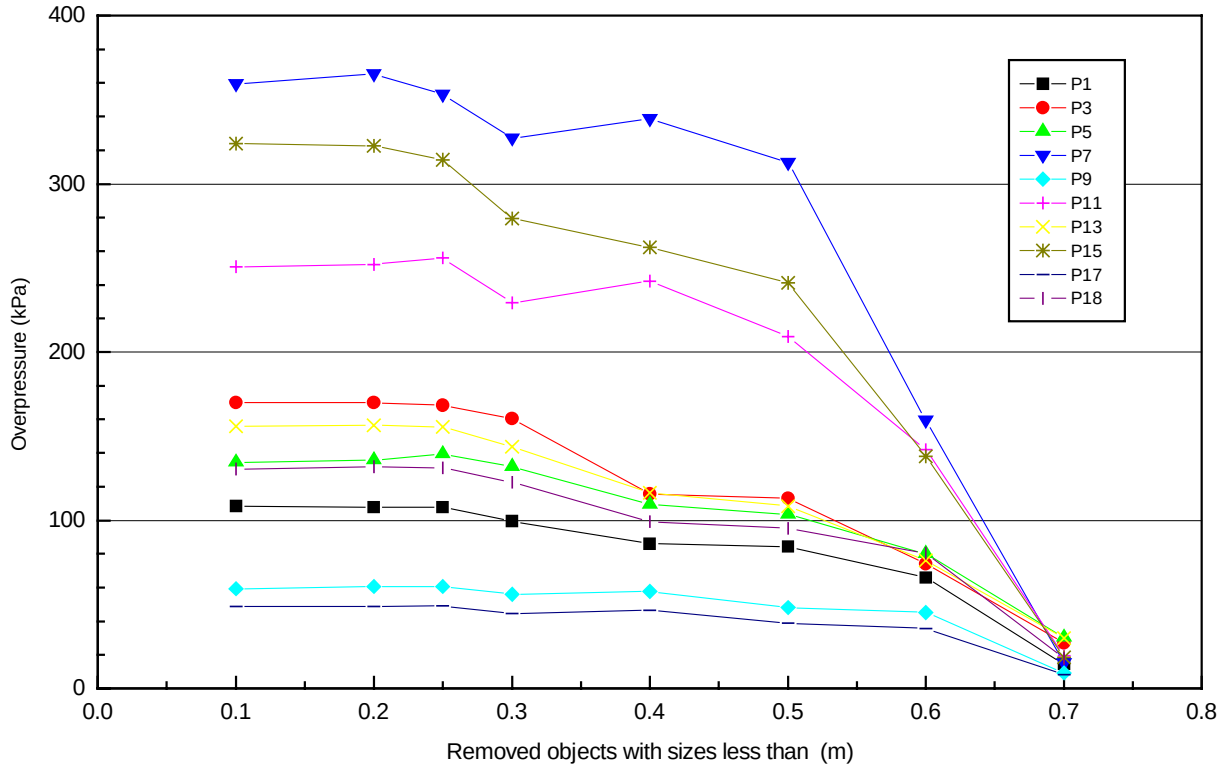

Figure 4: Influence of minimal obstacle diameter in obstacle database on overpressure.

7.8 5.8 Overall evaluation of the Chemical Plant case

7.8.1 General

The Chemical Plant obstacle configuration as a whole can be subdivided into a number of specific obstructed subregions.
The application of the correlations to the subregions and combination of subregions showed that a very large band of predictions for the overpressure is obtained for a specific situation by substituting possible values for all parameters in the correlation. On the one hand, this is due to the various ways in determining an average diameter; on the other hand, the configuration in combination with the ignition location differs very substantially from the configurations used to derive the correlation. The correlation is not capable of including the influence of the aspect ratio and of an ignition location at the edge of the configuration.

The correlation results when using the hydraulic diameter appear to be of the same order as the numerical results.

Except for the subregion containing the pipebridge, the influence of the ignition location according to the AutoReaGas calculations is not very strong. Edge ignition resulted always in lower overpressures than ignition inside the configuration. This observation may not be valid in other cases where the flame may be accelerated due to a higher level of obstruction in combination with the longer flame path.

An acceptable result was obtained when the correlation was used with the average hydraulic obstacle diameter D_{hym} in combination with an average value for the flame path length L_p. The average flame path length is equal to the radius of a hemisphere with a volume equal to the volume of the obstructed region under consideration.

7.8.2 Comments on the covering of the white spots

1 *Missing correlations*
The missing correlations concern 1D situations and jet ignition. The available correlations for 2D and 3D expansion are sufficient for the present case.

2 *Criterion to separate between 2D and 3D correlation*
The issue is of importance in part of the case only. The aspect ratio of that part is less than 5. The guidance given in section 2.1 advises one to take the 3D correlation in that case. The evaluation in section 4.3 shows that the less conservative results are obtained indeed by applying the 3D correlation.

3 *Definition of obstructed region*
The absence of a strict procedure to determine the boundaries of the obstructed region does not cause problems in this case. By applying the Yellow Book procedure, there is no problem in this case to decide whether an obstacle be-

longs to an obstructed region. A minor problem may be caused by the stacks present in the case. A strict application of the procedure results in adding the space between two stacks to the volume of the obstructed region. This is considered to be of no influence in this case.
The intuitive determination of the obstructed region almost completely coincides with the region defined according to the Yellow Book procedure.

4 *Multiple obstructed regions*
This white spot is not an issue in this case. The obstructed region can be composed of differently shaped obstructed subregions with specific obstacle characteristics. The overall lay-out however is not such that one could expect more than a single obstructed region.

5 *Differently shaped obstacles*
The case contains many non-cylindrical obstacles. The procedure adopted to cope with non-cylindrical obstacles is to turn these into cylinders with a length equal to the longest dimension of the obstacle and an equal cross-section area. There is, at present, no indication about the physically correctness of that procedure. Especially for flat plates, the procedure is very questionable.

6 *L_p in the case of aspect ratios other than unity and ignition location outside centre of configuration*
For aspect ratios differing from unity and central ignition, the value for L_p may vary between half the height, width or length of the obstructed region. The additionally provided guidance stated that the overpressure will not increase anymore after the moment the flame propagated the shortest L_p if the overpressure is less than a specific value at that moment. The specific value was arbitrarily chosen to be 30 kPa.
Application of this guidance in this case does not result in much confidence. The flat cloud in combination with the z-co-ordinate of the ignition location results in a smallest L_p of 4 m. Overpressures for Lp = 4 m were always very low, while the final overpressures were much higher.
For edge ignitions, the flame path length will always be longer than in the case of central ignition. Therefore the correlation will provide higher overpressures in the first situation, while in reality, lower values will be obtained in the majority of the situations, due to the influence of (back- and side-)venting. At the present, it is not possible to define when the pressure increasing effect due to a combination of a long flame path and a high volume blockage ratio is larger than the pressure reducing effect of back- and side-venting.
In the case of the Chemical Plant, edge ignition resulted in a lower overpressure than central ignition, so the correlation can be applied safely when used with the L_p for central ignition.

7 *Obstructed region larger than gas cloud*
This white spot will be an issue in many cases, including the present one. The

influence of obstacles located immediately outside the vapour cloud is neglected. It can be argued though that the influence might be considerable. Clearly, this issue should be investigated in more detail to arrive at a complete package of guidance for the application of the MEM.

8 *Single value for explosion overpressure*
The ARG simulations show the distribution of overpressures to be very non-homogeneous. A practical model like MEM requires a single value for the source overpressure. The use of an average maximum overpressure seems acceptable in case one is interested in blast. However, if one is interested in blast characteristics ‘close’ to the source, or if one is interested in consequences inside the source, more sophisticated models should be used.

8

9 6 Application to the LNG Terminal case

9.1 6.1 Description of case

The digital file containing the LNG Terminal case to be assessed in GAMES covers a volume of length: 175 m (x-direction), width: 57 m (y-direction) and height: 15.5 m (z-direction).
Figures 5.a, 5.b, 5.c and 5.d show an overview and various cross-sections.

The case mainly consists of a number of pipebridges running parallel to the x- and y-axes. The largest obstructed region can be found between the co-ordinates x: 25 - 85 m and y: 20 - 45 m. Two minor obstructed regions are located at approximately x: 1 - 10 m, y: 30 - 38 m and at x: 153 - 167 m, y: 30 - 45 m. There is an isolated obstructed region consisting of some large vessels surrounded by walls at x: 113 - 132 m, y: 15 - 27 m.

We will adopt the next nomenclature for the various parts (the dimensions given are not yet the boundaries of the obstructed subregions (OSR) but an indication of where the part considered is located):

- OSR 1 from x = 28 to 82 m and from y = 21 to 44 m;
- OSR 2 from x = 153 to 167 m and from y = 30 to 45 m;
- OSR 3 from x:= 1 to 10 m and from y = 30 to 38 m;
- OSR 4 from x = 113 to 132 m and from y = 15 to 27 m;
- OSR 5 pipebridge 1, running parallel to the x-axis from x = 15 to 175 m and width from y = 38 to 44 m;
- OSR 6 pipebridge 2, running parallel to the x-axis from x = 1 to 97 m and width from y = 6 to 10 m;
- OSR 7 pipebridge 3, running parallel to the y-axis from y = 10 to 47 m and width from x = 1 to 6 m;
- OSR 8 pipebridge 4, running parallel to the y-axis from y = 1 to 45 m and width from x = 88 to 95.

The database contains many objects describing the ground surface. The ground surface appears to be not completely horizontal but its z-co-ordinate varies between 2.5 and 3 m. For reasons of simplicity, the ground surface was chosen to be at z = 3 m. The ground surface is then represented by a single large plate.
The differences in height of the total obstacle configurations is slight. The height is mainly determined by the height of the pipebridges which is at z = 7 and 8 m (height 4 and 5 m). The height of pipebridge 4 is about 8 m.
The height of obstructed region 1 varies from 2 to 5 m for the largest part. There is a single large vertical cylinder with some pipework with a height of 12 m (see also

picture in progress report 1). Some pipework in obstructed region 3 reaches a height of 10 m. The height of the isolated obstructed region 4 is taken to be 3 m. This initial attempt to subdivide the total configuration into obstructed regions is visualised in Figure 6.

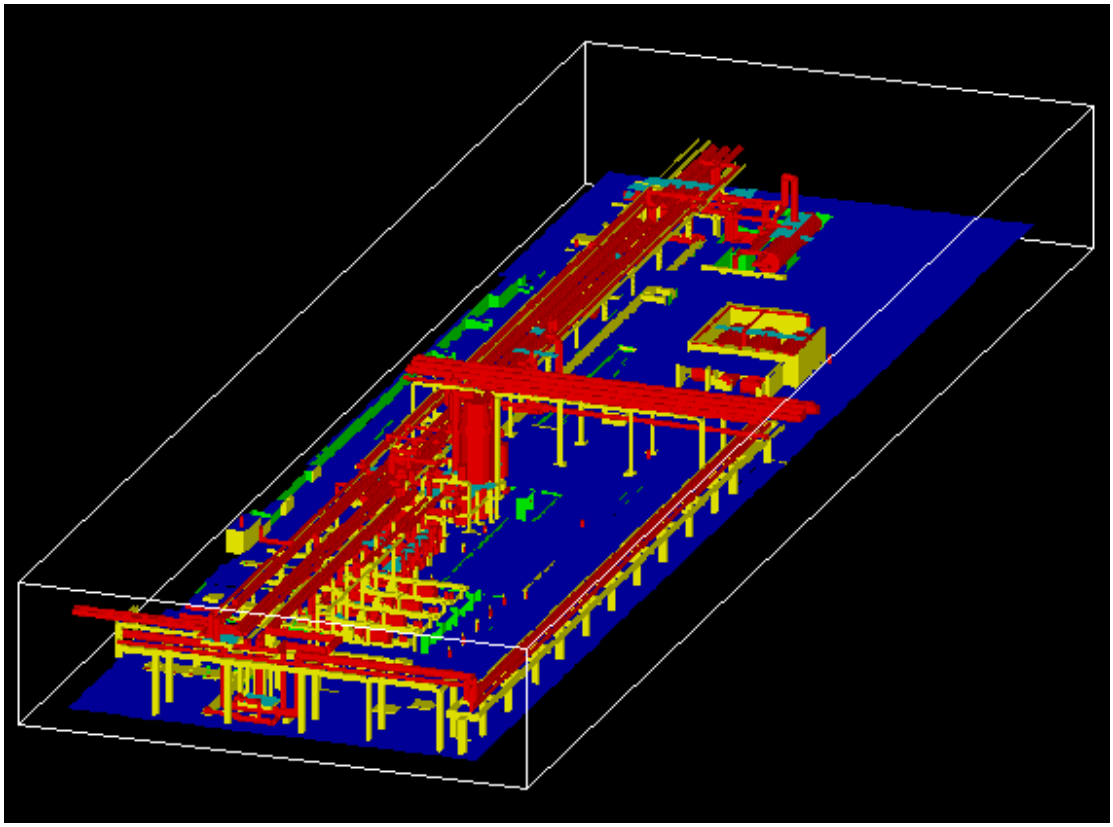

Figure 5.a: View of the LNG Terminal case: overall view.

Figure 5.b-d: View of the LNG Terminal case: b: horizontal projection on yx-plane; c: vertical projection on xz-plane; d: vertical projection on xy-plane.

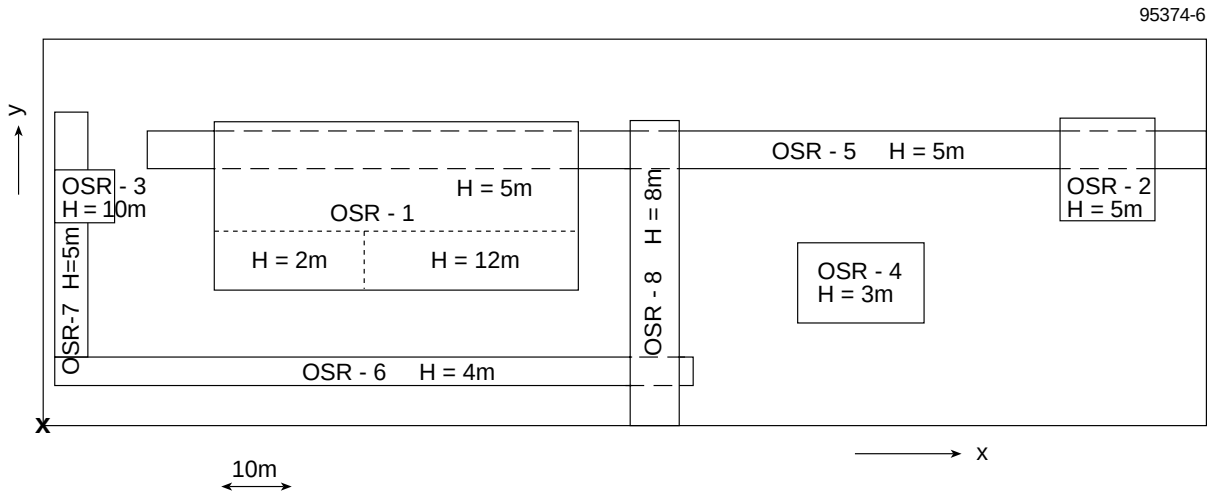

Figure 6: LNG Terminal case initial subdivision into obstructed regions.

9.2 6.2 First impression of potential explosion severity

The dimensions of the total obstacle configuration described by the database is quite large. On the other hand, there seems only a single part with a high obstacle density which is expected to generate higher overpressures. That is, OSR-1, OSR-2 and OSR-3 are expected to produce lower overpressures due to the smaller dimensions and their probably lower obstacle densities.

The effect of the pipebridges has to be investigated. The Chemical Plant case showed that ignition at the short edge resulted in a very low overpressure. It is therefore interesting to investigate whether an explosion in OSR-1 results in flame acceleration in OSR-5 to finally produce higher overpressures in OSR-2. It also may be possible that explosions in OSR-1 and OSR-2 have to be regarded as two separate explosion sources.

A question is also to what explosion the combination of OSR-1, -7, -6 and -8 will result. Is such an explosion governed by OSR-1 only or do the other OSRs have a contribution?

Considering the comments given above, it is logical to first investigate subcases before investigating the case as a whole.

The investigation will be performed assuming a cloud of a stoichiometric methane/air mixture filling the entire obstacle configuration up to a z-co-ordinate of 11 m. So, only the high vertical cylinder with adjacent equipment in OSR-1 extends outside the cloud.

Contrary to the Chemical Plant case, there is no obstructed subregion present for which one may consider the correlation for 2 dimensional expansion. The application of the correlations will therefore be restricted to equation 2 in combination with S_L = 0.45 m/s.

9.3 6.3 Application of correlation to obstructed subregion 1

The two main questions in applying equation 2 to OSR-1 are:

- what is the volume of OSR-1?
- what is the average obstacle diameter?

Values for L_p and VBR can be derived if the volume is known.

The step-by-step procedure of the Yellow Book, given in Annex A, will be applied to determine the boundaries of OSR-1.

Figure 7 shows details of OSR-1.

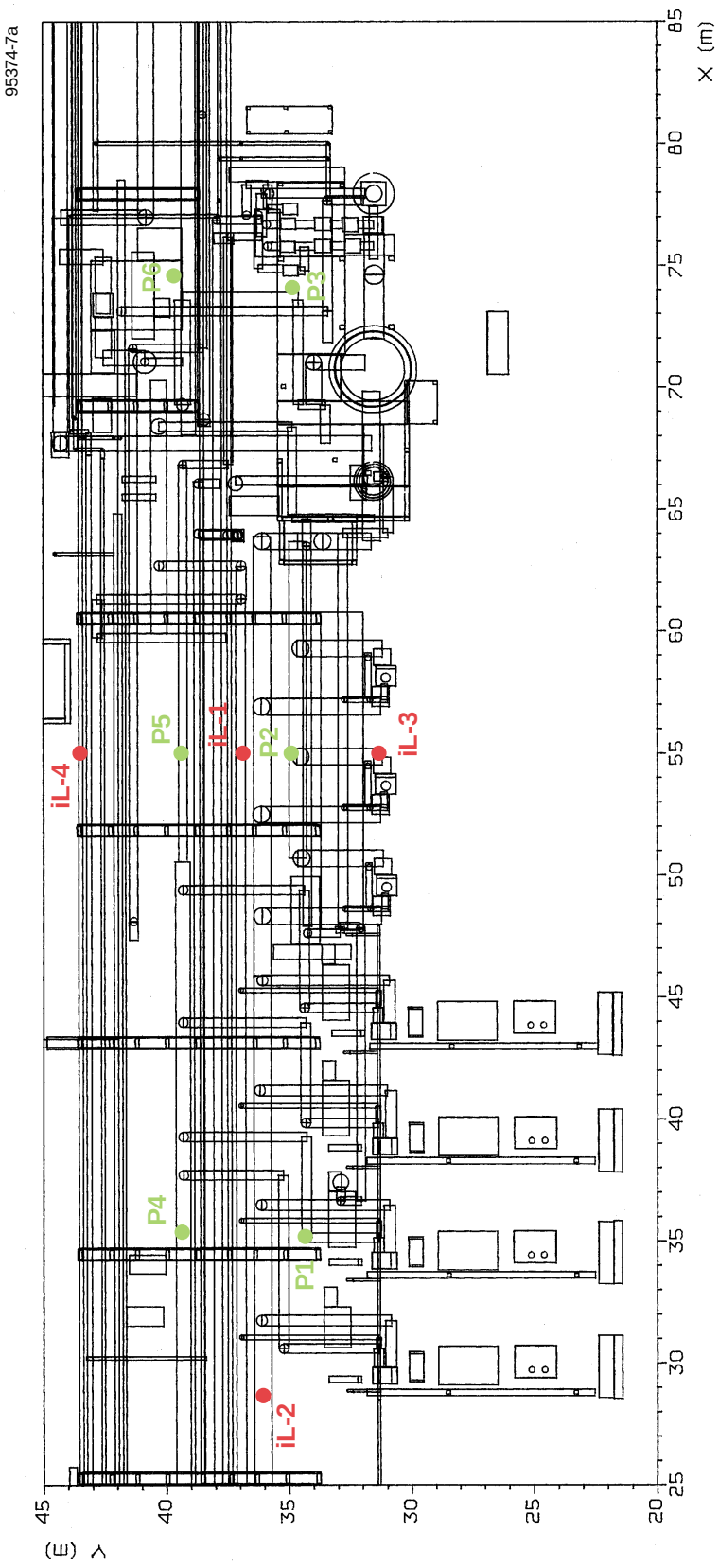

Figure 7.a: Details of OSR-1: horizontal projection on the xy-plane.

Figure 7.b-c: Details of OSR-1: b: vertical projection on the xz-plane; c: vertical projection on the yz-plane.

9.3.1 Determination of V_{or}

Step 1

This is the obstacle database.

Step 2

We will assume an ignition location inside OSR-1.

Step 3 and 4

These steps are to decide if an adjacent obstacle belongs to the initial obstructed region consisting of the obstacles immediately surrounding the ignition location. One of the criteria is that the initial obstructed region is extended with all obstacles within a range of 10 times the diameter of an obstacle in the initial obstructed region. For instance, if the diameter D1 of the obstacle closest to the ignition location equals 1 m, then all obstacles within 10 m should be included in the obstructed region. The extended initial obstructed region is to be extended again if more obstacles fall under the criteria applied to the extended initial obstructed region.
An obstacle does not belong to the obstructed region if the distance to any obstacle in that obstructed region is larger than 10 times the diameter of any obstacle inside the obstructed region or if the distance of the obstructed region is 25 m or larger.

It will soon be clear while applying the procedure that all obstacles in the LNG Terminal case belong to a single obstructed region according to the Yellow Book procedure; even OSR-4.

Step 5

In order to limit the first assessment to OSR-1 and to determine the V_{or} of OSR-1, we will assume that a single box containing the obstacles of OSR-1 is located between x = 28 to 82 m, y = 21 to 44 m and z = 3 to 15.5 m. The dimensions of the box are length 54 m, width 23 m and height 12.5 m.

Step 6

Without conflicting the criteria for the obstructed region, the volume of the box can be reduced by leaving out free space. Also, the height of the box is limited to the height of the cloud. A study in detail of the obstacle configuration inside OSR-1 resulted in the shape of V_{or} visualised in Figure 8.
The single box defined in step 5 is reduced to 4 subboxes:

- subbox 1: x = 28 - 45, y = 21 - 31, z = 3 - 5, volume = 340 m^3;
- subbox 2: x = 28 - 63, y = 31 - 35, z = 3 - 8, volume = 700 m^3;
- subbox 3: x = 28 - 63, y = 35 - 44, z = 3 - 7, volume = 1540 m^3;
- subbox 4: x = 63 - 82, y = 29 - 44, z = 3 - 8, volume = 1425 m^3.

The total volume of OSR-1 equals V_{or} = 4005 m^3.
Close examination of the obstacle configuration did not reveal any possibility to reduce V_{or} by 10% or more. The conclusion is that a volume of 4005 m^3 for the OSR-1 is a practical minimum value.

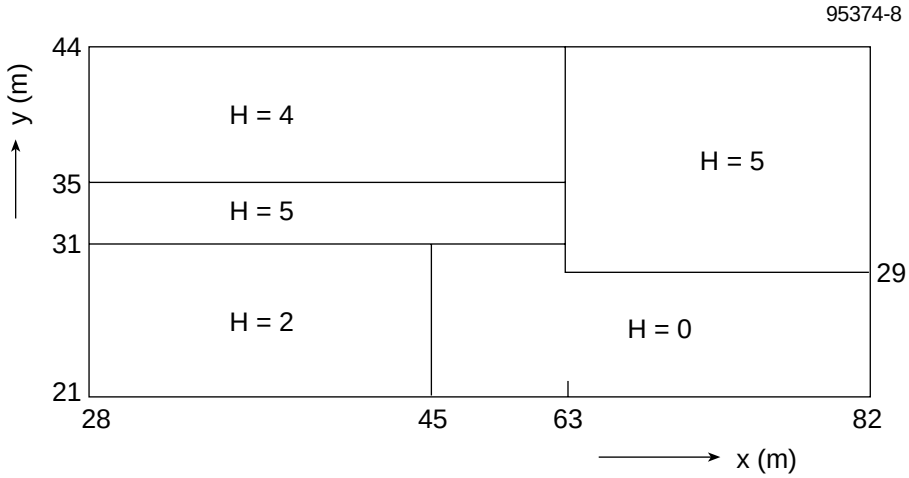

Figure 8: Subdivision of box containing OSR-1 into subboxes. H: height of subbox in metres.

9.3.2 Determination of the average diameter D and the volume blockage ratio VBR

Application of equations 5, 6 and 7 to OSR-1 results in:

- D_{arm} = 0.32 m;
- D_{ham} = 0.23 m;
- D_{hym} = 0.48 m;

and

- VBR = 0.06.

9.3.3 Determination of L_p

A number of values for Lp are possible depending on the ignition location.
The following ignition locations will be considered:

- IL-1 at (x,y,z) = (55,36,5), central ignition;
- IL-2 at (x,y,z) = (28,36,5), centre of short edge;
- IL-3 at (x,y,z) = (55,31,5), centre of long edge;
- IL-4 at (x,y,z) = (55,44,5), centre of long edge.

The next values for L_p are interesting for evaluation:

- L_{p1} = 2 m, approximate distance to top of OSR-1;
- L_{p2} = 11.5 m, half the width of OSR-1;
- L_{p3} = 23 m, width of OSR-1;
- L_{p4} = 27 m, half the length of OSR-1;
- L_{p5} = 54 m, length of OSR-1;
- $L_{p,ave}$= 12.4 m, radius of hemisphere with equal volume as OSR-1.

9.3.4 Determination of overpressure

Substituting the values for L_p, VBR, S_L and D in the correlation, equation 2, results in Table 15 for the overpressure P_0.

Table 15: Overpressures for OSR-1.

L_P (m)	P_0 (kPa) D_{arm} = 0.32 m	D_{ham} = 0.23 m	D_{hym} = 0.48 m
2	0.3	0.6	0.1
11.5	36	71	16
23	244	480	106
27	379	746	165
54	2549	5017	1110
12.4	45	88	19

The overpressures calculated for L_p = 2 and 54 are unrealistically low and high, respectively.

9.3.5 ARG calculations

ARG simulations were performed in which the obstacle configuration was limited to the obstacles within OSR-1. The ignition locations were IL-1, -2, and -4. Pressures were sampled at six locations (P1 to P6, see Figure 7.a).

Maximum overpressures calculated for the various ignition locations and pressure sampling locations are given in Table 16.

Table 16: Maximum overpressures calculated with ARG.

Location (x, y, z)	Po (kPa) IL-1	IL-2	IL-4
P1 (35, 34, 5)	36	24	7
P2 (55, 34, 5)	21	89	7
P3 (75, 34, 5)	73	82	7
P4 (35, 39, 5)	72	30	9
P5 (55, 39, 5)	22	70	9
P6 (75, 39, 5)	81	96	9
average	51	65	8

Table 16 shows that the overpressure increases at increasing distances from the ignition location. Despite the fact that IL-2 is located in the centre of the short edge, the maximum overpressures is higher than in the case of central ignition (IL-1). Edge ignition in the Chemical Plant case always resulted in a lower overpressure than central ignition.

9.3.6 Evaluation

The correlation results for the Lp values according to half the width, the width and the equivalent radius give results in the same order as the averaged numerical results. The best results seems to be those when a smallest value for the diameter is used (D_{ham}).

This is in contradiction to the results of the Chemical Plant case where the best results were obtained when the largest value for the diameter was used.
A difference between the Chemical Plant case and the subcase of LNG Terminal considered here is the lower VBR. The average L_ps are comparable because the V_{or}s are more or less the same. A difference is present in aspect ratio.

9.4 6.4 Application of correlation to obstructed subregion 2

The initial boundaries for OSR-2 were taken from x = 153 to 167 m and from y = 30 to 45 m. Closer examination and application of the procedure in Annex A resulted in slightly different boundaries. Figure 9 shows the boundaries. As in the previous section, application of the Yellow Book procedure to determine an obstructed region results in the complete LNG Terminal obstacle configuration becoming a single obstructed region. It is assumed for the limitation of the boundaries of OSR-2, the sections through pipebridge 1 at x = 147 m and x = 168 m are boundaries.
OSR-2 now consists of three subboxes:

- subbox 1: x= 150 - 168, y = 27 - 36, z = 3 - 6, volume 486 m^3;
- subbox 2: x = 147 - 168, y = 36 - 45, z = 3 - 8, volume 945 m^3;
- subbox 3: x = 157 - 165, y = 45- 47, z = 3 - 8, volume 80 m^3;

with a total volume V_{or} = 1511 m^3.

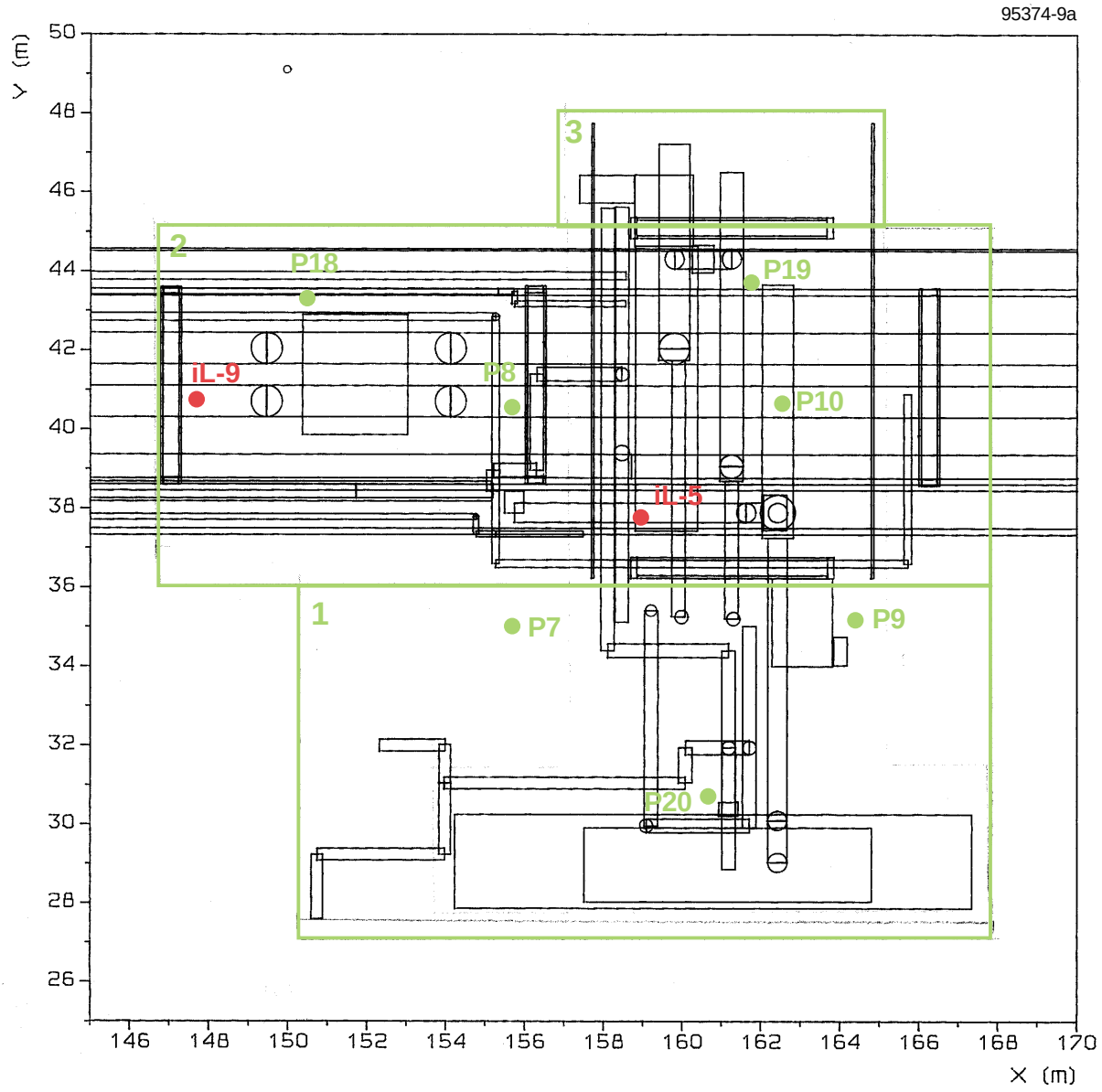

Figure 9.a: Subdivision of OSR-2 into subboxes: horizontal projection on the xy-plane.

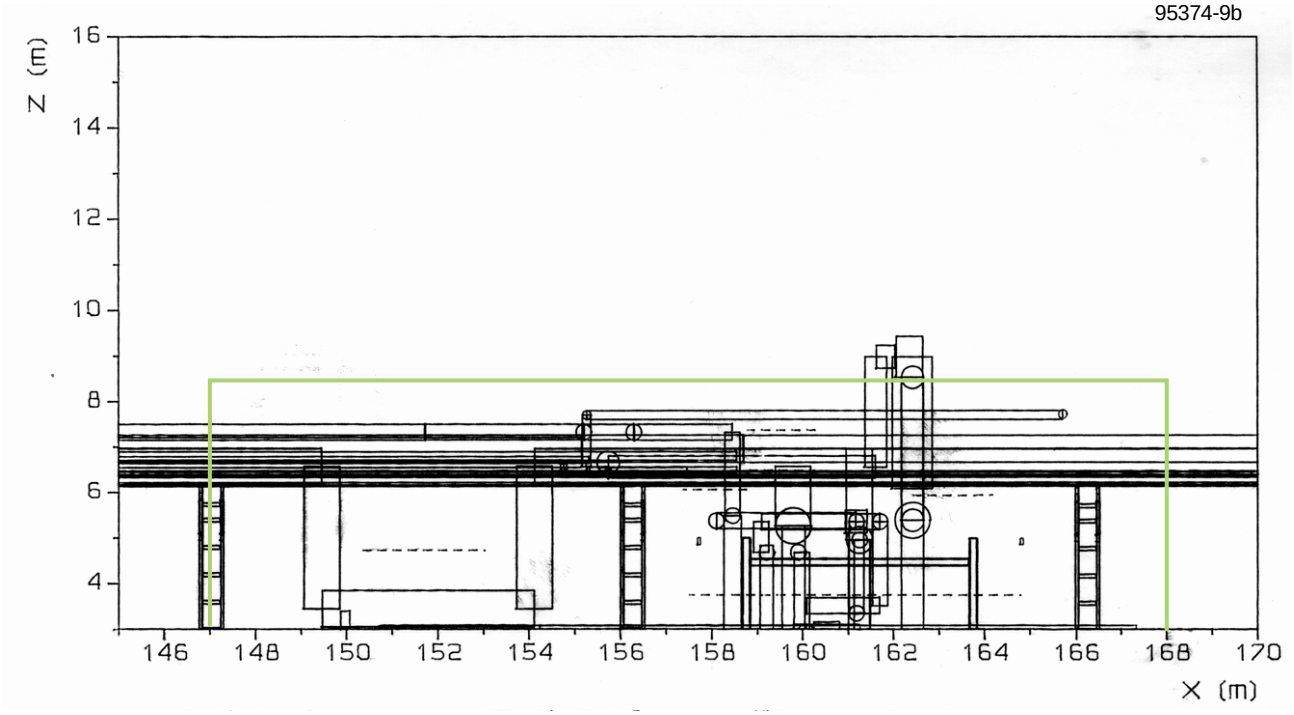

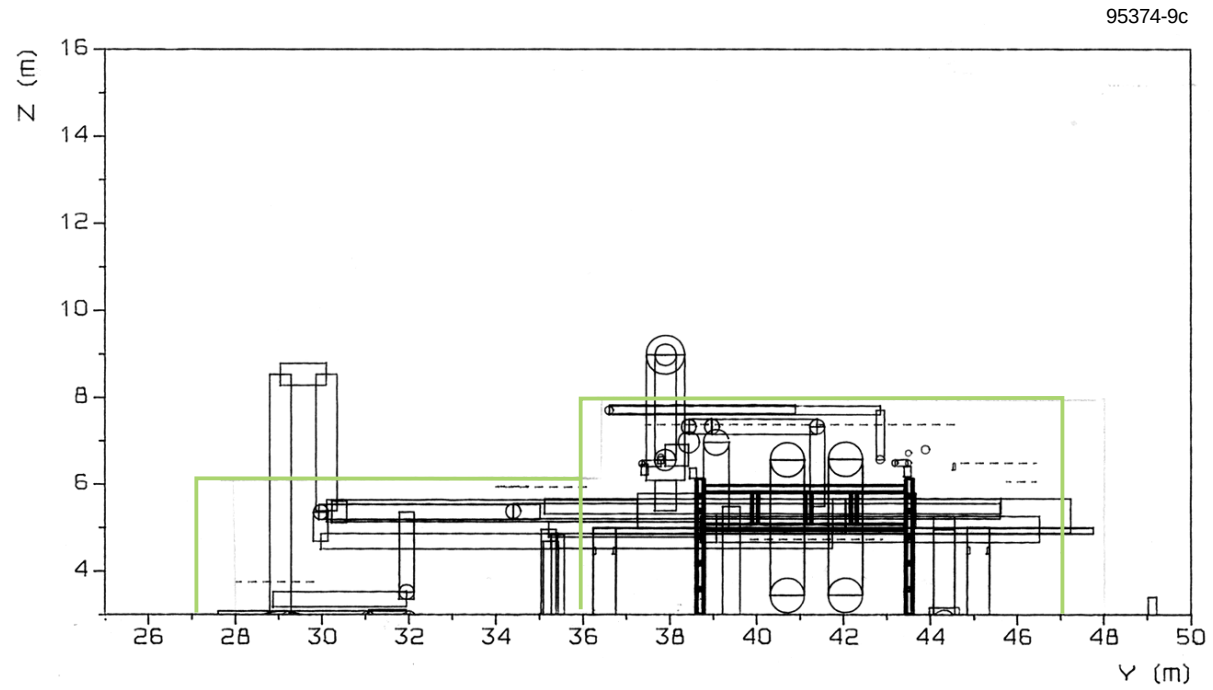

Figure 9.b-c: Subdivision of OSR-2 into subboxes: b: vertical projection on the xz-plane, c: vertical projection on the yz plane.

Calculation of the various average diameters results in:
- D_{arm} = 0.31 m;
- D_{ham} = 0.21 m;
- D_{hym} = 0.46 m;

and
- VBR = 0.04.

When the next ignition location is taken:
- IL-5 at (x,y,z) = (159,37,5), central ignition;

the next values for L_p are of interest:
- $L_{p,1}$ = 2 m, average distance to top;
- $L_{p,2}$ = 10 m, average distance to all edges;
- $L_{p,ave}$ = 9.0 m, radius of hemisphere with volume V_{or}.

Application of the correlation (equation 2) results in.

Table 17: Overpressures for OSR-2.

L_P (m)	P_0 (kPa) D_{arm} = 0.31 m	D_{ham} = 0.21 m	D_{hym} = 0.46 m
2	0.1	0.2	0
10	9	19	4
9	6	14	3

ARG calculations were performed using all obstacles enclosed within the space bounded by: x = 147 to 168 m, y = 27 to 47 m and z = 3 to 8 m and using IL-5 for the ignition location.
The maximum overpressures for locations P7, P8, P9 and P10 (see Figure 9a) were:
- P7: 18 kPa;
- P8: 28 kPa;
- P9: 20 kPa;
- P10: 21 kPa.

The average maximum overpressures equals 22 kPa.

Table 17 shows that variation of the parameters for the correlation within a realistic range results in a wide range of overpressure predictions. Acceptable results were obtained when using D_{hym} together with an average L_p. Here, this combination results in a too low overpressure (3 kPa).
A reason why this underprediction occurs may be that the procedure to determine the obstructed region according to the Yellow Book is too conservative, especially for small obstructed volumes. If the procedure would allow a reduction in V_{or} of 50%, the overpressure would increase despite the smaller L_p.
Room for volume reduction is available, see Figure 9. A reduction of 50% in V_{or} doubles the VBR to 0.08 and reduces the average L_p to 7.1 m. The correlation predicts the overpressures of Table 18 when using these values.

Table 18: Overpressures for OSR-2 with reduced V_{or}.

L_P (m)	P_0 (kPa) D_{arm} = 0.31 m	D_{ham} = 0.21 m	D_{hym} = 0.46 m
2	0.7	1.5	0.3
10	58	129	26
7.1	23	50	10

It appears that even with a 50% volume reduction the correlation using Dhym and Lp,ave results in too low overpressures when compared with the numerical results. Although the Yellow Book procedure to determine Vor is thought to be conservative, a reduction of 50% does not seem to be possible.
The conclusion is that the choice of parameters for the correlation which worked well in the Chemical Plant case is not appropriate in the present case of OSR-2. Maybe the low value for the VBR of OSR-2 (0.04) is responsible for this.

9.5 6.5 Application of the correlation to a combination of obstructed subregions 1, 2 and 5

9.5.1 Introduction

The combination of the obstructed regions 1 and 2 via pipebridge 1 into one large obstructed region is interesting for the application of the Multi-Energy Method. When ignited at the short ends, the pipebridge in the Chemical Plant case did not generate much overpressure. Here in the LNG Terminal case, the number of pipes and pipe layers is even less than in the Chemical Plant case. It may be expected therefore that a flame, initiated in either OSR-1 or OSR-2, will decelerate during propagation through the pipebridge. The result will be two separate explosions; one in OSR-1 and one in OSR-2.

9.5.2 ARG simulations

An ARG simulation was performed to investigate if any support for the idea of two separate explosions could be found.
The simulation was made with all obstacles inside OSR-1, OSR-2 and pipebridge 1 (OSR-5) for ignition location IL-2. An overview of the results is given in Table 19.

The ARG pressure histories for the pipebridge (P11 and P12) and for OSR-2 show two peaks. The first peak appears before the flame arrived at the sampling location and must therefore be due to a pressure wave. This pressure wave is initiated by the explosion in OSR-1. The second peak in the pressure histories inside the pipebridge and OSR-2 is due to the combustion in and near these locations.
The overpressures in OSR-1 are similar to the overpressures calculated previously considering OSR-1 only with IL-2 (65 kPa). The acceleration of the flame while propagating through OSR-1 causes a pressure wave which reduces from 60 to

33 kPa inside the pipebridge to 25 kPa inside OSR-2. Later the flame travels through the pipebridge and decelerates (overpressure from 70 kPa inside OSR-1 to 14 and 7 kPa closer to OSR-2). Inside OSR-2, the flame accelerates again to an overpressure of 11 kPa (near the 17 kPa in the case of an isolated OSR-2 with central ignition IL-5).

Table 19: ARG results for the combination of OSR-1,-2 and -5 with IL-2.

	$P_{0,max}$ (kPa)	$P_{0,average}$ per OSR (kPa)
P1	26	63
P2	94	
P3	80	
P4	31	
P5	70	
P6	76	
P11	60 - 14	
P12	33 - 7	
P7	26 - 7	25 - 11
P8	26 - 12	
P9	21 - 12	
P10	25 - 12	

Simulations have been performed with ignition locations IL-1, IL-5 and IL-6. The latter being in the centre of the pipebridge 1 at (x,y,z) = (99,37,5). Some divergence problems occurred during the simulations in these cases.
The results of the simulation before divergence showed however the same trend as the one ignited in IL-2: two separate explosions in OSR-1 and OSR-2, with a pressure wave preceding the combustion pressure wave in the acceptor-obstructed region. The overpressures being equal to the overpressures in the explosion of the isolated obstructed subregion.

9.5.3 Application of the correlation

Application of the correlation is restricted to a single explosion source. According to the ARG simulation, the combination of OSR-1, OSR-2 and OSR-5 consists of two separate blast sources. The overpressures in each blast source are almost independent of the ignition location.
Application of the correlation to the combined obstructed regions is therefore not expected to provide accurate answers for the overpressure inside the obstructed region.

9.6 6.6 Application of the correlation to a combination of obstructed subregions 1, 3, 6, 7, and 8

The assessment of the combination of obstructed regions 1,2 and 5 resulted in the conclusion that an explosion due to an ignition location in OSR-1 is not influenced by an explosion due to an ignition location in OSR-2. The next item to consider is then the influence of pipebridges 2, 3 and 4 (OSR-6, 7, and 8) and OSR-3 on the explosion potential of the LNG Terminal case. It may expected that the flame, after leaving OSR-1 where ignition is assumed, will decelerate in the open space in between OSR-1 and the surrounding pipebridges. Some acceleration of the flame when it enters the pipebridges may perhaps be expected.

9.6.1 Determination of parameters

The first step to determine the V_{or} of the combination of OSR-1, 3, 6, 7, and 8 according to the Yellow Book procedure is to define a box containing all obstacles in these OSRs. Such a box has dimensions: x from 1 to 97 m, y from 1 to 45 m and z from 3 to 11 m.

An intuitive subdivision into subboxes results in Figure 10a. The subboxes containing OSR-1 according to paragraph 5.3 is extended with subboxes containing the other OSR-1, assuming dimensions according to paragraph 5.1.

The Yellow Book procedure is a more strict procedure to subdivide this initial box into subboxes and to reduce the volume V_{or}.
The result of the first step to reduce the initial box into subboxes using the Yellow Book procedure is presented in Figure 10.b. According to the procedure, the height of the initial box can be lowered if the distance between obstacles is greater than 25 m. The height of the space in between these obstacles is then the height of the obstacle or subregion to which the flame propagates.
A further reduction in the height locally becomes questionable. The procedure is not very strict about the height of the space in between two volumes containing obstacles, and various values for the height appear to be possible.
In order to remain conservative, a next step to further reduce V_{or} will not be taken.

The following values were calculated for input in the correlation.

For the volume of the obstructed region according to the Yellow Book procedure:

- V_{or} = 17985 m^3;
- VBR = 0.027;
- D_{arm} = 0.35 m;
- D_{ham} = 0.24 m;
- D_{hym} = 0.48 m.

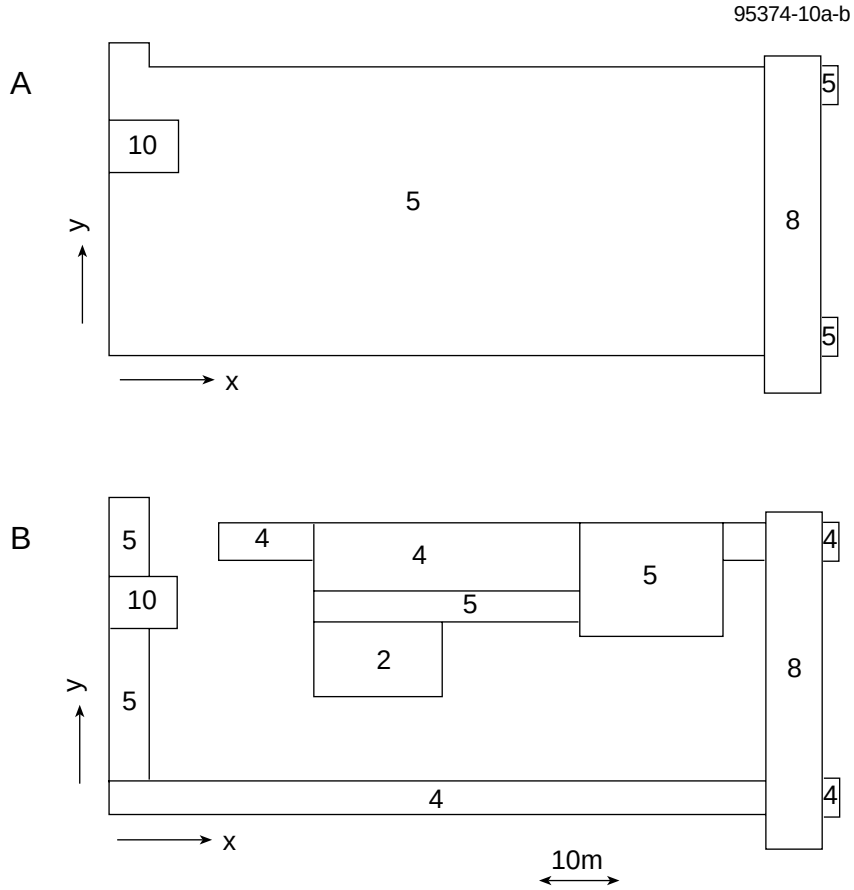

Figure 10: Subdivision into multiple subboxes; A: intuitive subdivision; B: subdivision according to Yellow Book procedure. The numbers indicate the local height in metres.

For the volume of the obstructed region determined intuitively:

- V_{or} = 9482 m^3;
- VBR = 0.048;
- D_{arm} = 0.33 m;
- D_{ham} = 0.23 m;
- D_{hym} = 0.47 m.

Although the pipe diameters and VBRs vary considerably for the various subboxes in both alternative approaches, the average pipe diameters as stated above do not. This indicates that the only difference between the two approaches concerns empty space only.
Also possible values for L_p are the same in both approaches, except the average value based on volume.

The following ignition locations will be considered:

- IL-3 at (x,y,z) = (55,29,5); the centre of the combined obstructed regions considered;
- IL-4 at (x,y,z) = (55,44,5); the centre of the long edge;

- IL-7 at (x,y,z) = (0,27,5); the centre of the short edge, which results in the following values for L_p:
- L_{p1} = 2 m, average distance to the top of the combined obstructed regions;
- L_{p2} = 20.5 m, half the width of the combined obstructed regions;
- L_{p3} = 41 m, the width;
- L_{p4} = 46 m, half the length;
- L_{p5} = 92 m, the length;
- $L_{p,aveYB}$ = 20.5 m, radius of hemisphere of volume 17985 m^3;
- $L_{p,aveIN}$ = 16.5 m, radius of hemisphere of volume 9482 m^3.

9.6.2 Correlation results

The combination of all possible values for the various parameters results in a range of overpressure predictions; these are collected in Table 20. The results for L_p = 2 m are not in the table. The overpressures for L_p = 2 m all appeared to be negligible (< 1 kPa).

Table 20: Overview of overpressure predictions using the correlation.

	P_0 (kPa)					
	VBR = 0.027			VBR = 0.048		
L_p (m)	D_{arm}= 0.35 m	D_{ham}= 0.24 m	D_{hym}= 0.48 m	D_{arm}= 0.33 m	D_{ham}= 0.23 m	D_{hym}= 0.47 m
20.5	19	39	9	90	189	44
41	125	262	60	607	1273	294
46	171	359	83	834	1747	404
92	1153	2416	558	5608	11756	2716
20.5	19	39	9	-	-	-
16.5	-	-	-	50	104	24

9.6.3 ARG calculations

AutoReaGas calculations were performed using an obstacle database equal to all obstacles present in the combination of OSR-1, -3, -6, -7 and -8. Calculations were performed using ignition locations IL-3, IL-4 and IL-7.

Overpressures were sampled at P1 to P6 (all in OSR-1) and at:

- P13 at (x,y,z) = (6,35,5); the centre of pipebridge 3 (OSR-7);
- P15 at (x,y,z) = (40,5,5); the centre of pipebridge 2 (OSR-6):
- P16 at (x,y,z) = (92,25,5); the centre of pipebridge 4 (OSR-8).

See Figure 10.a for ignition and pressure sample locations. Results are in Table 21.

Table 21: ARG maximum overpressures.

Location	P_0 (kPa) IL-3	IL-4	IL-7
P1	32	27	27
P2	7	8	15
P3	71	24	49
P4	29	24	17
P5	11	9	21
P6	52	35	40
P14	13	11	10
Average	31	20	26
P13	5	4	12
P15	7	4	22
P16	5	8	7
Average	5.6	5.3	13.7

Ignition in OSR-1 (IL-3 and IL-4) does not result in significant overpressures outside OSR-1. Overpressure is generated in the pipebridges only by ignition in IL-7. Presumably, this overpressure is due to the other direction of flame propagation, which is parallel to the pipebridge OSR-6 for IL-7 and perpendicular to the pipebridge OSR-6 for IL-3 and IL-4.

9.6.4 Evaluation

Application of the correlation to an obstructed volume like the combined one considered here shows that no insight is obtained into the overpressure distribution inside the obstructed volume itself.
A reasonable result is obtained when using the correlation with D_{hym}, $L_{p,ave}$ and the intuitive V_{or}. Applying the correlation with the Yellow Book V_{or} gives a reasonable result in combination with D_{ham}. This implies that the procedure in the Yellow Book to determine V_{or} might be too conservative in a sense that too much empty space is included.
In general, it appears that a smaller average diameter has to be chosen to get an acceptable overpressure prediction for lower VBRs.

9.7 6.7 Blast outside obstructed regions

The exercises performed in the previous paragraphs demonstrated the inapplicability of the correlations to predict the overpressure inside obstructed regions with a highly non-homogeneous obstacle distribution and/or with a large aspect ratio. In those situations it is complicated to decide on a choice for V_{or}, L_p and D.
Until now the attention has been focused on prediction of the source strength, which is described by overpressure P_0, and total combustion energy, the latter being determined by V_{or}.

The objective of the MEM is to predict the blast characteristics outside the vapour cloud and outside the obstructed region. It is therefore interesting to investigate the influence the various combinations of the parameters have on the blast characteristics in order to get insight into the required accuracy with which the parameters have to be applied.

The blast chart of the MEM is given in Figure 1. It shows that for source strengths higher than 6 (P_0 > 50 kPa) the blast overpressures at greater distances (r'>2) are independent of the source strength.
The source overpressure P_0 is uniform within the cloud (r' < r'_0). The blast overpressure equal to the source overpressure for r' is about $2r'_0$ (at about r'= 0.6), which is the radius of the fully expanded burnt hemispherical flammable cloud. For r' > $2r'_0$, the blast decays with distance according to acoustic law (a straight line in a log P - log r' scale):

For source strengths of class < 6, the blast overpressure decay P(r') can be approximated by two straight lines:

$$P(r') = P_0 \qquad \text{for } r' < 0.6 \qquad (8)$$

$$\log P(r') = \log P_0 - (\log r' - \log 0.6) \qquad \text{for } r' > 0.6 \qquad (9)$$

The overpressure P at a certain distance r depends on the choice of P_0 and r'.
For a scaled distance greater than twice r'_0:

- doubling P_0 results in doubling the overpressure P at a certain r' and in doubling r' with a certain overpressure P;
- doubling r' results in halving the overpressure P for a specific P_0.

The emphasis on the determination of the influence of changing the parameters of the correlation on the blast will be on the diameter D and on the volume of the obstructed region V_{or}.

9.7.1 Influence of changing the diameter D

It can be deduced easily using equation (2) that varying D according to:

$$D2 = \alpha D1 \qquad (10)$$

results in:

$$P_{0,2} = \alpha^{2.05} P_{0,1} \qquad (11)$$

Changing D does not influence V_{or}, so the scaled distances do not have to be changed.
Changing from D1 to D2 will increase the overpressure at a certain distance by a factor $\alpha^{-2.05}$, or change the actual distance for a certain P with the same factor.

For source overpressures larger than 50 kPa, changing D only influences the blast characteristics at scaled distances smaller than 2, for MEM class 6, and 1 for MEM class 7.

The exercises in the previous paragraphs on the determination of D often show a variation of 50% in diameter for D_{hym} and D_{ham} with respect to D_{arm}.
If D_{hym} in such a case is used instead of D_{arm}, the distances at which a certain overpressures occurs is reduced by 45%. Similarly, if D_{ham} is used instead of D_{arm}, that distance is increased by a factor 4. This factor of four will be much lower in most cases, as P_0 will increase for smaller D and will exceed easily the limit of 50 kPa. Nevertheless, the influence of varying D on distances can be strong, especially for smaller P_0.

9.7.2 Influence of changing V_{or}

The procedure adopted to determine V_{or} is the procedure from the Yellow Book (Annex A). While applying this procedure, the Volume Blockage Ratio VBR will increase while V_{or} decreases. Because the reduction procedure will not neglect obstacles, D will not change.
As the external dimensions of the obstructed region will change, L_p will change too. To investigate the influence of changing V_{or} correctly, it is assumed here that L_p is the radius of a hemisphere with volume V_{or}. Now $L_p = r_0$.

Varying V_{or} varies both P_0 and E (scaled distance).
It can be deducted that for:

$$V_{or,2} = \beta V_{or,1} \tag{11}$$

the MEM input parameters vary according to:

$$P_{0,2} = \beta^{-1.83} P_{0,1} \tag{12}$$

and

$$r'_2 = \beta^{-1/3} r'_1 \tag{13}$$

A reduction in V_{or} increases the pressure P at a certain distance r due to the increase in P_0, but reduces P due to the increase of r'.

Substituting (12) and (13) in (8) and (9) results in:

$$P_2 = \beta^{-1/3} P_1 \qquad \text{for } P_0 > 50 \text{ kPa (MEM class 6)} \tag{14}$$

and

$$P_2 = \beta^{-1.5} P_1 \qquad \text{for } P_0 < 50 \text{ kPa} \tag{15}$$

In order to get a feeling for the variation in blast overpressure induced by the factor β, the equations (14) and (15) will be applied to two examples.

According to paragraph 2.2, it is useful to apply the Yellow Book procedure for the determination of V_{or} until a further reduction of 10% is not possible.
A 10% reduction equals $\beta = 0.9$, which means that the error in the blast peak overpressure induced by the criterion for stopping the procedure will be 4 to 17% according to (14) and (15), respectively. These values are acceptable given the accuracy of the correlations.

The procedure to define the obstructed region (steps 1 to 4 of the procedure in Annex A) can be evaluated for the situation considered in paragraph 6.6, with the influence on the outside blast in mind.
According to the Yellow Book procedure, the combination of the obstructed subregions 1 ,3, 6, 7 and 8, should be regarded as a single large obstructed region. The open space in between OSR-1 and the pipebridge cannot be excluded. Therefore, the volume of the obstructed region is $V_{or} = 17985\ m^3$. According to an intuitive approach, the volume of the obstructed region results in $V_{or} = 9482\ m^3$.
The reduction from the Yellow Book volume to the intuitive volume by the factor $\beta = 0.53$ leads to an increase in peak blast overpressures by a factor of 2.6.

The conclusion is that the criteria in the Yellow Book procedure to include or exclude free space in the obstructed region should be more validated than they are at present, because a conservative estimate for the obstructed region may result in an unsafe prediction of the blast overpressures.

9.7.3 Large or small obstructed region

In the case of a flammable cloud covering the obstructed regions 1, 3, 6, 7 and 8 as in paragraph 6.6, the blast outside can be calculated using the MEM for various assumptions for the volumes of the obstructed region:

- case 1 assume that only OSR-1 generates blast;
- case 2 assume that the obstructed volume according to the Yellow Book procedure generates blast;
- case 3 assume that the intuitive obstructed volume generates blast
  a: using D_{arm} and b: using D_{hym}.

Table 22 shows the distances to the centres of the various obstructed regions for specific blast overpressures

Table 22: Distances for specific blast levels.

		Distance r (m)			
	blast:	25 kPa	10 kPa	5 kPa	1 kPa
case 1 (D_{arm})	V_{or} = 4005 m^3 D_{arm} = 0.32 m P_0 = 45 kPa	56	130	242	1036
case 2 (D_{arm})	V_{or} = 17985 m^3 D_{arm} = 0.35 m P_0 = 19 kPa	-	96	197	983
case 3a (D_{arm})	V_{or} = 9482 m^3 D_{arm} = 0.33 m P_0 = 50 kPa	90	191	352	1473
case 3b (D_{hym})	V_{or} = 9482 m^3 D_{hym} = 0.47 m P_0 = 24 kPa	-	98	192	930

It is interesting to note that the distances for cases 1, 2 and 3b do not differ much. For cases 2 and 3, the numerical average overpressure was about 20 kPa. It may be expected that the blast, when calculated numerically, also will not differ much from the blast according to the MEM.
The conclusion is that blast is only produced by OSR-1; the pipebridges do not contribute to the blast in this case.
Although the Yellow Book procedure results in a large volume V_{or} and consequently a low P_0, the blast at some distance is comparable with the blast calculated using other assumptions.

The conclusion is also that following a strict procedure, like the one in the Yellow Book, in this particular case with a complicated obstructed region, results in acceptable blast overpressures at long distances. The high source overpressures in the specific parts of the obstructed region, which are the actual explosion sources, will not be identified.

9.8 6.8 Overall evaluation of the LNG Terminal case

9.8.1 General

The LNG Terminal obstacle configuration consists of a number of large elongated obstructed regions, the pipebridges, which connect a single large volume with a congestion of obstacles with a couple of smaller congested volumes. The pipebridges enclose a considerable volume of space without obstacles.

As in the Chemical Plant case, the correlations were applied first to single obstructed subregions. A large band of predictions of the overpressures was obtained when using the correlation depending on the location of the ignition source and the definition of average obstacle diameter.

In general, the results from the correlations were lower than the numerical results when compared to the Chemical Plant case.
The correlation results when using the arithmetic obstacle diameter in combination with the radius of an equivalent hemisphere for L_p appear to be of the same order as the numerical results.

A larger diameter should be used in the correlation to get acceptable results in comparison with the Chemical Plant case. The reason for this is not completely clear. In comparison with the Chemical Plant case, the obstructed subregions 1 and 2 of the LNG Terminal case have a lower volume blockage ratio and a much lower height than in the Chemical Plant case.
Despite the low height of OSR-1, the overpressure according to the numerical calculation is much higher than according to the correlation using the height for Lp. This is probably due to the relatively large length of OSR-1. Apparently, the flame is capable of accelerating despite the venting through the top and the low VBR.

The low overpressure in OSR-2 according to the correlation is probably caused by the criteria of the Yellow Book to define the obstructed region. Using half the value of the obstructed volume according to the Yellow Book procedure and D_{arm} results in an acceptable overpressure in comparison with the numerical result.

The presence of various pipebridges complicates the application of the correlation. The numerical simulation shows that the overpressures inside the pipebridges are relatively low and the conclusion is that OSR-1 and OSR-2 should be considered as separate explosion sources of different strengths.

The application of the correlation to the combination of OSR-1 and OSR-3 together with three pipebridges, is problematic. The obstacle distribution inside the obstructed region varies considerably. The numerical calculation shows low as well as high overpressures depending on the location. This makes it difficult to deduce a single average maximum overpressure. The strict Yellow Book procedure results, however, in acceptable values for far field blast overpressures.

In the case of OSR-2, it is suspected that too much free space is included in the obstructed region using the Yellow Book procedure.
If this is indeed the case, then the blast overpressures outside the obstructed region may be underpredicted. A numerical calculation of the blast may provide the answer.

In order to determine blast outside the obstacle configuration, only the contributions from OSR-1 and OSR-2 should be taken into account. The pipebridges and the free space enclosed do not significantly contribute to blast. The two obstructed regions should be considered as separate explosion sources.

9.8.2 Comments on the covering of the white spots

1 *Missing correlations*
The case considered is clearly a 3D expansion situation. The available correlation 3D expansion is sufficient here.

2 *Criterion to distinguish between 2D and 3D correlation*
Not applicable in this case.

3 *Definition of obstructed region*
Contrary to the Chemical Plant case, the definition of the obstructed region is a problem in this case. The impression exists that the criteria in the procedure to define the obstructed region according to the Yellow Book include too much free space.
The approach adopted in the Yellow Book is a conservative one, as a high number for the source strength class should be adopted. In combination however with the application of the correlation to determine the source strength class, the procedure may lead to too low predictions for the outside blast.

4 *Multiple obstructed regions*
The numerical simulation shows that various blast waves are produced by different parts of the obstructed region if the whole obstacle configuration is situated within a flammable cloud. The pipebridges are not able to accelerate the flame.
The procedure in the Yellow Book is not able to distinguish multiple explosion sources within a single obstacle configuration. The procedure results in a large V_{or} with a low VBR with consequently a low P0. Because of the large E the blast in the far field will not differ much from the blast resulting from a smaller but more congested volume.

5 *Differently shaped obstacles*
The case contains many non-cylindrical obstacles. The procedure adopted to cope with non-cylindrical obstacles is to turn these into cylinders with a length equal to the longest dimension of the obstacle and an equal cross-section area. There is, at present, no indication of the physically correctness of that procedure. The procedure is very questionable, especially for flat plates.

6 *L_p in the case of an aspect ratio other than unity and ignition location outside the centre of configuration*
The height of the obstructed region (maximally 5 m) is very low compared to the other dimensions (40 to 100 m). Using the height for L_p in the correlation will not result in any overpressure. This is not correct, as the numerical results demonstrate.
Also, the model derived in Annex E to take the aspect ratio into account is incorrect, as the overpressure increases considerably after the flame has left the obstructed region through the top.

In some situations, edge ignition resulted in higher overpressures than central ignition, despite the fact that VBRs are lower than in the Chemical Plant case. Obviously the longer path the flame can travel while accelerating is responsible for the higher overpressures.
The flame accelerating and the influence of top and back venting in combination with the flame path length cannot yet be explained on the basis of simple and clear models. More research is required on this aspect, as it appears to be a very important issue in the determination of the source overpressure.

7 *Obstructed region larger than gas cloud*
This white spot will be an issue in many cases, due to the low height of the present case; it is not very important in this case.

8 *Single value for explosion overpressure*
The ARG simulations show the distribution of overpressure to be very non-homogeneous. A practical model like MEM requires a single value for the source overpressure. The use of an average maximum overpressure seems acceptable if one is interested in blast. However, if one is interested in blast characteristics ‘close’ to the source, or if one is interested in consequences inside the source, more sophisticated models should be used.

10 7 Application to the Gas Processing case

10.1 7.1 Description of case

The third case to be assessed in the project is an experiment conducted by British Gas plc in a test rig typical of onshore storage or gas processing sites. The information on the experiment and on the test rig was made available via the EU sponsored Explosion Modelling Evaluation (EME) project (EMEG, 1997).
The case was chosen because experimental data is available so there is no requirement to rely on numerical simulations to evaluate the applicability of the correlations.

The test rig comprises a mixture of pipework, vessels and support structure in a cuboidally shaped region. The congested region of the test rig had maximum dimensions of approximately 8.3 m length, 5.3 m width and 3.5 m height.
The digital file containing the Gas Processing case covers a volume of 207.5 m^3 enclosed by: x from 5 to 11.3 m, y from 0 to 8.9 m and z from 0 to 3.7 m. Figures 11.a, b, c and d show an overview and various cross-sections.
The obstacle configurations consist of three support structures closely located to each other. The first layer of obstacles above ground level consists of large cylindrical vessels (diameter about 0.8 m) with axes parallel to the x-axis. The higher layers consist of smaller pipes (about 0.1 to 0.3 m diameter) orientated parallel to the x- and y-axes. The vertically orientated obstacles consist mainly of the legs of the bearing structure.

10.2 7.2 Test performed

The experiment published was performed with propane as the fuel. The whole obstacle configuration was covered with a plastic sheet to retain the gaseous mixture inside the rig. The plastic sheet was not removed prior to ignition.
The concentration of the propane in air was 4.2%.
Ignition occurred in the centre of the rig at (x,y,z) = (8.35, 4.15, 0).
There were 16 pressure transducers mounted inside the obstacle configuration (T1 to T16) and 3 pressure transducers outside the configuration (T17, T18 and T19), the last 3 being mounted at a height of 1 m above ground level.
Figure 12 shows the location of the pressure transducers.
Figure 13 shows a typical pressure history obtained during the experiment (transducer T1).
The peak overpressures measured are gathered in Table 23. The average of the measured peak overpressures inside the obstacle configuration is 24 kPa.

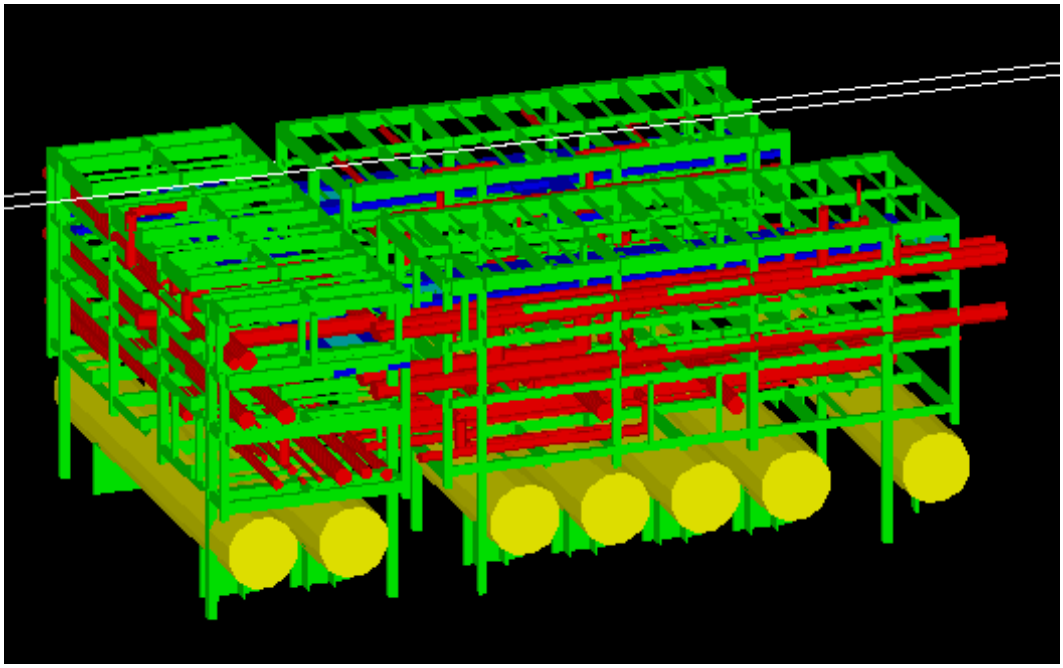

Figure 11.a: View of the Gas Processing case: overall view.

Figure 11.b: Views of the Gas Processing case: horizontal projection on xy-plane.

Figure 11.c: Views of the Gas Processing case: vertical projection on xz-plane.

Figure 11.d: Views of the Gas Processing case: vertical projection on xy-plane.

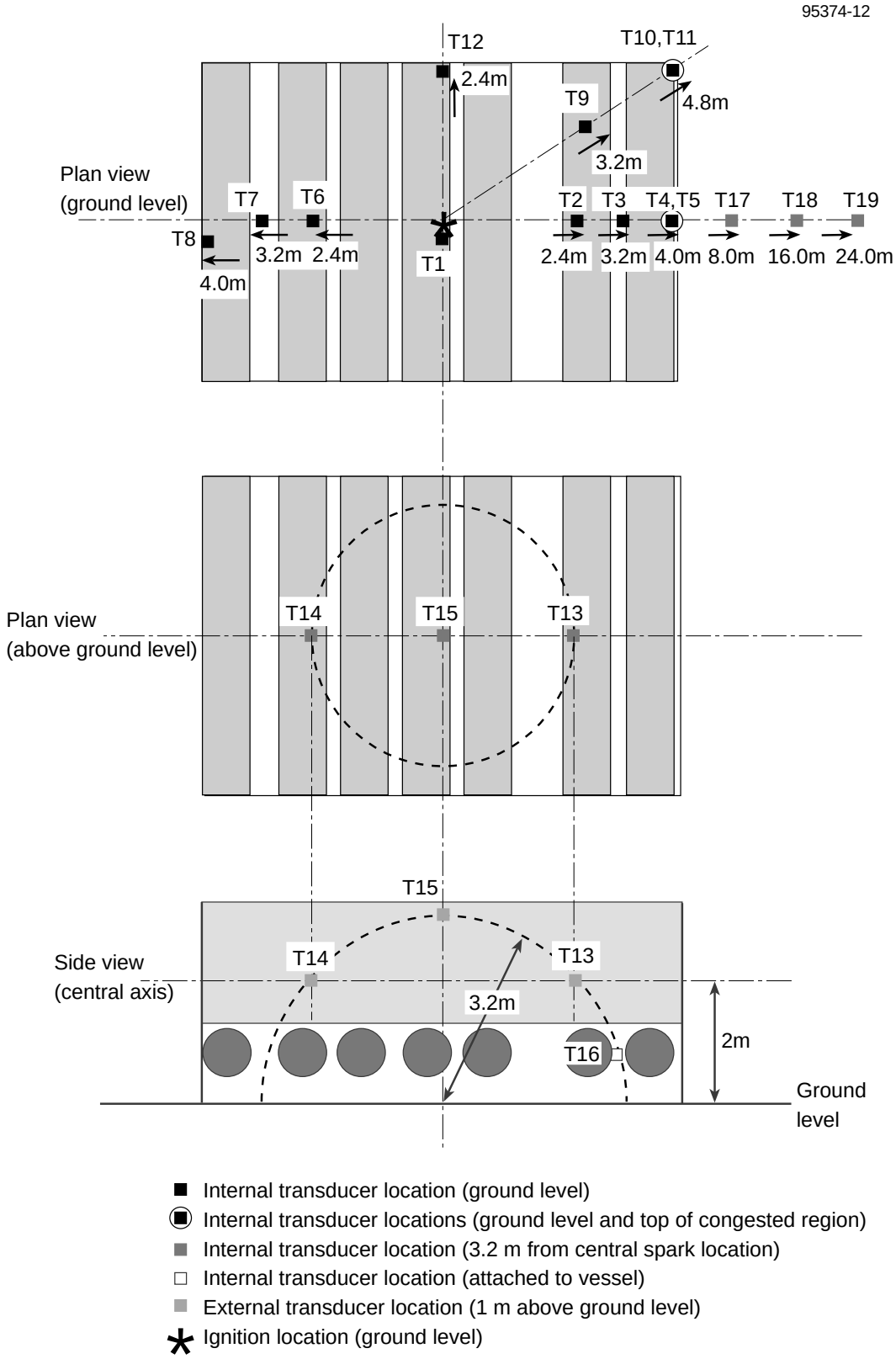

Figure 12: Location of pressure transducers (EMEG, 1997).

Figure 13: Example of pressure signal (EMEG, 1997).

Table 23: Measured overpressures.

A: Peak overpressures inside obstacle configuration

Transducer	T1	T2	T3	T4	T5	T6	T7	T8	T9	T10	T11	T12	T13	T14	T15	T16
overpressure (kPa)	24	24	27	36	30	23	23	22	23	36	14	19	21	20	20	25

B: Peak blast overpressures outside obstacle configuration

Transducer	T17	T18	T19
distance to ignition (m)	8	16	24
peak overpressure (kPa)	34	16	12

10.3 7.3 AutoReaGas calculation

As experimental results are available, this case offers an opportunity to check the validity of the AutoReaGas calculations. The calculations were performed for this

case in exactly the same way as they were calculated for the other cases: using a cell size of 1 m^3 and a C_t factor of 65.
Overpressures inside the obstructed region were calculated in 7 locations. The maximum values varied from 21.3 to 28.3 kPa. The average of the maximum values is 24 kPa, which is equal to the average of the maximum overpressure recordings during the tests. This remarkable result provides confidence in the AutoReaGas caculations which serve as the basis for the evaluation of the correlations.

10.4 7.4 Application of correlation to obstructed region

Although the obstacle configuration consists of three bearing structures, the free space in between them is small compared to the overall dimensions of each of the bearing structures. The obstacle configuration is therefore to be considered a single obstructed region.

The volume of the obstructed region can be determined easily from Figure 11:
- V_{or} = 154 m^3.

Application of equations 5, 6 and 7 to the obstructed region results in values for the various diameters:
- D_{arm} = 0.11 m;
- D_{ham} = 0.07 m;
- D_{hym} = 0.25 m.

The volume blockage ratio calculated is:
- VBR = 0.14.

The interesting values for L_p for central ignition are:
- L_{p1} = 2.65 m, half the width;
- L_{p2} = 3.5 m, the height;
- L_{p3} = 4.15 m, half the length;
- L_{p4} = 5.3 m, the width;
- L_{p5} = 8.3 m, the length;
- $L_{p,\ ave}$ = 4.2, the radius of a hemisphere with volume V_{or}.

For propane we take:
- S_L = 0.52.

Applying the correlation using the set of parameter values defined above results in a wide variety of overpressures (Table 24).

Table 24: Overpressures.

L_p (m)	P_0 (kPa) D_{arm} = 0.11 m	D_{ham} = 0.07 m	D_{hym} = 0.25 m
2.65	87	219	16
3.5	186	470	35
4.15	298	752	52
5.3	583	1275	108
8.3	2004	5062	372
4.2	308	778	57

10.5 7.5 Blast outside obstructed region

Blast outside the obstructed region can be calculated using the contributing energy and a value for the overpressure and applying Figure 1.

With a VBR of 14%, the combustion energy is:

E = (1-0.14) x 154 x 3.5 = 464 MJ

The blast overpressure is calculated at the same locations as the blast measurements (Table 23B) using a source overpressure P_0 of 57 kPa together with 100% and 50% of the energy. The 'efficiency' factor is applies because of the conclusion of GAME stating that less than 100% of the available energy contributes to the explosion for source overpressures of less than 1 bar. The factor of 50% is deduced from Figure 6 of the GAME report (Eggen, 1994).
Table 25 show the results.

Table 25: Blast predictions using MEM for P_0 = 57 kPa.

Distance to centre (m):	P_S (kPa) 8	16	24
E = 464 MJ	56	37	24
E = 232 MJ	51	29	18

10.6 7.6 Evaluation and conclusion

In comparison with the average peak overpressure measured during the test, the best predictions using the correlations are obtained by using D_{hym}. Using D_{arm} or D_{ham} results in high and unrealistic overpressures. The experimental average peak overpressure of 24 kPa is in between the predictions using D_{hym} and L_{p1} and L_{p2}. Using D_{hym} and $L_{p,ave}$ results in an overprediction by a factor of 2.5.

A similar result was obtained for the reduced problem within the Chemical Plant case in paragraph 5.3. There the overpressure was also in between the values predicted by using for L_p the two shortest distances to the edges of the obstructed region where the flame leaves the region. Venting will reduce further pressure generation inside the obstructed region (venting through the top was not possible in the Chemical Plant case of paragraph 5.3).

The outer dimensions of obstacle configuration in this case are within the range of dimensions of the configurations in MERGE used to derive the correlation. The same counts for the VBR. The difference is that different types, dimensions and orientations of obstacles are present. Because the obstacle configuration in MERGE is considered to produce high overpressures it could be expected that the predictions using the correlation for this case are high compared with the experimental result.

Taking the overpressure corresponding to the average flame path length and D_{hym} (57 kPa) results in an MEM class number of about 6.3, while the test gives a class of about 5.3.
Even when an efficiency factor of 50% is adopted, the blast overpressures are overpredicted.
It is expected that better predictions are possible if the influence of the aspect ratio can be taken into account.

11 8 Application to the Hydrogen case

11.1 8.1 Description of case

In order to investigate the influence of reactivity it was decided to investigate a case with hydrogen as the fuel.
Equation (2) shows that the reactivity from the fuel influences the overpressure through the laminar burning velocity S_L to the power of 2.7.
The laminar burning velocity of hydrogen is 3.5 m/s, which is a factor 7.8 higher than S_L for methane. As a result, the correlation predicts overpressures for hydrogen which are a factor $7.8^{2.7} = 254$ higher than for methane.
As very high overpressures are expected, the obstacle configuration to be considered for this case should be small and should have a low VBR to be realistic.

The obstacle configuration selected is the obstacle configuration of the obstructed subregion OSR-2 of the LNG Terminal case. Figures 9 a,b and c show vertical and horizontal projections of the configuration. Figure 14 shows a three-dimensional view.

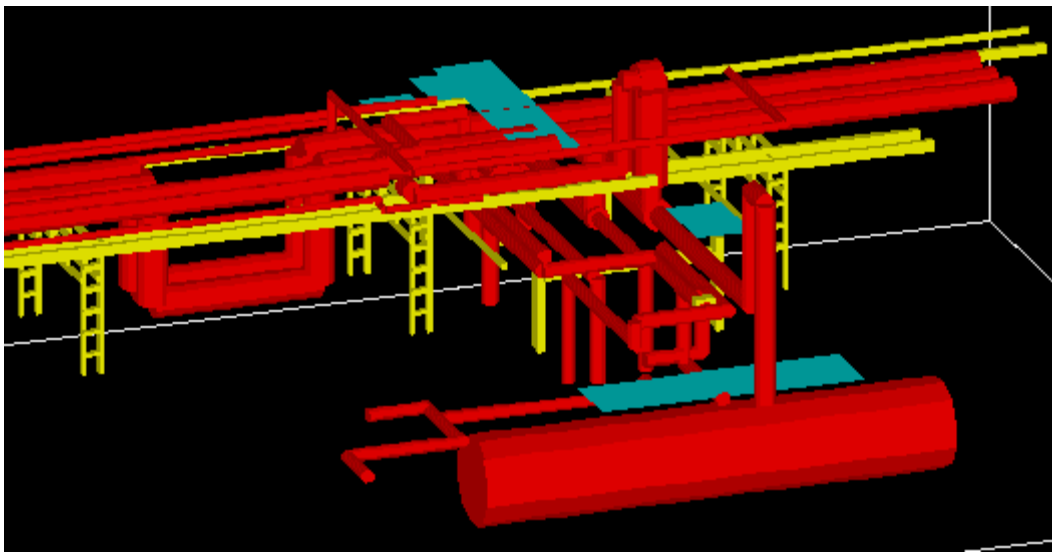

Figure 14: Three-dimensional view of the Hydrogen case.

11.2 8.2 Application of correlation and ARG simulations

The procedure for the application of the correlation is similar to paragraph 6.4.

The obstructed volume according to the Yellow Book procedure consists of three subboxes:

- subbox 1: x= 150 - 168, y = 27 - 36, z = 3 - 6, volume 486 m^3;
- subbox 2: x = 147 - 168, y = 36 - 45, z = 3 - 8, volume 945 m^3;
- subbox 3: x = 157 - 165, y = 45- 47, z = 3 - 8, volume 80 m^3;

with a total volume V_{or} = 1511 m^3.

Calculation of the various average diameters results in:
- D_{arm} = 0.31 m;
- D_{ham} = 0.21 m;
- D_{hym} = 0.46 m;

and:
- VBR = 0.04.

The following ignition locations were taken:
- IL-5 at (x,y,z) = (159,37,5), central ignition;
- IL-9 at (x,y,z) = (147,41,5), centre of edge.

The following values for L_p are of interest:
- $L_{p,1}$ = 2 m, average distance to top;
- $L_{p,2}$ = 10 m, average distance to all edges;
- $L_{p,ave}$ = 9.0 m, radius of hemisphere with volume V_{or}.

Application of the correlation (equation 2) results in the values in Table 26.

Table 26: Overpressures for OSR-2.

L_p (m)	P_0 (kPa) D_{arm} = 0.31 m	D_{ham} = 0.21 m	D_{hym} = 0.46 m
2	26	58	12
10	2196	4880	977
9	1644	3652	732

ARG calculations were performed using all obstacles enclosed within the space bounded by: x = 147 to 168 m, y = 27 to 47 m and z = 3 to 8 m and using IL-5 for the ignition location.

Initially, the ARG simulations were performed using a cell size of 1 m. The pressure peaks appeared to be of very short duration (less than 1 ms). Because of this very short duration, the peak values are cut off due to the rather large cell size. Therefore the calculations were repeated using a cell size of 0.5 m.

The maximum overpressures for locations P7, P8, P9, P10, P18, P19 and P20 (see Figure 9.a) calculated with a cell size of 0.5 m are given in Tables 27.a and 27.b, while the pressure histories are shown in Figures 15 and 16.

Table 27.a: ARG overpressures for various locations for IL-5.

Location	P7	P8	P9	P10	P18	P19	P20	Average
overpressure (kPa)	185	220	220	510	580	300	415	347

Table 27.b: ARG overpressures for various locations for IL-9.

Location	P7	P8	P9	P10	P18	P19	P20	Average
overpressure (kPa)	180	290	780	1340	100	500	630	546

Central ignition (IL-5) of the highly reactive mixture results in high overpressure in the centre of the obstructed region. The overpressure even increases while the flame propagates through the obstructed region while accelerating. A shock is already created inside the mixture and a detonation can be expected in the case of a longer flame path.

The acceleration until detonation is more clear in the case of edge ignition (IL-9). Overpressure near the ignition is about 100 kPa and the pressure sharply increases at locations farther away from the ignition location. The highest pressure is obtained in P10, which is in a direction parallel to the pipebridge. Outside the pipebridge where obstacle density is considerably lower, the overpressure increase is less (P20).

It is expected that the cell size is still too large to prevent the peaks from being cut-off. Pressures will increase when the cell size is reduced further.

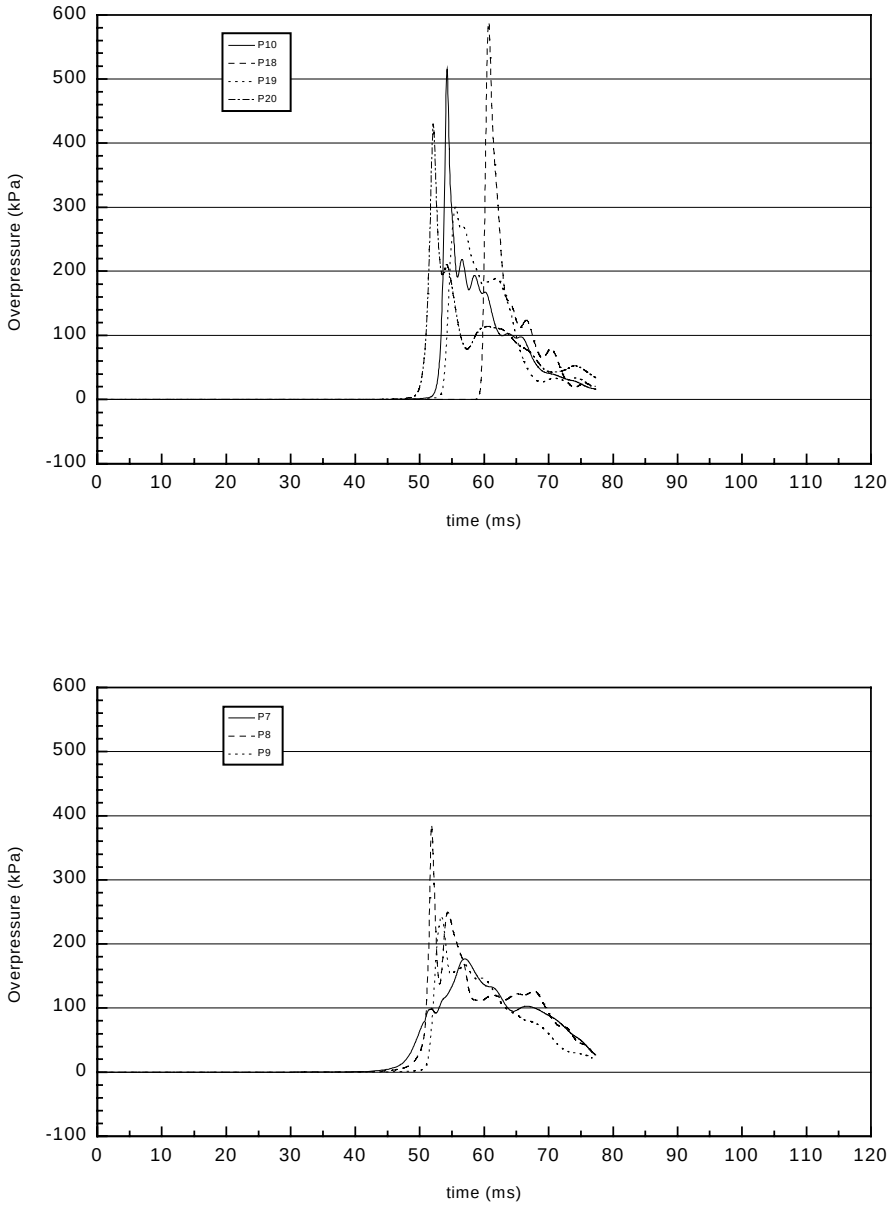

Figure 15: Pressure histories according to ARG for ignition location IL-5.

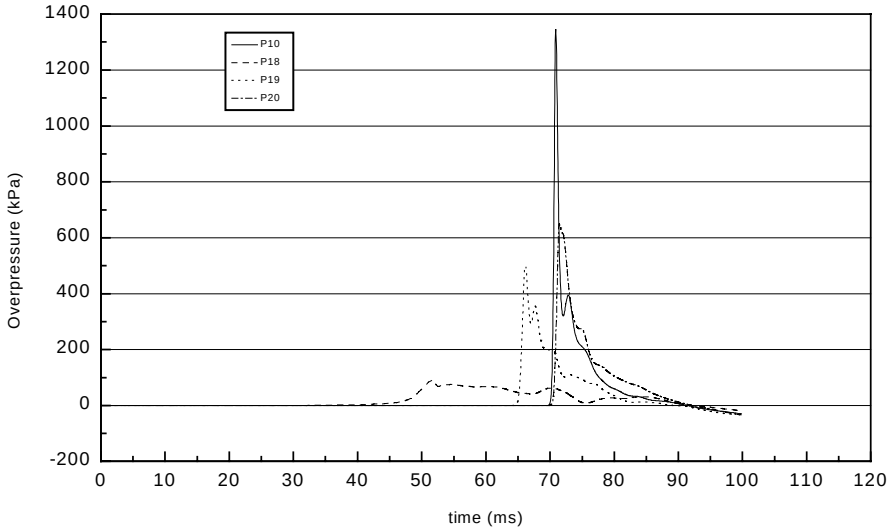

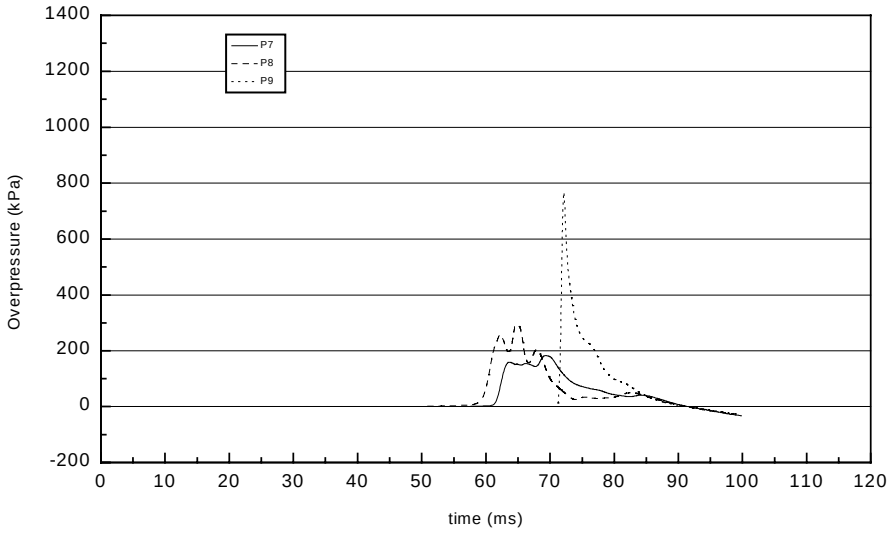

Figure 16: Pressure histories according to ARG for ignition location IL-9.

11.3 8.3 Evaluation and conclusion

The correlation predicts rather low overpressures when the shortest distance from the ignition location to the nearest boundary of the obstructed region is used (L_p = 2 m). For other flame path lengths and for D_{arm} and D_{ham}, extremely high overpressures are predicted. Their value is that in fact a detonation is predicted in those cases and that overpressures will be in the order of 20 bar.

The average values of the overpressures calculated by AutoReaGas have no real meaning here. The numerical calculations clearly demonstrate wave propagation inside the obstructed region rather than a homogeneous pressure rise.

The influence of the laminar burning velocity is evaluated best using D_{arm}, as this diameter gave the best results in the LNG Terminal case. The combination with the average flame path length of 9 m gives 16 bar, which is in line with what can be expected.
The influence of the laminar burning velocity in the correlation is based on the fractal scaling theory developed by Shell Research. The factor 2.7 is derived from measurements on flame structures using hydrocarbons like methane and propane. Nevertheless, the scaling appeared to work very well for acethylene also. Overpressures in the same obstacle configurations could be predicted for other fuel types with an accuracy of 10%, based on the experiments using methane (Mercx et al. 1994).

12 9 Overall evaluation and guidance obtained

12.1 9.1 General

The correlations derived in GAME are based on experiments with symmetrical obstacle configurations consisting of well-defined obstacles orientated in regular patterns. Ignition of the flammable mixture occurred in the centre of the obstacle configuration which implied an equal distance from the ignition location to all open edges.
As a consequence, the accuracy of an overpressure prediction according to the correlation for a realistic obstacle configuration depends on the extent to which the realistic configuration differs from the experimental one. The most important differences comprise:

- the ratios of the outer dimensions of the obstructed region (aspect ratio);
- the ignition location;
- the homogeneity of obstacle distribution within an obstructed region.

The influence of aspect ratio is demonstrated in the Chemical Plant case. Overpressures in sub-obstructed regions having a more or less cubical shape can be predicted much better than in sub-obstructed regions with an elongated shape. For instance, the large pipebridge present in the case. The distance from the ignition location to the centre of an edge is either very short or very long, which results in a large under- or overprediction of the numerically predicted peak overpressure.

The influence of aspect ratio and the ignition location are both related to the flame path length and the possibility of early venting. Overpressure may be vented through one or more of the boundaries of the obstructed region while the flame is still burning through parts of the obstructed region located farther away from the ignition location. Early venting (side-, top- or backventing) occurs in a direction opposite to the flame propagation direction.
In the case of edge ignition, venting starts immediately after ignition. In most cases simulated numerically, this early venting results in lower overpressures than for the situation in which the same obstacle configuration is ignited in the centre. An exception is the Sub Obstructed Region 1 in the LNG Terminal case. Here, edge ignition resulted in a higher overpressure than central ignition. The flame burns very slowly initially due to backventing, but after propagating a certain distance, the backventing is overruled by the acceleration due to obstacle-induced turbulence. Apparently, the remaining flame path length is long enough to accelerate the flame to a speed greater than the flame path length in the central ignition case is able to.

The MERGE experiments, underlying the correlation, have a highly regular pattern. The repeatibility of obstacles, the equal obstacle spacing and the small obstacle diameter was chosen intentionally to obtain high overpressures. As a consequence, the correlation is expected to provide safe and conservative values.
The exercises performed in the four cases have shown that the correlations easily overpredict the numerical results. As correlation overpressure decreases for increasing obstacle diameters, the best results were obtained by choosing a rather large value for the average obstacle diameter.
The exception again is the LNG Terminal case where, despite the low numerical overpressures, the arithmetic average diameter had to be used in order to obtain acceptable results. It is not clear why the LNG Terminal case provided answers different from the other cases. The obstacle configuration is different obviously: a large width and length in combination with a rather low height (length: 157 m, width: 57 m, height of cloud: 5 m), and a low volume blockage ratio.

The non-homogeneity of the obstacle configuration in the LNG Terminal case resulted in a non-homogeneous distribution of maximum overpressures inside the obstructed region considered. This is an effect which cannot be predicted by the correlation at all.

12.2 9.2 The correlation and parameters

12.2.1 Correlation

The expansion possibilities in the cases and subcases considered were all three-dimensional. The subcase of the Chemical Plant case in which obstacles located between two parallel floors were considered appeared to be of a three-dimensional expansion nature also. The length and width of that case were too small in relation to the height to obtain two-dimensional expansion during a large part of the combustion process.

12.2.2 Volume blockage ratio or volume of the obstructed region

In cases were the obstructed region is compact and has a more or less homogeneous obstacle distribution, the determination of its volume is not problematic. The volume can either be estimated or the procedure of the Yellow Book can be followed. The Chemical Plant and Gas Processing cases have shown that one may arrive at different values for the volume of the obstructed region V_{or} depending on how strictly the procedure is applied, but that the variations will not have an important influence on the overpressure. The variation in overpressures are within the accuracy of the correlation with respect to the underlying experimental results.
The determination becomes more problematic when obstacle-poor spaces are enclosed by the obstructed region, when the boundaries of the obstructed region are irregular and when the geometrical situation is close to the criteria given in the Yellow Book procedure.

The criteria in the Yellow Book procedure are probably too conservative, but there is a lack of knowledge to better quantify them. In combination with a high class number for MEM, the procedure will result in conservative predictions. In case the procedure is coupled with the correlation, the overpressure inside the obstructed region will be underpredicted, as the exercise with the LNG Terminal subcase in paragraph 6.4 has demonstrated (obstructed subregion 2). Also, the blast overpressures at great distances may be underpredicted as is demonstrated with the theoretical approach in paragraph 6.7.
Nevertheless, the Yellow Book procedure resulted in an acceptable average overpressure for the LNG Terminal subcase described in paragraph 6.6 (combination of obstructed subregions 1, 3, 6, 7 and 8) in combination with a smaller (arithmetic) value for the average diameter.

The Yellow Book procedure specifically fails for the obstructed subregion 2 of the LNG Terminal case probably due the relatively small outer dimensions of that subregion in combination with the low obstacle density.
The criteria in the Yellow Book procedure to build up the obstructed region should be probably coupled with the outer dimensions of the obstructed region already defined.

The numerical exercises for the LNG Terminal case and its subcases have demonstrated that the pipebridges do not contribute to the explosion overpressure. Obstructed subregions connected via pipebridges can be regarded as separate explosion sources. Obviously, the space in between obstructed regions does not have to be totally obstacle free in order to consider the regions separate explosion sources. Also in the Chemical Plant subcase of the isolated large pipebridge, no acceleration of the flame inside the pipebridge is observed.

12.2.3 Average obstacle diameter

The three definitions used to calculate an average diameter can result in a considerable variation in results. For all cases but the LNG Terminal one, the best results were obtained when using the hydraulic diameter. The hydraulic diameter results always in the largest value for the average diameter. The larger the diameter, the lower the correlation overpressure. A larger diameter is preferred in order to reduce the conservatism of the correlation.
Using a larger diameter in the LNG Terminal case results in an underprediction of the overpressure. There, the arithmetic average gives the best results. The large dimensions in combination with the low obstacle density (volume blockage ratio) may be responsible.

12.2.4 Flame path length

The exercises with the cases have shown that a wide range of values is possible for the flame path length. For elongated or flat obstructed regions, the distance from the ignition location to the shortest edge (the top included) results in very low

overpressures. Using the longest distance to an edge, on the other hand, results in far too high overpressures.
In order to deal with the problem of aspect ratios other than one, a simple model is presented in Annex E. There it is assumed that the pressure will not rise after the flame leaves the obstructed region through the nearest edge if the pressure at that instant is below a certain limit. The underlying physics is that the flame speed acceleration for pressures below that limit is too low to overtake pressure reduction due to venting.
Observed in the exercises is that the final average numerical overpressures are in between the predicted values using the correlation with values for the flame path length according to the distances of the ignition location to the two nearest edges (Chemical Plant subcase of paragraph 5.3) or the second and third nearest edge (Gas Processing case). Furthermore, it is not clear whether there is a single value for the overpressure limit. The exercises still show an increase in overpressure after the start of venting through one of the edges also at a low overpressure level.

The best results are obtained where an average value for L_p is used. The average value is the radius of a hemisphere with a volume equivalent to the volume of the obstructed region V_{or}. Acceptable results are obtained for aspect ratios smaller than about 5.
Central ignition is implicit when the radius of a hemisphere is adopted for L_p. The numerical results however show lower overpressures, in most cases, for edge ignition. Applying an average flame path length would cover all ignition locations in most cases.

12.2.5 Laminar burning velocity

The influence of the laminar burning velocity on the outcome of the correlation was investigated in the fourth case (Hydrogen case) only. The input value for the laminar burning velocity is not recognised as a problem. The MERGE experiments (Mercx et al, 1994) already demonstrated the validity of the concept of fractal scaling. This concept is adopted in the correlation.

12.3 9.3 Guidance and remaining white spots

The following statements, considerations and rules can be kept in mind while applying the correlations to a realistic situation.

12.3.1 9.3.1 General

12.3.2 Reminder

A general consideration to start with is that the correlation will provide the best results when the obstacle configuration of the realistic situation resembles, as closely as possible, the obstacle configuration used in the experiments underlying the correlation. These were configurations with cubical outer dimensions, single

size obstacles equally spaced, completely filled with flammable mixtures which were centrally ignited.

12.3.3 Comparison

The first thing to do is to compare the case under consideration with one of the cases and subcases assessed in this report

12.3.4 9.3.2 Choice of a correlation

White spot 1: missing correlations
White spot 2: lack of criterion to choose between correlations
There are only two correlations, which, in practice, will cover the majority of cases. The cases considered here generated no sound information to decide whether to choose the correlation for 2- or 3-dimensional expansion.

Guidance provided for choice between correlations
Take the dimensions of the obstructed region as: length L, width W and height H. If a confining plane is present for instance orientated in the directions of L and W, then it is advisable to choose the 2-dimensional correlation if:

- L > 5H;
- W > 5H;
- the dimensions of the confining plane are of about the same size as L and W.

12.3.5 9.3.3 Determination of volume of obstructed region

The procedure of the Yellow Book to determine the volume of an obstructed region consists of two parts:

- to build-up the obstructed region;
- to reduce the volume of a box containing all the obstacles of the obstructed region.

White spot 3: criteria for build-up of obstructed region
White spot 4: separation distances
The criteria to decide whether or not an obstacle belongs to an obstructed region are conservative. The procedure will lead to an obstructed region including probably too many obstacles.
The reduction of the volume by reducing the free space in an enclosing box uses the same criteria and the result will be a too large volume.
A too large volume results in too large blast overpressures in case a high explosion class number is adopted as recommended in the Yellow Book.
A too large volume implies a too low volume blockage ratio. In combination with the correlation, too low blast overpressures may be predicted. Reduction of the volume results in a reduction of the contributing energy but this is more than compensated for by the increase of the source overpressure.
The conservatism of the correlation is expected to cover this effect.

An as small as possible volume of the obstructed region is required to get conservative results when applying the correlation.
In order to be able to better calculate the obstructed volume better criteria should be derived. This is not possible within the present project.
The criteria of the procedure to build up the obstructed region are probably too coarse; they should probably be related to the size of the obstructed region.

The Yellow Book procedure will lead to a too large volume especially for small obstructed regions. The combination with a low obstacle density will result in very low overpressure as the subcase OSR-2 of the LNG Terminal case revealed (volume of 1000 m^3 and VBR of 4%).

The problem of multiple explosion blast sources in a single obstructed region or because of multiple obstructed regions still remains unsolved. The Yellow Book procedure for defining an obstructed region may lead to multiple regions, but validation for the criteria is lacking.
Some consideration to this subject has been given in Annex D of this report. The impression is that a separation distance should be in the order of the size of the obstructed region in which ignition occurs. Experimental validation or evidence for this concept is lacking.

Guidance provided for obstructed region
Apply the procedure of the Yellow Book for the definition of the obstructed region and its volume. Be cautious in cases of small volumes in combination with a low obstacle density as too low overpressures may be calculated (volume < 1000 m^3 and VBR < 5%). In those cases, study the OSR-2 LNG Terminal sub-case.

Guidance provided for multiple explosion blast sources
The application of the Yellow Book procedure for the definition of an obstructed region may lead to separated obstructed regions and thus to multiple explosion blast sources. The condition for that is an obstacle free space in between the regions. This will hardly ever be the case. In many industrial situations, units will be coupled via pipebridges or large diameter obstacles present in an obstructed region which will require a very large free distance to outside obstacles.
Sub-cases of the LNG Terminal and the Chemical Plant cases have shown though that the pipebridges present did not contribute to the explosion as long as the long edges of such a pipebridge are not situated along an obstructed region. A comparison of a situation at hand with the LNG Terminal and Chemical Plant case might provide some guidance to whether or not to include or exclude a specific pipebridge.

12.3.6 9.3.4 Determination of average obstacle diameter
Three ways of calculating an average diameter have been investigated: the arithmetic, harmonic and hydraulic means. For the arithmetic and harmonic mean, an

equivalent cylinder was calculated for non-cylindrical obstacles based on an equivalent cross-section area.

White spot 5: how to deal with non-cylindrical obstacles
As the correlation tends to overpredict source overpressures, the choice of a larger diameter appears to result in reasonable answers. In most cases the use of the hydraulic mean diameter resulted in acceptable answers. Only in the LNG Terminal case where the arithmetic mean provided the best answers did overpressures tend to be relatively higher than in the other cases. This effect must be attributed to the low volume blockage ratio and large outer dimensions of the obstructed region. Probably, the correlation is less conservative for these situations which can be counterbalanced by using a smaller diameter.

Provided guidance for the mean diameter
Use the hydraulic mean for obstructed regions similar to the Chemical Plant and Gas Processing case. Use the arithmetic mean diameter in case there is more similarity to the LNG Terminal case.

Provided guidance for non-cylindrical obstacles
It may be expected that non-cylindrical obstacles having a similar cross-section area as a cylindrical obstacle will have a larger effect on flame acceleration. Maybe, a drag factor should be included in the transition of a non-cylindrical to a cylindrical obstacle. This was not investigated in the present project.
The transition to cylindrical obstacles is not an issue when the hydraulic diameter is used.

12.3.7 9.3.5 Determination of flame path length

The determination of the flame path length turned out to be a complicated parameter. The correlation is in fact unable to cope with influences of: an aspect ratio other the one and an ignition location outside the centre of the obstructed region including edge ignition. The subject was discussed extensively in the previous paragraphs.

White spot 6: which Lp to choose in the case of non-point symmetrical situations
The proposed approach stated earlier in this report is that if there is a distance between ignition point and an edge for which the correlation predicts an overpressure of less than 30 kPa if this distance is taken as the flame path length, the overpressure will not increase anymore.
This approach does not hold for edge ignition. Also, the numerical simulations show different behaviour. On the other hand, the proposed approach seems attractive from a practical point of view. Clearly, more (experimental) investigation is required to come up with sound guidance.
At this moment it is not possible to incorporate the influence of non-symmetrical situations.

Provided guidance for the flame path length
The flame path length should be taken as the radius of a hemisphere having the volume of the obstructed region. An conservative value for the overpressure will be obtained in most situations.

White spot 7: influence of obstructed region larger than the vapour cloud
It can be argued that overpressure will increase as the cloud expansion occurs partially inside an obstructed region. The efficiency, that part of the combustion energy inside the obstructed region which contributes to blast, will increase.

Provided guidance for clouds smaller than the obstructed region
Do not take an efficiency smaller than one into account.

12.3.8 9.3.6 Other remaining deficiencies

White spot 8: a single value for the explosion overpressure
The AutoReaGas calculations showed that the overpressure distribution in obstructed regions having an irregular obstacle distribution in not homogeneous. The maximum overpressures are different for different locations inside the obstructed region.
The overpressure resulting from the correlation should be such that the maximum blast overpressures outside the obstructed regions are calculated as accurately as possible. This means that the correlation overpressure should not be equal to the peak maximum overpressure in the obstructed region if this peak is limited to a small part of the entire region.
Thus, the correlation overpressure should be merely an average of the maximum overpressures occurring inside the obstructed region.

12.4 9.4 Possible extensions of the blast charts

The Multi-Energy Method is a practical tool for determining the blast overpressures from vapour cloud explosions. The reality is simplified into a one-dimensional problem. The blast charts are for hemispherical clouds having an energy density of 3.5 MJ/m^3. The blast charts result from numerical calculations using a constant flame speed inside the cloud.
Other blast charts can be composed in order to differentiate more between the numerous situations which may be present in reality. Other blast charts may include:

- other energy densities;
- non-constant flame speeds: linear or exponential functions;
- obstructed regions with an aspect ratio other than one;
- arrival times to be able to superimpose blasts from various sources.

13 10 Conclusions and recommendations

The correlations to determine a single overpressure in an explosion blast source for application in the Multi-Energy Method were applied to four realistic situations in order to investigate the problems encountered.
The correlations consist of a relation between parameters describing the obstructed region containing a flammable vapour cloud and describing the fuel.
Results of numerical calculations using the CFD code AutoReaGas served as a reference for comparison with the results of the correlations; the numerical results for the realistic situation for which experimental results are available.

The emphasis in this project was on the parameters Volume Blockage Ratio and Average Obstacle Diameter. The results of numerical calculations were used as a reference for comparison with results from the correlations. Due to this approach, attention had to be given to the other parameters as well.

The Multi-Energy Method is a practical one-dimensional tool to determine blast from vapour cloud explosions. The correlations to determine the source strength were derived for homogeneous and symmetrical situations.
The more a realistic situation deviates from the homogeneous and symmetrical situation, the less accurate the predictions for the overpressures in the source and in the blast will be. The approach for application should therefore be a conservative and safe one.

The exercises performed showed that the procedure given in the new Yellow Book can be used for the determination of the volume of the obstructed region in order to arrive at the Volume Blockage Ratio. This procedure is the best there is at the present. It is not fully consistent but differences which may arise from that inconsistency will not lead to deviations outside the band of uncertainty of the correlations. Only for small and low obstacle density obstacles may the procedure lead to less safe answers.

The average obstacle diameter to use should not be chosen too small. It was found that in most cases, the hydraulic diameter of all obstacles together provided the best answers.

A safe upperbound in most situations and scenarios appears to be to use the hydraulic diameter in combination with a flame path length equal to the radius of a hemisphere with a volume equivalent to the volume of the obstructed region. This approach is fully in line with the concept of the Multi-Energy Method.

The ‘white spots’ encountered while applying the correlations in the four cases are all related to the deviations of the ideal simplified situation. They comprise:

- obstructed regions having different values for length, width and height;

- criteria for the definition of an obstructed region;
- criteria for multiple explosion sources;
- non-homogeneous obstacle distributions in size, location and orientation;
- non-central ignition locations.

All these items refer to the obstacle configuration. No problems were encountered in incorporating the influence of the fuel.

An approach is suggested in order to pass the white spots while applying the correlations.
For the white spots: ‘obstructed region with aspect ratios other than unity’ and ‘multiple explosion sources’, the suggested approach has a physical footing. However, experimental validation is lacking completely. Also, the results of the numerical exercises do support some of the physical phenomena occurring but seem to indicate that more complex criteria are requested. For instance, in the case of an aspect ratio other than unity, there does not seem to be a general overpressure threshold below which the flame will not accelerate after it has reached the nearest edge of the obstructed region.

For situations where more than a single explosion source may be expected, and for situations where the radius of an equivalent hemisphere appears to be an unacceptable approach, experimental data should be generated to develop and validate procedures for the application of the Multi-Energy Method and the correlations.

14 11 References

Berg, A.C. van den; The, H.G.; Mercx, W.P.M.; Hayhurst, C.J.; Clegg, R.A.; Robertson, N.J. and Birnbaum, N.K. (1995),
'Gas Explosion Hazard Analyses Using the CFD Code AutoReaGas',
Proceedings of the 6th Annual PETRO-SAFE Conference on Pipelines, Terminals and Storage, 31 January – 2 February 1995, Houston, Texas, USA.

Selby, C.A. and Burgan, B.A. (1998),
'Joint Industry Project on blast and fire engineering for topside structures phase 2',
Steel Construction Institute, SCI Publication number 253, Ascot, England, 1998.

CPR14E (1997) (Yellow Book),
Methods for he calcultion of physical effects due to releases of hazardous materials (liquids and gases),
Sdu Uitgevers, The Hague 1997.

Eggen, J.B.M.M. (1995),
'GAME: development of guidance for the application of the Multi-Energy Method',
TNO report PML 1995-C44, August 1995, Rijswijk.

EMEG (1997),
'Explosion Model Evaluation Group, Specifications of test cases for gas explosions - test case C1',
EME project, DGXII, Brussels, Belgium, 1997.

Mercx, W.P.M.; Johnson, D.M. and Puttock, J. (1994),
'Validation of scaling techniques for experimental vapour cloud explosion investigations',
AIChE Loss Prevention Symposium, Atlanta, Georgia, USA, 1994.

15 12 Acknowledgement

This project could only be accomplished due to the participation of the following companies and organisations:

- Air Liquide (F);
- BP International Ltd. (UK);
- Elf Atochem (F);
- ENEL SpA CRIS (I);
- Gaz de France (F);
- Health and Safety Executive (UK);
- ICI (UK);
- INERIS (Fr);
- Norsk Hydro (N);
- RIVM (NL);
- Snamprogetti SpA (I).

Their contribution to the discussions during the progress meetings are highly appreciated.

16 13 Authentication

W.P.M. Mercx
Project leader/Author

A.C. van den Berg
Author

D. van Leeuwen
Author

Dr. J. Weerheijm
Group leader

Annex A Procedure for the determination of the boundaries of the obstructed region according to the Yellow Book

Copy of paragraph 5.5.3 of CPR14E (1997)

16.1.1 5.5.3 Procedure for the division of an area into obstructed and unobstructed regions

A procedure to subdivide a region into obstructed and unobstructed parts is presented next.

The procedure given is thought to be a safe and conservative one in a sense that always a too large volume of the obstructed region will be selected. The procedure offers a possibility for optimisation, i.e. reduction, of the obstructed volume. This optimisation procedure can be followed but obviously requires more time. The optimisation procedure in itself will not lead to unsafe situations.

The procedure to build up an obstructed region is based on the effect obstacles have on the generation of turbulence in the expansion flow ahead of the flame. A zone with obstacle-induced turbulence will exist behind an obstacle. The length of this zone is related to a characteristic dimension of the obstacle. However, if the scale of an obstacle becomes larger it is assumed that the length of the influenced zone is bounded by an upper value.

The procedure is as follows.

- *Step 1: break-down structures into basic geometrical structural shapes*

Structures in a potentially hazardous area like an industrial site may be regarded as being composed of (or fairly good bounded by) basic geometrical shapes:
- cylinders with length l_c and diameter d_c;
- boxes with dimensions b_1, b_2, b_3;
- spheres with diameter d_s.

- *Step 2: assume an ignition location*

After ignition of a flammable cloud in a congested area the flame will travel outward, so the orientation with respect to the flame propagation direction of each obstacle is known.

- *Step 3: determine obstacle orientation*

Let the smallest dimension oriented in a plane perpendicular to the flame propagation direction be D_1 then:

$D_1 = l_c$ or d_c for cylinder
D_1 = smallest of b_1 and b_2, b_2 and b_3, or b_1 and b_3 for a box
$D_1 = d_s$ for a sphere

Let the obstacle dimension parallel to the flame propagation direction be D_2.

- *Step 4: build-up of obstructed region*

An obstacle belongs to an obstructed region if the distance from its centre to the centre of any obstacle in the obstructed region is smaller than 10 times D_1 or 1.5 times D_2 of the obstacle under consideration in the obstructed region (D_1 and D_2 belonging to any obstacle in the obstructed region).
If the distance between the outer boundary of the obstructed region and the outer boundary of the obstacle is larger than 25 m, then the obstacle does not belong to that obstructed region.

Note: there are values given to three factors. These are a factor times D_1 and a factor times D_2 (respectively 10 and 1.5) for obstacle distances and a value (25 m) for the distance between obstructed region and obstacle to determine if the obstacle is part of that obstructed region. It is not yet possible to quantify these values accurately. The values given are thought to be safe.

- *Step 5: defining a box containing the obstructed region*

The obstructed region is defined as a box that contains all the obstacles in the obstructed region:
including: the space between a confining surface and an obstructed region where the distance between that surface and any obstacle in the obstructed region is less than 10 times D_1 or 1.5 times D_2 (for instance, the earth's surface)
excluding: parts of cylinders or boxes that obviously do not belong to the obstructed region like upper parts of chimneys, distillation columns (vertically oriented cylinders) or pipes (horizontally oriented cylinders) connecting, for instance, chemical units, each potentially being an obstructed region, at a chemical plant. The excluded parts may form an obstructed region themselves.
The free volume of the obstructed region V_r is the volume of the box minus the space occupied by the obstacles. In case it is not possible to calculate or estimate the volume occupied by the obstacles, assume V_r equals the total volume of the box.

- *Step 6: subdivision into multiple boxes*

The box containing the obstructed region smooths the outer boundary of the actual obstacle boundaries, thereby including additional space free of obstacles. In case this free space is not included in the obstructed region by the procedure for building up the obstructed region but by drawing the box around the obstructed region, sub-division into multiple directly adjacent boxes is acceptable for reducing the volume of the obstructed region.

- *Step 7: define additional obstructed regions if appropriate*

If not all obstacles present are inside the obstructed region, perhaps more obstructed regions within the cloud can be defined.
In that case, the region where ignition occurs is called the ‘donor’ region; the other regions are ‘acceptor’ regions.
The direction of flame propagation, required for the orientation of the obstacles in the acceptor region, depends on the orientation of the acceptor region with respect to the donor region.

If separate obstructed regions are located close to one another, they may be initiated more or less at the same time: then coincidence of their blasts in the far-field may not be ruled out and the respective blasts should be superposed.
At the present, their is no guidance on the minimum separation distance between donor and acceptor regions at which they can be assumed to be separate explosions. Due to this lack, a great possibility of reducing the hazards of a vapour cloud explosion cannot be applied. The procedure for applying the Multi-Energy Method described in the next section contains a safe and conservative approach to cover this deficiency.

Remarks

Due to the choice of having a high initial blast strength for an obstructed region, the need to have a clear definition of an obstructed regions grows.
The exact boundaries of an obstructed region are, in fact, not so important for the determination of blast. According to the blast charts (Figure 5.8), the energy E has to be raised to the power of 1/3.
Nevertheless, a solid definition might be required.

The subdivision of a hazardous site into obstructed and unobstructed regions and the attribution of a source strength to each region is a major issue of ongoing research. As a simplified Multi-Energy Method is applied here, a simplified procedure for the subdivision into obstructed and unobstructed regions is adapted.

In order to obtain a rather straightforward, easy to apply and fully closed procedure, a number of obvious influences which lead to reduction of the explosion severity have been neglected. This indicates that further optimisation is possible, but this should be obtained through consultation with experts.

Annex B Procedure for the application of the Multi-Energy Method according to the Yellow Book

Copy of paragraph 5.5.4 of CPR14E (1997)

16.1.2 5.5.4 Procedure for the application of the Multi-Energy Method

The procedure of vapour cloud explosion blast modelling according to the Multi-Energy concept can be subdivided into a number of steps. Figure 5.9 shows these successive steps to be taken.

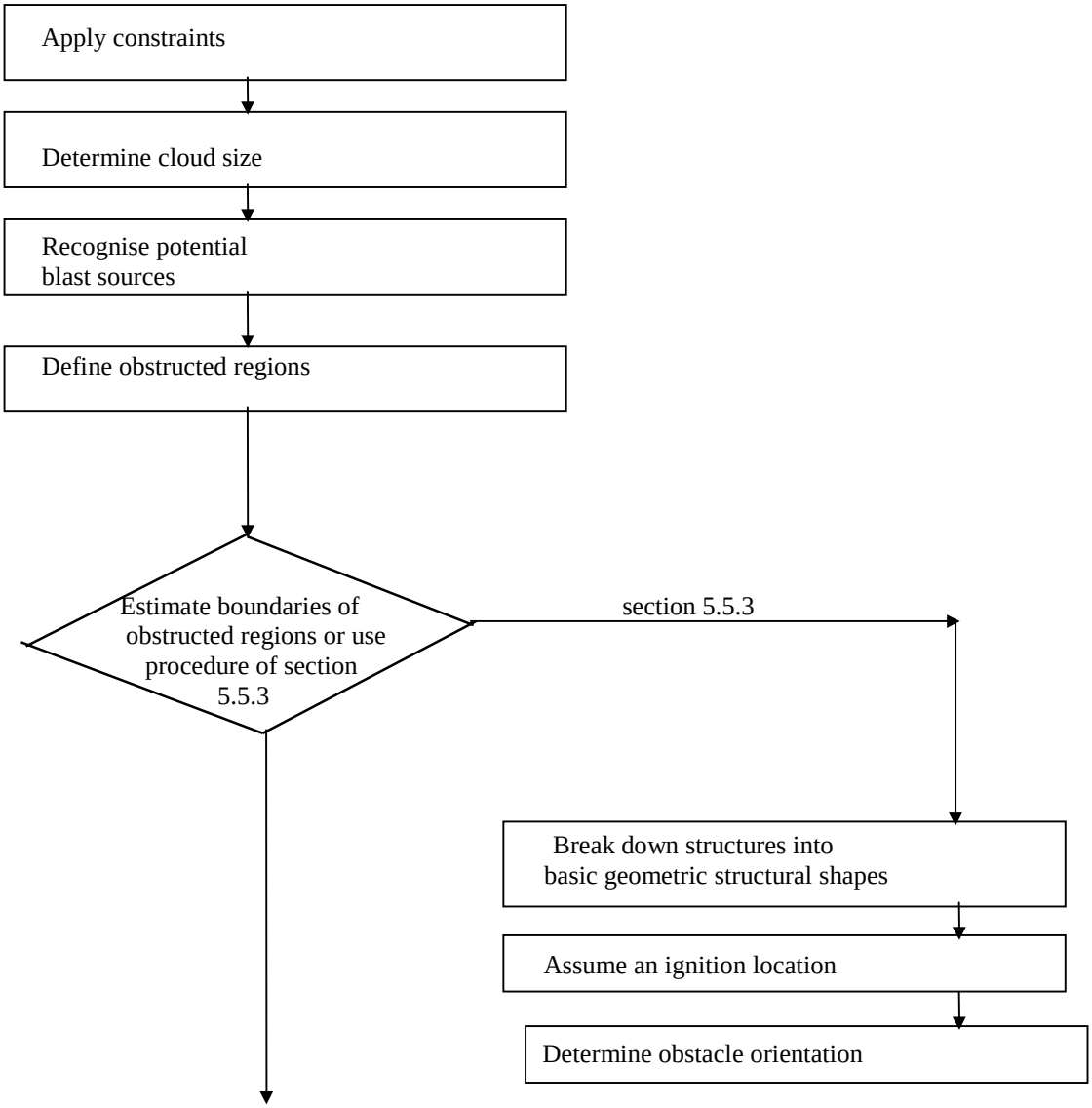

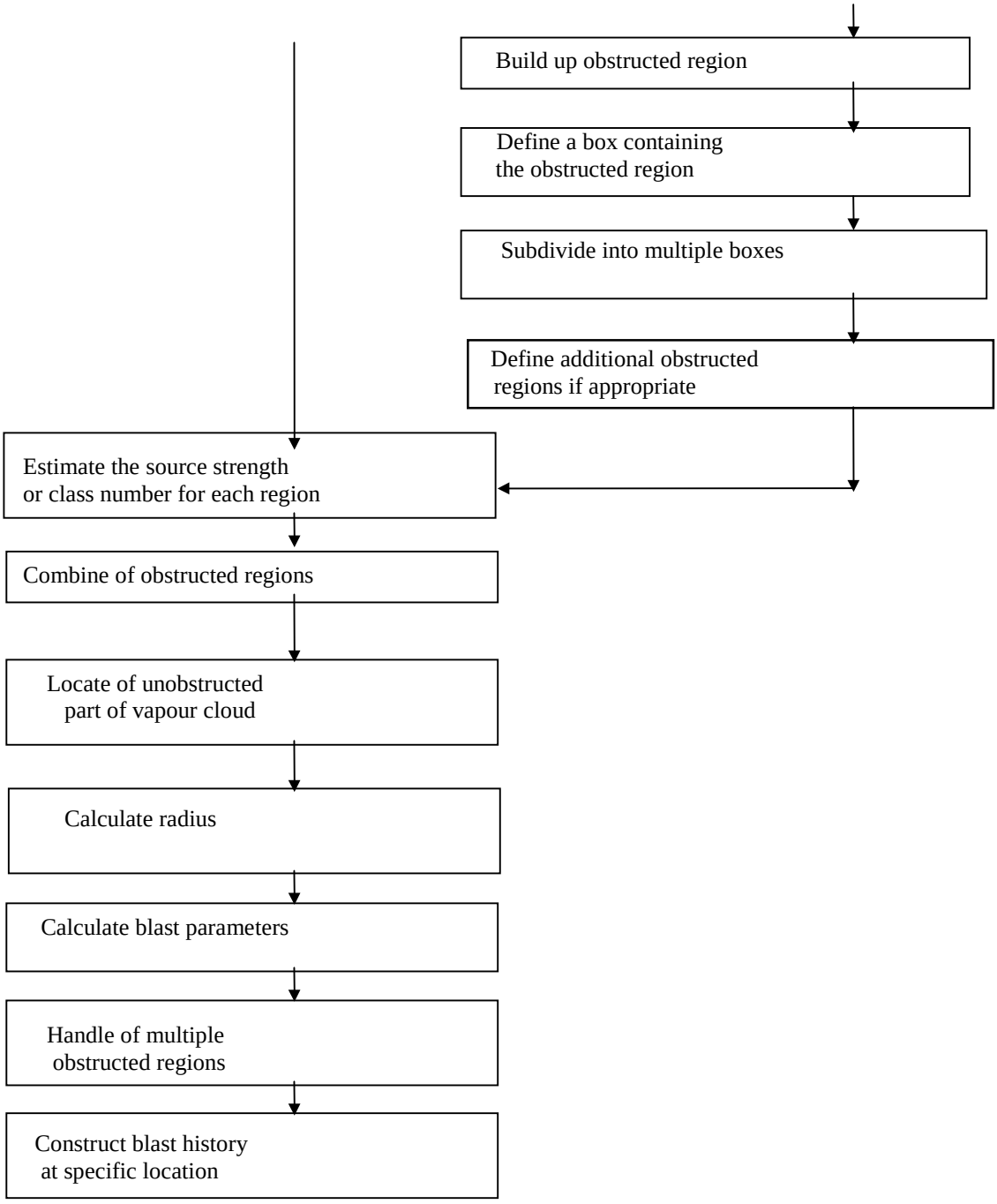

Figure 5.9: Flow diagram for application of the method.

- *Step 1: apply constraints*

- Realise that the Multi-Energy Method is to determine the blast parameters from 'unconfined' vapour cloud explosions. Blast from vented vapour cloud explosions and from internal explosions should be assessed by other methods.
- Realise that the Multi-Energy Method is a simplification of reality. It does not take into account directional blast effects due to the inhomogeneous distribution of confinement and obstruction of the vapour cloud or due to the non-point symmetrical shape of the vapour cloud. Use other, more sophisticated, models to assess these aspects.
- Assume that blast modelling on the basis of deflagrative combustion is a sufficiently safe and conservative approach. Keep in mind that unconfined vapour cloud detonation is extremely unlikely and has only one single precedent, to our present knowledge.

- *Step 2: determine of cloud size*

- Determine the mass quantity after an accidental release that can contribute to the formation of a flammable cloud.

In general, a dispersion calculation will preceed the explosion calculation. See section 5.7 on how to calculate the flammable mass quantity within a cloud.
If no dispersion calculation is made, the mass quantity has to be estimated. In a safe approach, one could assume that the whole mass inventory contained within the process unit under consideration contributes to the formation of a flammable cloud. In the case of pool evaporation, one could multiply the evaporation rate by a certain time period to come up with a mass quantity.

- Calculate the volume V_c of a cloud with a density ρ containing the flammable mass quantity Q_{ex} at stoichiometric concentration c_s (c_s in %) with:

$$V_c = 100 \cdot Q_{ex} \cdot \rho / c_s \qquad (m^3) \qquad (5.7)$$

- *Step 3: recognise of potential blast sources*

- Identify potential sources of blast in the vicinity of a postulated location of the centre of the cloud.

Potential sources of strong blast are, for example:
- extended spatial configuration of objects, e.g. process equipment at chemical plants or refineries, piles of crates;
- the space between extended parallel planes, e.g.:
  - underneath groups of closely parked cars in car parks or marshalling yards;
  - open buildings, e.g. multi-storey car parks;

- the space in tube-like structures, e.g.:
  - tunnels, bridges, corridors;
  - sewage systems, culverts;
- an intensely turbulent fuel-air mixture in a jet due to release at high pressure.

- *Step 4: define obstructed regions*

- Define obstructed regions with the procedure given in the previous section or estimate boundaries of obstructed regions and determine the free volume V_r of each obstructed region.

- Determine the maximum part of the cloud V_{gr} that can be inside the obstructed regions.

- Calculate the volume V_o of the unobstructed part of the vapour cloud with:

$$V_o = V_c - V_{gr} \qquad (m^3) \qquad (5.8)$$

- Calculate the energy E of each region, obstructed as well as unobstructed, by multiplying V_{gr} and V_o by the combustion energy per unit volume.

- *Step 5: estimate the source strength or class number for each region*

As explained before, a conservative approach is to choose a class number of 10 for each obstructed region. Other numbers may be chosen based on additionally obtained information if required. Choose a low initial blast strength for the remaining unobstructed regions: number 1. In case initial low turbulence motion is expected in unobstructed regions, for instance, due to the momentum of the fuel release, a number of 3 is advised.

- *Step 6: combine of obstructed regions*

In case more than one obstructed region has to be considered:
- define an additional blast source (obstructed region) by adding all the energies of the separate blast sources together and by assuming a centre for the additional blast source. This centre can be determined by considering the centres of the separate blast sources and their respective energies.

- *Step 7: locate unobstructed part of vapour cloud*

- Determine a centre for the unobstructed vapour cloud volume. This centre can be determined by considering the centres of the separate unobstructed regions and their respective energies.

Now a certain number of explosion centres and their respective energies E have been determined. For each centre, the blast parameters as a function of distance to its centre can be calculated with the blast charts given in Figure 5.8.

- *Step 8: calculate radius*

- Model the blast from each source by the blast from an equivalent hemispherical fuel-air charge of volume E/E_v m^3 (E_v = 3.5 MJ/m^3 is an average value for most hydrocarbons at stoichiometric concentration).
  Get an impression of the scale by calculating the radius r_o for each blast source from:

  $$r_o = (3/2 \cdot E/(E_v \cdot \pi))^{1/3} \quad \text{(m)} \quad (5.9)$$

- *Step 9: calculate blast parameters*

The blast parameters at a specific distance r from a blast source can be read from Figure 5.8 A, B and C after calculating the scaled distance r'.

- Calculate the scaled distance r' with:

  $$r' = r/(E/p_a)^{1/3} \quad \text{(-)} \quad (5.2)$$

- Depending on the class number 1, 3 or 10, read the scaled peak side-on overpressure P_s', the dynamic peak pressure p_{dyn}' and the scaled positive phase duration t_p' from the respective blast charts in Figure 5.8.

- Calculate the peak side-on overpressure P_s, the peak dynamic pressure p_{dyn} and the positive phase duration t_p with:

  $$P_s = P_s' \cdot p_a \quad \text{(Pa)} \quad (5.3)$$

  $$p_{dyn} = p_{dyn}' \cdot p_a \quad \text{(Pa)} \quad (5.5)$$

  $$t_p = t_p' \cdot (E/p_a)^{1/3}/a_a \quad \text{(s)} \quad (5.4)$$

- Determine the shape of the blast wave from the Figure 5.8.

- Calculate the positive impulse i_s by integrating the overpressure variation over the positive phase, which can be approximated by multiplying the side-on overpressure by the positive phase duration and by a factor of 1/2:

$$i_s = 1/2 \cdot P_s \cdot t_p \qquad \text{(Pa·s)} \qquad (5.6)$$

- *Step 10: handle multiple obstructed regions*

If separate blast sources are located close to one another, they may be initiated more or less at the same time. Therefore, coincidence of their blasts in the far-field may not be ruled out, and the respective blasts should be superposed This should be accomplished by taking the respective quantities of combustion energy of the sources in question together.
To determine the parameters in the blast wave at a specific distance, one should use the blast source as defined in step 6.

- *Step 11: construct the blast history at a specific location*

Combustion in the unobstructed region is considerably different to combustion in an obstructed region. Blast from an obstructed region will result in sharp and relatively short peaks (shock waves). The relatively slow combustion in an unobstructed region will result in pressure waves of long duration. Due to the influence of the respective energies however, either of the blast waves can be of importance at a specific location.

It may be assumed that the blast history at a specific location consists of the blast parameters and blast shape resulting from the obstructed region on which the blast parameters of the unobstructed region is superposed.

Annex C Application of procedure to determine obstructed region boundaries

Copy of paragraph 5.6.2 of CPR14E (1997)

16.1.3 5.6.2 Definition of an obstructed region

The boundaries of obstructed regions can be chosen by carefully considering the layout of a hazardous site. In case of doubt, or in case a more precise definition is required, the more time-consuming procedure of section 5.5.3 can be followed. That procedure will be followed here.

As an example of the build-up of obstructed regions on a hazardous site, an LPG storage and distribution centre is chosen. The picture in Figure 5.10 shows an overview. Figure 5.11 gives a map from which becomes clear that the LPG installation at San Juan Ixhuatepec near Mexico City was the basis for this example [Pietersen, 1984].

The facility comprises six spherical storage tanks; four with a volume of 1600 m^3 and two with a volume of 2400 m^3. An additional 48 horizontal cylindrical bullet tanks are situated near the large spheres.
The total storage capacity is about 16000 m^3.
The storage is subdivided into six zones, see Figure 5.12.
Horizontal distances are given in Figure 5.13.

Additional dimensions are:
- the minimum height underneath the bullet tanks is 2 m;
- the minimum height underneath the spheres is 2 m;
- additional pipework on top of cylinders and spheres has a height of 0.5 m;
- the storage area is surrounded by an open corridor of 30 m width;
- alongside the length of the outer cylinders, stairs with a width of 1.5 m are situated.

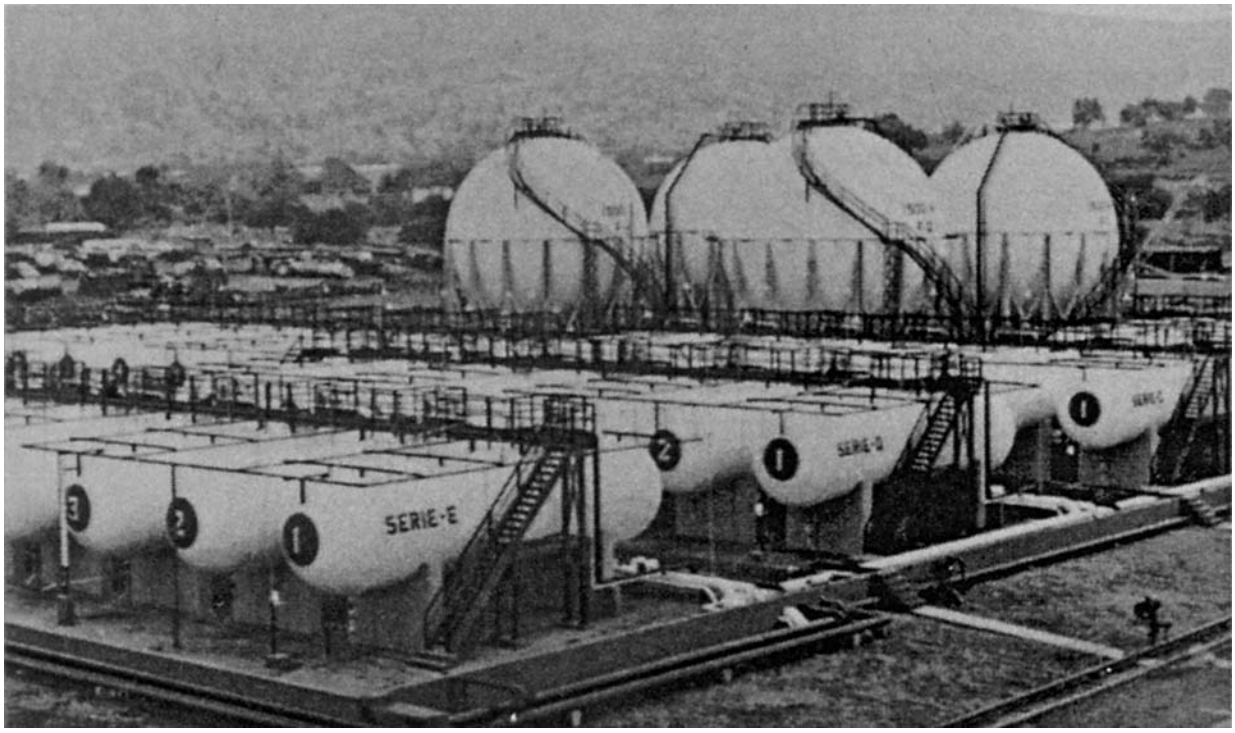

Figure 5.10: Picture of LPG storage facility.

At first glance, it will be clear that any of the groups of cylinders or spheres are an obstructed region.

- *Step 1: break-down of structures into basic geometrical structural shapes*

The structures consist of big spheres and cylinders. Other structures like stairs, walkways, supports and pipes will not be considered here. This is a valid approach: the dimensions of the large obstacles will dominate the process of building an obstructed region: 10 times D_1 of a big obstacle will override 10 times D_1 of a small obstacle located near the larger one (step 4). Figure 5.12 shows all major basic geometrical structural shapes.

- *Step 2: assume an ignition location*

Assume ignition in the centre of the southern group of cylinders in zone 4 (Figure 5.13).

The build-up of the obstructed region is started by taking the cylinder west of the ignition location as a start (marked as 1).

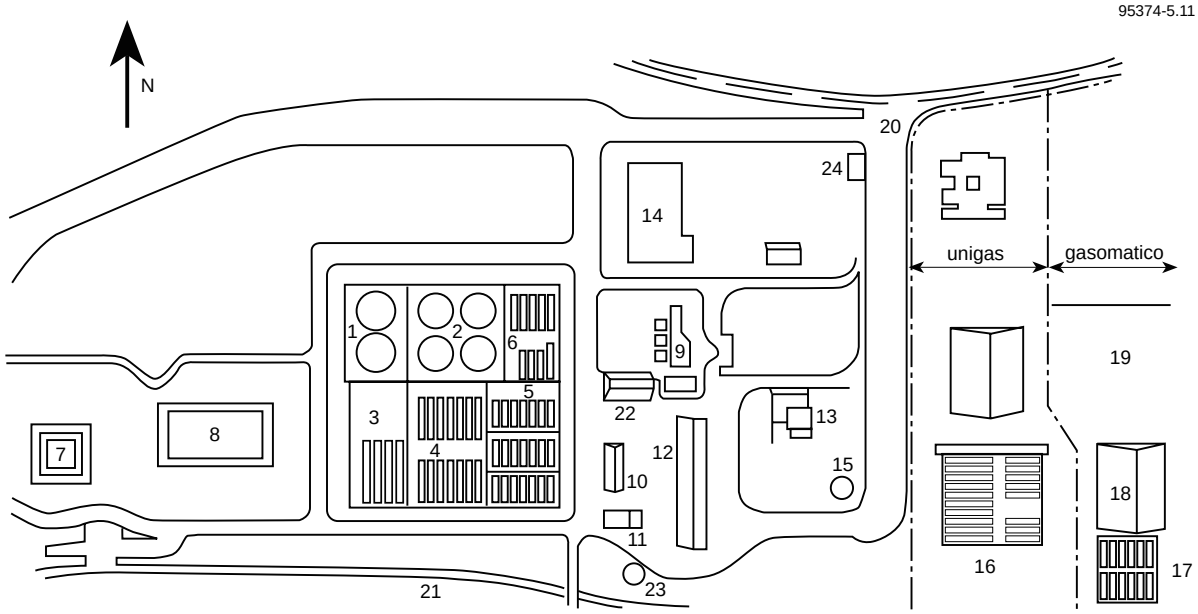

Legend:

1	2 spheres of 2400 m^3, ds = 16.5 m
2	4 spheres of 1600 m^3, ds = 14.5 m
3	4 cylinders of 270 m^3, dc = 3.5 m, length = 32 m
4	14 cylinders of 180 m^3, dc = 3.5 m, length = 21 m
5	21 cylinders of 36 m^3, dc = 2 m, length = 13 m
6	6 cylinders of 54 m^3, dc = 2 m, length = 19 m 3 cylinders of 45 m^3, dc = 2 m, length = 16 m
7	flare pit
8	pond
9	control room
10	pumphouse
11	fire pumps
12	car loading
13	gas boiler store
14	pipe/valve manifold
15	waterpower
16	LPG storage Unigas
17	Storage Gasomatico
18	battling Terminal
19	depot cars with bottles
20	entrance
21	rail car loading
22	store
23	watertank
24	garrison

Figure 5.11: Plan of LPG installation.

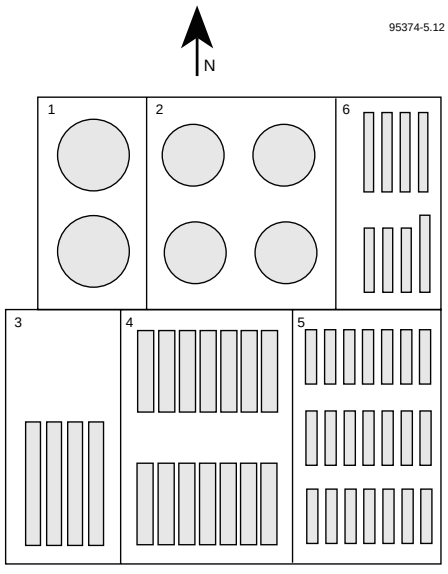

Figure 5.12: Division into zones.

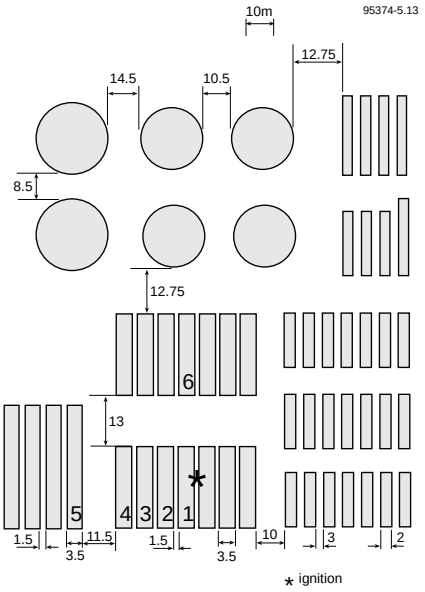

Figure 5.13: Build-up of obstructed region.

- *Step 3: determine obstacle orientation*

In order to decide if cylinder 2 is part of the obstructed region, values for D_1 and D_2 have to be determined. Following the direction of flame propagation from the ignition location via cylinder 1 towards cylinder 2, the orientation of the axis of cylinder 1 is perpendicular to the direction of flame propagation. Therefore, both D_1 and D_2 equal the diameter 3.5 m in this case.

- *Step 4: build-up of obstructed region*

The distance between cylinder 1 and the adjacent one, cylinder 2, is 1.5 m. This distance is shorter than 10 times D_1 and also shorter than 1.5 times D_2. Thus, cylinder 2 is part of the obstructed region.

The obstructed region is enlarged to include cylinders 1 and 2 now.

It is obvious that all seven cylinders of the southern group in zone 4 are within one obstructed region.

The distance between the east cylinder in zone 3 (number 5) and the west cylinder of the obstructed region (number 4) is 11.5 m. D_1 and D_2 both equal 3.5 m still. Thus, cylinder 5 belongs to the obstructed region too.
It is derived very easily that all four cylinders of zone 3 belong to the obstructed region also.

The distance between the northern and southern group of cylinders in zone 4 is 13 m. In this case, D_1 = 3.5 m and D_2 = 21 m. The distance of 13 m is shorter than 10 times D_1 and 1.5 times D_2. Thus, cylinder 6 and all other cylinders in that group are part of the obstructed region.

Repeating the procedure for the other cylinder groups as well as the spheres results in one obstructed region covering all cylinders and spheres.
Additional pipework and stairs located within a distance of D_1 or D_2 from a sphere or cylinder belongs to the obstructed region too.

- *Step 5: define box containing the obstructed region*

A box containing all obstacles in the obstructed region has dimensions of length 108.5 m, width 110 m and height 19.5 m (Figure 5.14; 19.5 m is the height of the highest cylinder including pipework on top).
The space underneath the obstacles is part of the obstructed region too; the distance of 2 m to a confining surface (the earth) is smaller than 10 times D_1 or 1.5 D_2 or all big obstacles.

A single big box in this case includes large volumes of free space, due to the large variation in height between cylinders and spheres. A sub-division in multiple directly adjacent boxes is therefore beneficial.

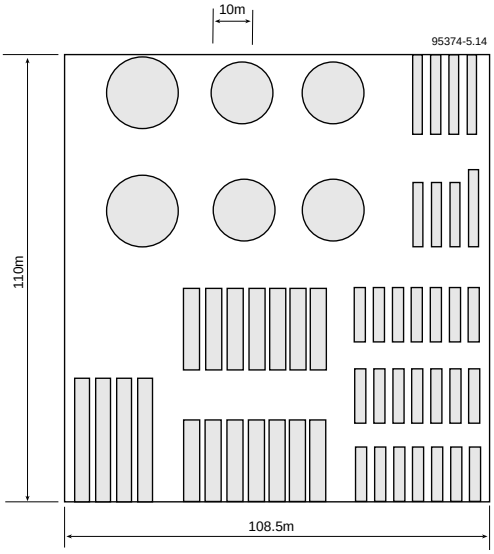

Figure 5.14: Single box.

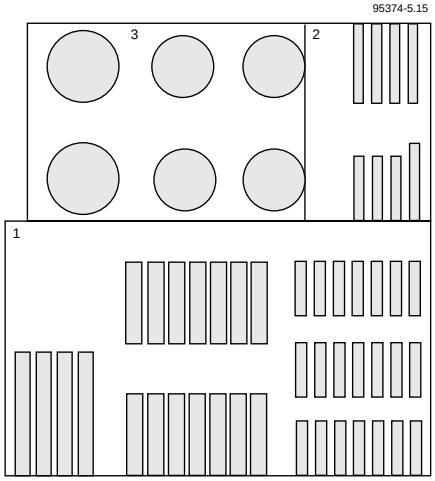

Figure 5.15: Three boxes.

- *Step 6: subdivision in multiple boxes*

A first subdivision into 3 boxes is shown in Figure 5.15.

Box 1 contains the cylinders in zones 3, 4 and 5;
dimensions: length 108.5 m, width 65 m and height 6 m.

Box 2 contains the cylinders in zone 6;
dimensions: length 45 m, width 31.25 m and height 4.5 m.

Box 3 contains all spheres in zone 1 and 2;
dimensions: length 65.5 m, width 45 m, height 19.5 m.

A second further subdivision is possible as the free space in box 1 north of zone 3 does not belong to the obstructed region. All other free space between groups of cylinders are part of the obstructed region and cannot therefore be excluded by further subdivision into multiple boxes.

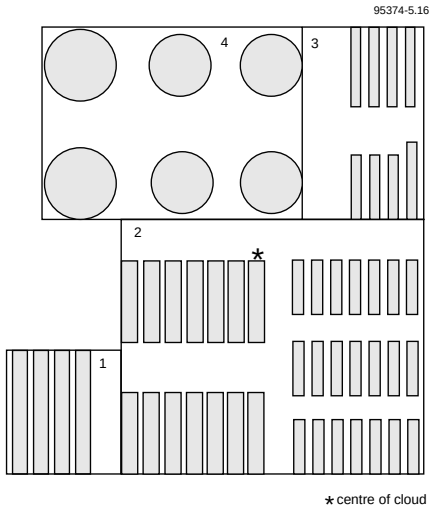

Figure 5.16: Four boxes.

We now have four boxes (Figure 5.16).

Box 1 contains the cylinders in zone 3 and the space between zones 3 and 4;
dimensions: length 32 m, width 31.5 m, height 6 m.

Box 2 contains the cylinders in zones 4 and 5 and the space between zones 4 and 2, and 5 and 6;
dimensions: length 77 m, width 65 m and height 6 m.

Box 3 contains the cylinders in zone 6;
dimensions length 45 m, width 31.25 m and height 4.5 m.

Box 4 contains all spheres in zone 1 and 2;
dimensions: length 65.5 m, width 45 m, height 19.5 m.

The volume of the obstructed region is the sum of the volumes of the four boxes minus the space occupied by the obstacles:

Box 1	32	· 31.5	·	6	=	6048 m^3
Box 2	77	· 65	·	6	=	30030 m^3
Box 3	45	· 31.25	·	4.5	=	6328 m^3
Box 4	65.5	· 45	·	19.5	=	57476 m^3
	Total volume				=	99882 m^3

The volume of the cloud inside the obstructed region is determined by deduction of the volume of the cylinders and spheres of the volume of the obstructed region.

The storage capacity is 16000 m^3, which is assumed to equal the volume of the storage vessels.

So: V_{gr} = 99882 - 16000 = 83882 m^3

Obviously further subdivision is possible and acceptable as long as the rules for subdivision are followed. One has to balance the benefit from further subdivision (which can be rather small) with the required time to perform the subdivision (which can be rather long) in order to decide to which level of detail subdivision is carried out.

- *Step 7: define additional obstructed regions if appropriate*

As all obstacles present are inside the one obstructed region defined, no additional obstructed regions are requested.

Annex D Critical separation distances between obstructed areas

16.2 D.1 Introduction

The Multi-Energy (ME) method is a simple method for vapour cloud explosion blast modelling. A vapour cloud's explosive potential is modelled by the specification of an equivalent explosive fuel-air charge whose blast characteristics can be read from blast charts.
The ME method recognises that in gas deflagration, turbulence generative boundary conditions are the predominant factor in the generation of overpressure and blast. The mechanism of a gas explosion implicates that, as soon as the appropriate turbulence generative boundary conditions are lacking, the burning speed and the pressure build-up in the process of flame propagation will slump. The direct consequence of the ME concept is that an extended vapour cloud containing several obstructed areas, separated by *open spaces of sufficient extent*, will produce the same number of separate blast waves on ignition. In the modelling process of blast effects, the individual obstructed areas should be considered separately.

The objective of this report is to develop some practical simple guidance for the quantification of the term '*open spaces of sufficient extent*'. In other words: how large should an open space be between two obstructed areas to be treated as separate sources of blast? Or, the other way around, how closely should obstructed areas be located to one another, to be treated as one single blast source? Some general notion of the critical separation distance can be developed by considering the phenomena and mechanisms that govern the gas dynamics in gas deflagration.

16.3 D.2 Mechanisms and phenomena

Pressure build-up in gas deflagration is a consequence of the expansion, a process of flame propagation is attended by. Under isobaric conditions, a stoichiometric hydrocarbon-air mixture expands up to approximately a factor 8 in volume on combustion. The consequence is that a combustion process induces a flow field in its environment. The propagating flame front is carried along in this flow. The flame propagation will behave dependently on the flow structure met by the flame. The flow structure (i.e. velocity gradients and turbulence) is largely determined by the boundary conditions of the flowfield, i.e. the solid boundaries and objects present in the space in which a gas explosion develops. Boundary conditions, therefore, play a predominant role in the development of overpressure in gas deflagration.

Turbulence generative boundary conditions trigger a feedback coupling in the interaction between the combustion and the expansion flow. The turbulence intensifies the combustion rate and thereby flame speed and expansion flow velocity. Higher flow velocities go hand in hand with higher turbulence intensities, which in turn intensify combustion again, etc., etc.. As long as the proper turbulence generative boundary conditions are present, the development of flame speed and overpressure is a self-amplifying process.

During the development of a deflagration, the maximum pressures and medium velocities are produced just in front of the combustion zone. As soon as the flame propagates out of an obstructed and/or partially confined area, the proper boundary conditions to maintain the feedback coupling are lacking and the burning speed slumps. The combustion wave and pressure/velocity wave decouple. The pressure/velocity wave is the blast wave which propagates out and decays in space.

The turbulent motion induced by the boundary conditions will be limited to the medium originally present within the obstructed, turbulence generative area. Therefore, the explosive combustion will not extend beyond the medium originally present within the obstructed area. This observation may lead to a very simple theoretical delimitation of the critical separation distance.

16.4 D.3 Theoretical considerations

The isobaric expansion ratio of stoichiometric hydrocarbon-air mixtures is equal to approximately 8. In other words, a stoichiometric hydrocarbon-air mixture expands up to a volume 8 times as large as its original volume upon combustion. The distance covered by this isobaric expansion is dependent on the degree of confinement by which the expansion is limited. Basically, three different degrees of confinement can be distinguished:

- **3D expansion**

A spherical charge will expand up to a sphere of $\sqrt[3]{8} = 2$ times the original charge radius upon combustion. In more generalised terms: a fully unconfined cloud expands up to a distance of twice its original linear dimensions.

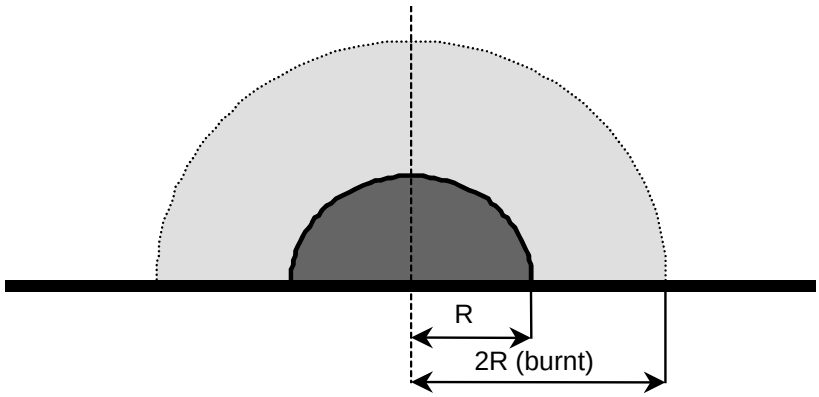

Figure D.1a: Unconfined charge expanding spherically.

- **2D expansion**

A cylindrical charge, confined by parallel planes, will expand up to $\sqrt{8} \approx 28$ times its original charge radius upon combustion.

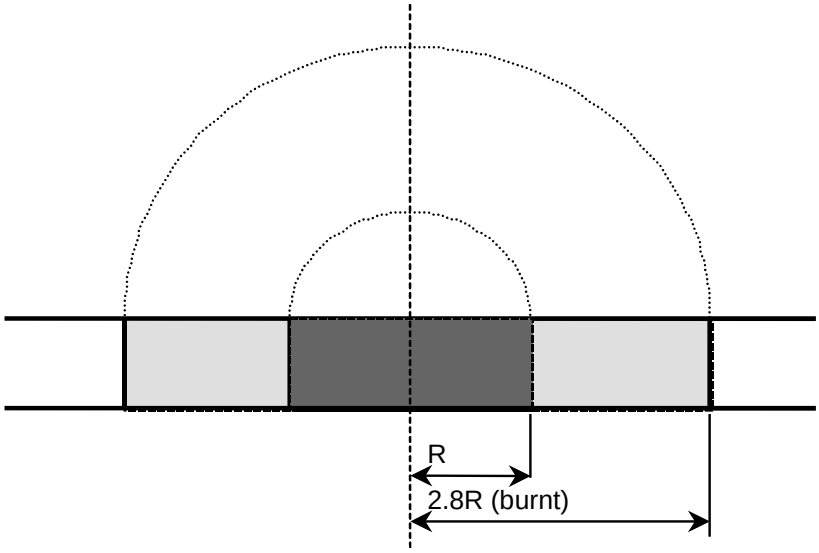

Figure D.1b: Charge confined between parallel planes, expanding radially.

- **1D expansion**

A charge confined by a tube or channel-like structure will expand up to 8 times its original linear charge size upon combustion.

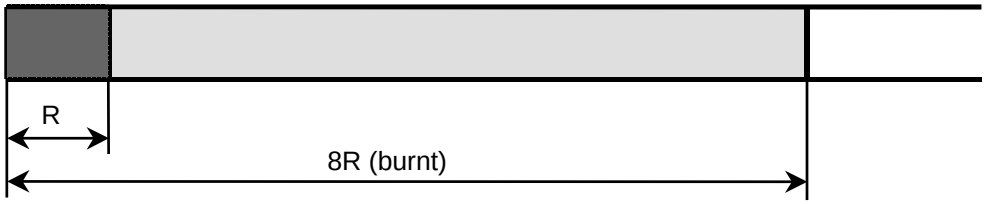

Figure D.1c: Charge confined by channel structure, expanding linearly.

Because of the assumed stoichiometry, these figures may be regarded as safe and conservative upper limits for the separation distance. However, for the 2D and 1D case, these figures may be substantially reduced.

If a space confined between parallel planes is completely filled with a flammable mixture, the expansion of the medium will partly take place outside the confinement where 3D expansion is possible. The flame jet will not only expand in a purely radial direction but upward as well. A mushroom-shaped flame jet is generally observed (Figure D.2a) which does not extend over the full 2.8 times the original charge radius.

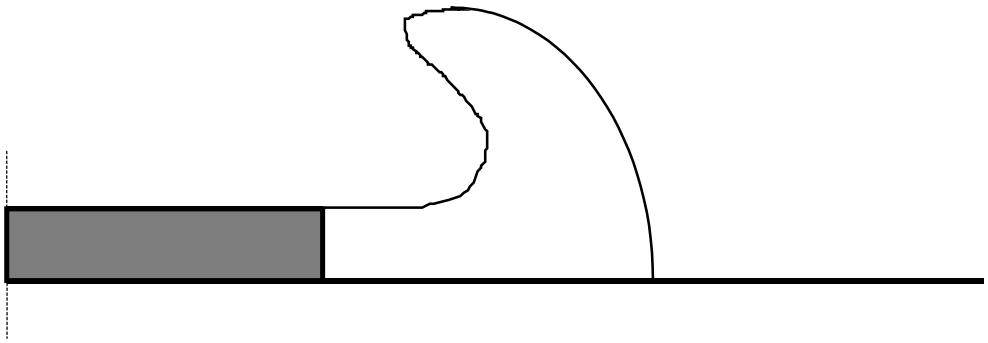

Figure D.2a: The mushroom-shaped flame jet produced by a charge confined between parallel planes.

Therefore, the recommended value for the separation distance for a flammable mixture confined between parallel planes may be reduced. Experimental data on the length of flame jets from this type of configuration are not available. For the time being, therefore, the recommended value for the separation distance is assumed equal to that for the 3D, unconfined charge, i.e. 2 times the linear dimension of the charge radius.

In the same way, the flame jet in the 1D case will possibly be substantially shorter than 8 times the linear dimension of the original charge as it expands from a channel into 3D space.
Fortunately, giving a concrete value for the 1D case is not relevant as most practical application of the ME concept is to chemical plants whose layout can be approximated by the 3D or 2D cases.

16.5 D.4 Experimental observations

Flame jet length
Experimental data on flame jet length are limited to dust or gas explosion venting. In such experiments the overpressure, induced by a gas explosion in a closed vessel, is relieved by venting through an orifice of a size which is generally substantially smaller than the cross-sectional dimension of the vessel.

Only few data on the flame jet length in vented explosions were found in papers by Wirkner-Bott (1992) and Bartknecht (1993). For vented *dust* explosions, Bartknecht (1993) poses a rough empirical relation which relates the flame jet length L_f to the vessel volume V.

$$L_f = 8.V^{0.3}$$

This expression also covers experimental data generated by Wirkner-Bott et al. (1992).

For vented *propane-air* explosions, Bartknecht (1993) poses the relation

$$L_f = 3.1V^{0.402}$$

The set-up venting experiments show some resemblance with the 1D case. They confirm the basic idea underlying the theoretical considerations that the flame jet length is approximately proportional to a linear dimension of the original cloud configuration.

Donor-acceptor experiments
At TNO Prins Maurits Laboratory, Van Wingerden (1988 and 1989) investigated a gas explosion developing in two subsequent obstructed areas separated by a free space, i.e. a separation distance. The obstructed areas consisted of a configuration of concrete cylinders confined between parallel planes.
The gap size between the two obstructed areas was varied. The results showed that as long as the separation distance was larger than the linear dimension of the donor array, the blast waves produced by the respective configurations were clearly separated. This result does not contradict the values for the separation distance, proposed above.

16.6 D.5 Generalisation

For application to realistic problems, i.e. the (petro-)chemical industries, the rules concerning the separation distance must be generalised. A plant can be regarded either as a spatial configuration of equipment (obstacles) or as a configuration of equipment confined between the floors of an open building. Such a configuration of obstacles definitely has not the idealised spherical or cylindrical shape the theoretical considerations were based on. Therefore, the rule for the critical separation distance is generalised.

The critical separation distance around a potential blast source area is equal to half its linear dimension in each direction. If the distance between potential sources is larger, the sources should be modelled as separate blasts. If not, they should be modelled as one single blast of summed energy content.

16.7 D.6 References

Bartknecht, W. (1993),
Explosionsschutz,
Springer Verlag,
Berlin, 1993.

Wirkner-Bott, I.; Schumann, S. and Stock, M. (1992),
Dust explosion venting: Investigation of the secondary explosion,
7th Int. Symp. on Loss Prev. and Safety Prom. in the Process Industries,
Taormina, Italy, 408 May, 1992.

Wel, P.G.J. van der (1993),
A review of blast phenomena during vented explosions,
TNO Prins Maurits Laboratory report no. PML 1993-C111.

Wingerden, C.J.M. van (1988),
Investigation into the blast produced by vapour cloud,
explosions in partially confined areas,
TNO Prins Maurits Laboratory report no. PML 1988-C195.

Wingerden, C.J.M. van (1989),
Experimental investigation into the strength of blast waves generated byvapour
cloud explosions in congested areas,
6th Int. Symp.'Loss Prevention and Safety Promotion in the ProcessIndustries',
Oslo, Norway, 1989, proceedings, pp. 26-1, 26-16.

Wingerden, C.J.M. van (1993),
Prediction of pressure and flame effects in the direct surroundings,
of installations protected by dust explosion venting,
J. Loss Prev. Process Ind.,Vol. 6, No.4, (1993), pp. 241-249.

Annex E Application of GAME correlation to obstacle configurations of high aspect ratio

16.8 E.1 Introduction

The aspect ratio of an obstacle configuration can be defined as its length/width or length/height ratio. All the experiments that, the GAME correlation was compiled from were performed in obstacle configurations of an aspect ratio approximately equal to 1. An obstacle configuration aspect ratio equal to 1 allows the flame front propagation process to develop more or less symmetrically. Over almost the entire flame path, the flame is allowed to maintain its approximately cylindrical or spherical (closed in itself) shape. Effects of *side or back relief* do not play a role.

Generally speaking, practical problems (plants in the chemical industries) are of quite different proportions. Often, practical plant equipment configurations are of a length/width ratio and/or a length/height ratio much higher than one. The aspect ratio of an obstacle configuration and/or the aspect ratio of the cloud in the obstacle configuration may largely influence the development of the flame propagation process and, therefore, may largely determine the ultimate explosion overpressure. A straight application of the GAME correlation to high aspect ratio obstacle configurations may result in a considerable overestimation of the explosion pressure. This report suggests a possible way to implement the aspect ratio of an obstacle configuration as an additional factor in the application of the GAME correlation.

16.9 E.2 Phenomena and experimental observations

The development of a deflagrative gas explosion is largely determined by the feedback coupling in the interaction of the combustion process with the structure of its self-generated expansion flow field ahead of the flame. The feedback is triggered by turbulence generative boundary conditions. The feedback coupling and consequently the self-amplification of the flame propagation process is optimum when a maximum medium velocity (and consequently a maximum turbulence intensity) is generated ahead of the flame as result of a minimum burning speed. In other words: when the ratio of medium velocity ahead of the flame and the flame front’s burning speed is maximum, the feedback coupling is optimum and the self-amplification capability of the process is maximum.
An optimum feedback coupling is obtained when the combustion products behind the flame front cannot expand freely backward. This is the case when the combustion products (the flame bubble) are fully enclosed either by the flame front itself and/or by rigid boundaries. Then, the expansion is fully utilised to generate flow ahead of the flame.

When a reactive mixture in an obstructed area is not ignited at the area's centre but at an edge, the flame propagation process finds the proper conditions to speed up only inside obstructed area. Then the combustion products behind the flame are not stagnant but expand partly freely backwards (back relief) without contributing fully to the medium velocity ahead of the flame. Then the expansion of the products is not fully utilised for the generation of flow in the reactants ahead of the flame front in the obstructed area. The feedback coupling is not optimum. Therefore, an edge-ignited obstructed area will develop more slowly than a centrally ignited area over the same distance of flame propagation.

Similar effects play a role in the development of a gas explosion in an obstacle configuration of aspect ratio higher than 1 (Figure E.1). The position of the flame front at three consecutive points in time has been indicated.

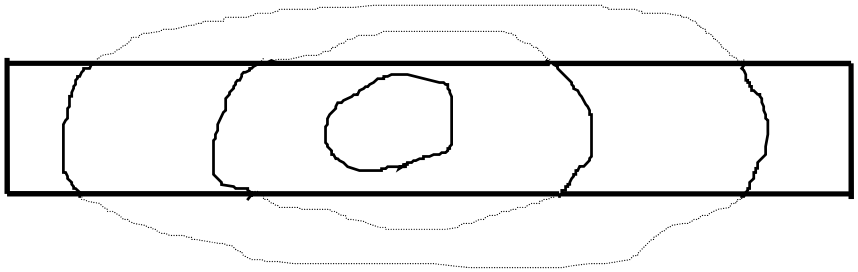

Figure E.1: Flame propagation in an obstacle configuration of an aspect ratio higher than 1.

The flammable mixture is ignited near the centre of the obstacle configuration. Initially, as long as the entire flame front propagates within the obstructed area, the flame bubble (closed in itself) develops more or less symmetrically because it finds similar boundary conditions all around. During this initial stage of flame propagation, the aspect ratio of the obstructed area does not play a significant role.
Then the flame propagates out of the obstructed area at the long sides into the open where the proper boundary conditions for pressure build-up are lacking. The consequence is that from that point on, the part of the flame front outside the obstructed area does not fully contribute to the generation of expansion flow ahead of the flame in the obstructed area and thereby does not contribute to the feedback any longer. The flame propagation inside the obstructed area is less supported by expansion from the back as a consequence of what is called *side relief*.

Almost all of the experimental data on gas explosions have been derived from experiments in obstacle configurations of aspect ratios approximately equal to 1. So far, only very limited data on gas explosion development in obstacle configurations of an aspect ratio substantially higher than one are available. Two sources of data were found: Van Wingerden (1988 and 1989) and Harris and Wickens (1989)

Van Wingerden (1988 and 1989) reports on a number of flame propagation experiments performed in a 4×4 m^2 rig consisting of a configuration of circular rows of

vertical 0.08 m diameter cylinders confined between parallel planes with a 0.16 m interspace. The cylinder configuration was characterised by a 50% area blockage in a row of cylinders and a pitch between the respective rows of 3 cylinder diameters. The obstacle configuration was filled with a stoichiometric ethylene-air mixture and ignited by a spark.

Ignition at the edge of the configuration showed a slower initial development than for central ignition. However, a higher ultimate flame speed and overpressure were obtained simply because the flame path length was twice as long and the number of obstacle rows passed by the flame was twice as high as in the case of central ignition.

Subsequently, the width of the obstacle configuration was varied from 4 to 2 and 1 m so that the configuration's aspect ratio varied from 1 to 2 and 4. The length of the rig (distance of flame propagation) was kept constant and equal to 4 m. The configurations were ignited in the centres of their short edges.
In aspect ratio 1 and 2 experiments, flame speed and overpressure quickly ran up to respective maximum values of over 600 m/s and 600 kPa within the 4 m propagation distance. Possibly the maximum flame speed was limited by choking flow conditions.
The aspect ratio 4 experiment, on the other hand, showed quite different behaviour, namely: a slow development which resulted in an ultimate flame speed of about 150 m/s and a maximum overpressure of approximately 30 kPa.

The key point in these experiments is the big difference in the flame speed and overpressure development between the aspect ratio 1 and 2 experiments on the one hand and the aspects ratio 4 experiment on the other. The experiments suggest that a certain width of configuration or a certain number of obstacles in lateral direction is required to develop a high level of flame speed and overpressure. If that width of configuration or that number of obstacles is present, the flame propagation process develops quickly and independently of side relief effects. If not, the flame propagation process develops slowly.

Harris and Wickens (1989) report on flame propagation experiments with natural gas, propane and cyclohexane-air mixtures in a very elongated $3 \times 3 \times 45 m^3$ fully unconfined rig whose cross-section was obstructed by vertical arrays of horizontal tubes. The tube arrays, characterised by an area blockage of 40%, were placed at a mutual distance of 1.5 m.
If the rig was ignited by a spark, a slow but gradual increase in flame speed over the full length of the rig was observed. If the rig was initiated with a flame jet at a flame speed higher than approximately 500 m/s, the high flame speed was more or less maintained. Initiation at lower flame speeds, on the other hand, resulted in a slump of the process down to much lower values, from which the slow and gradual speed-up started.

Generalisation
The experimental observations suggest some sort of a jump in behaviour. If the lateral dimension of the obstructed area is too small to develop some critical value of flame speed and overpressure before the flames reaches the lateral edge of the configuration, the development of the process will be largely governed by side relief and the ultimate explosion overpressure will be low. If, on the other hand, the lateral size is sufficient to exceed this critical value before the flame reaches the lateral edge of the configuration, the process will develop independently of side relief effects and the ultimate explosion overpressure will be high.

Modelling
Given a 3D obstructed area of dimensions: a length L, a width W and a height H. The area is characterised by an obstacle configuration of an average obstacle size D. The area is fully engulfed by a vapour cloud of a flammable mixture characterised by a laminar burning speed S_L.
The experimental observations suggest a way of implementation of the aspect ratio in the application of the GAME correlation which roughly reflects the behaviour observed experimentally. The procedure is as follows.

- Check the lateral dimensions of the obstructed area on pressure build-up capability. Apply the GAME correlation to the minimum dimension ½W or H. In other words: evaluate the parameter combination by taking the flame path length equal to the minimum of ½W or H.
- If the correlating overpressure is *below some critical value*, the ultimate explosion overpressure will be largely determined by side relief effects. The ultimate explosion overpressure is taken equal to the overpressure calculated on the basis of the minimum lateral dimension.
- If the correlating overpressure, on the other hand, *exceeds the critical value*, the ultimate explosion overpressure must be calculated on the basis of the real flame path length in the obstructed area.

For a choice of *the critical level of overpressure* the described experiments must be quantitatively interpreted. If the GAME correlation is applied to the above-mentioned experiments in which the aspect ratio of the obstacle configuration was varied from 1 to 2 and 4.

- VBR = 0.13;
- D = 0.08 m;
- S_L = 0.66 m/s;
- Sc = 0.08 m;
- the rig dimensions in the aspect ratio 2 experiments were $2 \times 4\ m^2$;
- ignited in the centre of the smallest dimension (2 m);
- a lateral flame path length of 1 m;
- the aspect ratio 4 experiment gives a flame path length of 0.5 m.

Evaluating the argument for the 2D correlating data:

$$ARG = LOG\left(\left[\frac{VBR \cdot L_p}{D}\right]^{2.25} \cdot S_L^{2.7} \cdot Sc^{0.7}\right)$$

- L_p = 1 m results in an overpressure of approximately 50 kPa (aspect ratio 2);
- L_p = 0.5 m results in an overpressure of approximately 10 kPa (aspect ratio 1).

The critical overpressure level must be somewhere between the two. Let's assume the critical overpressure level is in the middle, i.e. **P_{crit} = 30 kPa**. This value is simply extrapolated to hold for the 3D case as well. There is a lack of experimental data.

16.10 E.4 Demonstration

Application of the suggested procedure to the SNAMPROGETTI heat exchanger unit:

- VBR = 0.11;
- D = 0.6 m;
- S_L = 0.45 m/s;
- Sc = 0.6 m;
- L = 12 m, W = 10 m, H = 7.5 m;
- evaluate argument for the 3D correlating data with Lp equal to the minimum lateral dimension ½W or H, i.e.: Lp = 5 m:

$$ARG = LOG\left(\left[\frac{VBR \cdot L_p}{D}\right]^{2.75} \cdot S_L^{2.7} \cdot Sc^{0.7}\right)$$

- ARG = -1.2, which correlates with an explosion overpressure P_{exp} on the order of 5 kPa (MERGE-data);
- compare with critical overpressure P_{crit} = 30 kPa $\Rightarrow P_{exp} < P_{crit}$;
- conclusion: lateral pressure build-up capability of this obstacle configuration is not sufficient to develop the critical overpressure. Therefore, the ultimate explosion overpressure will be largely determined by side relief effects and will not be higher than 5 kPa.

A similar approach can be followed in cases where the flammable cloud is of limited thickness. If the cloud thickness H_{cl} is smaller than half the vertical proportion of the obstacle configuration H, twice the cloud thickness determines the lateral pressure build-up capability. So if $H_{cl} < 0.5H \Rightarrow L_p = 2H_{cl}$.
The basic assumption for this procedure is that under unconfined conditions, the flammable mixture expands up to twice its original linear dimensions on combustion.

The procedure proposed above is partly based on largely intuitive arguments and drastic simplification of the behaviour of gas explosion phenomena observed in just a very few experiments. In addition, a critical overpressure level had to be determined for which sufficient quantitative support is lacking. Therefore, the proposed procedure may be substantially adapted after the performance of a specific experimental programme.

16.11 E.5 Guidance application GAME correlation

Before the guidance can become fully concrete, in a way that two users in the same problem come up with similar answers, the data points in the correlation graphs must be brought back to a single line, a best fit, or the most realistic fit realising that the MERGE data probably constitute an upper bound: if agreement can be achieved, in relation of the best realistic correlation.

16.12 E.6 References

Wingerden, C.J.M. van (1988),
Investigation into the blast produced by vapour cloud,
explosions in partially confined areas,
TNO Prins Maurits Laboratory report no. PML 1988-C195.

Wingerden, C.J.M. van (1989),
Experimental investigation into the strength of blast waves generated byvapour cloud explosions in congested areas,
6th Int. Symp.'Loss Prevention and Safety Promotion in the ProcessIndustries',
Oslo, Norway, 1989, proceedings, pp. 26-1, 26-16,

Harris, R.J. and Wickens, M.J. (1989),
Understanding vapour cloud explosions - an experimental study,
55th Autumn Meeting of the Institution of Gas Engineers,
Kensington, UK, 1989.

Annex F AutoReaGas pressure histories for the various situations simulated with the Chemical Plant case

GAMES Chemical Plant: scenario NH01

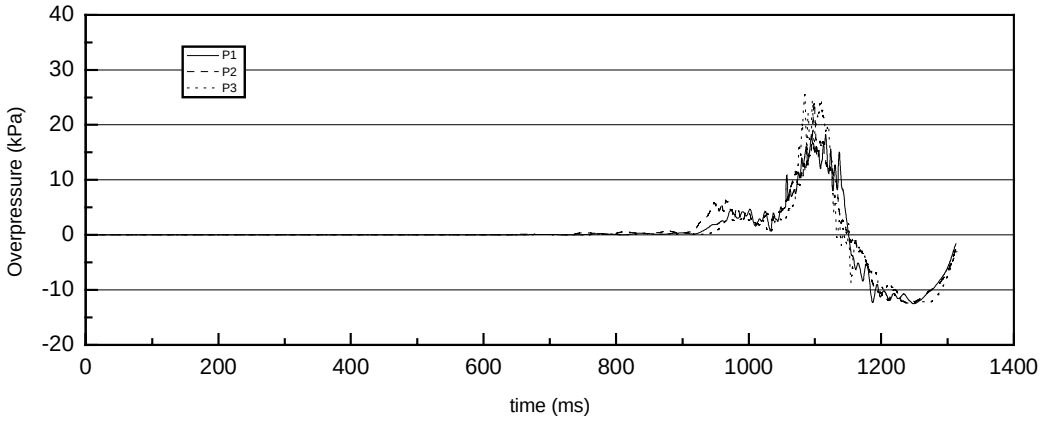

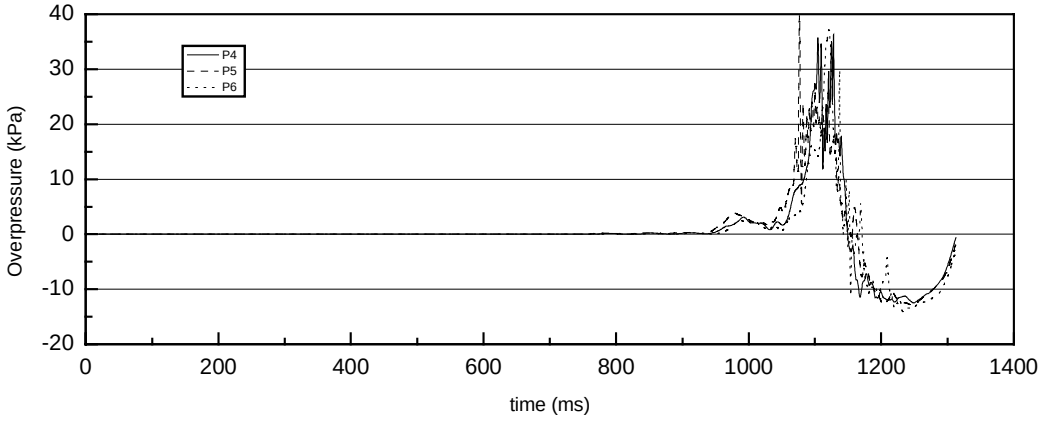

GAMESChemical Plant: scenario NH02

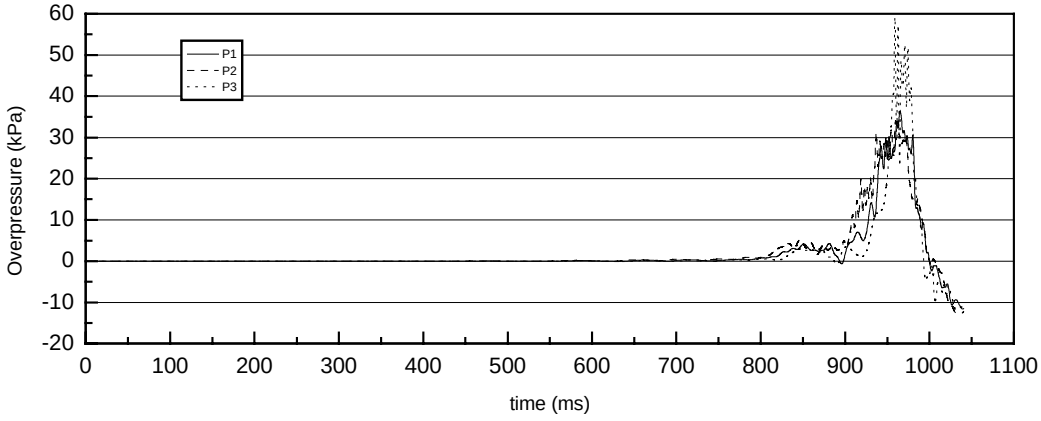

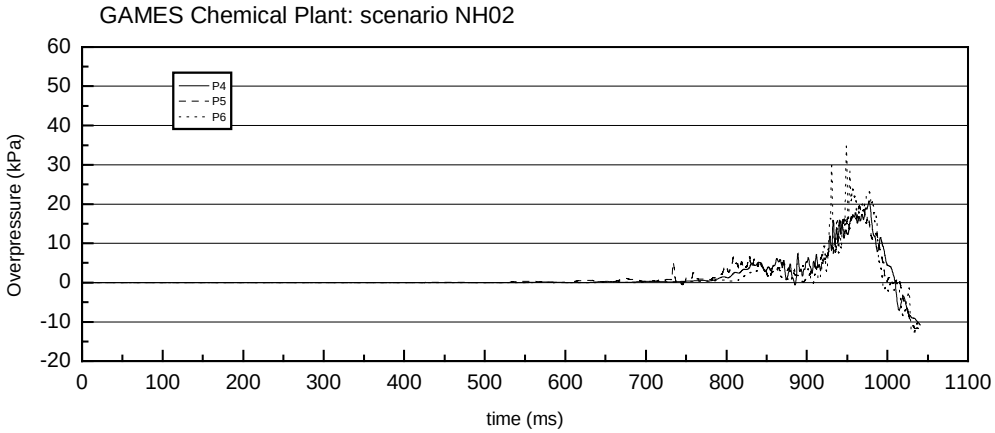
GAMES Chemical Plant: scenario NH02
P4
P5
P6
Overpressure (kPa)
time (ms)

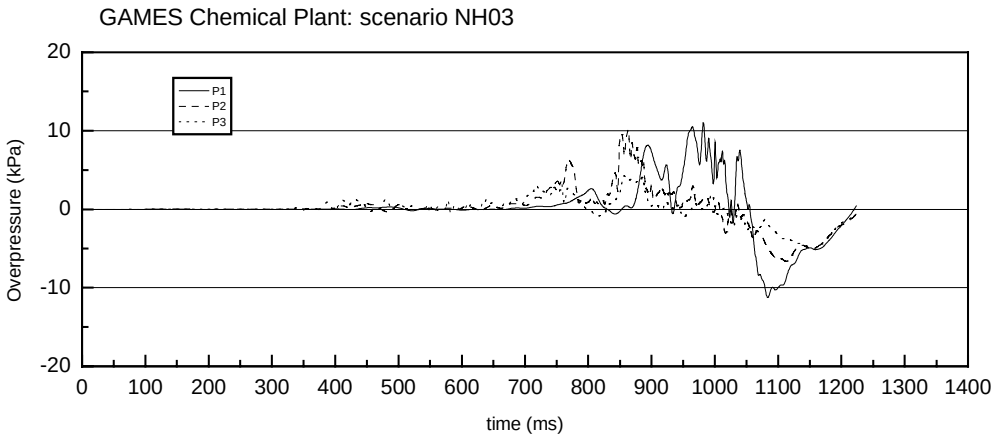
GAMES Chemical Plant: scenario NH03
P1
P2
P3
Overpressure (kPa)
time (ms)

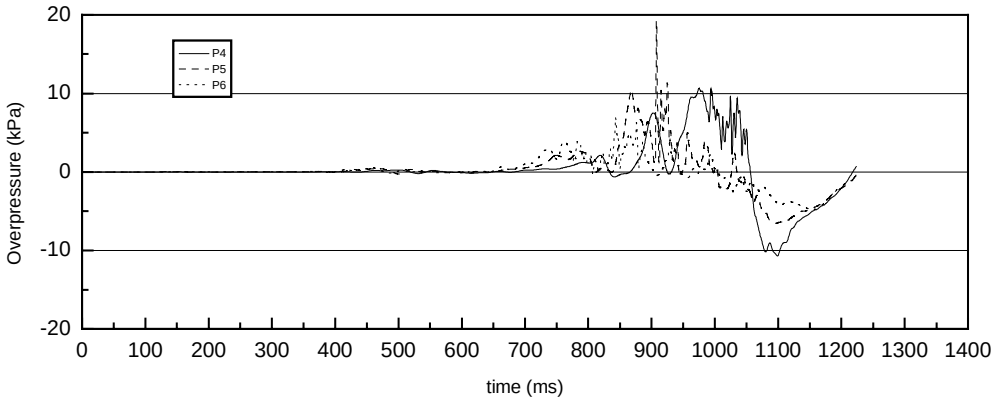
P4
P5
P6
Overpressure (kPa)
time (ms)

GAMES Chemical Plant: scenario NH04

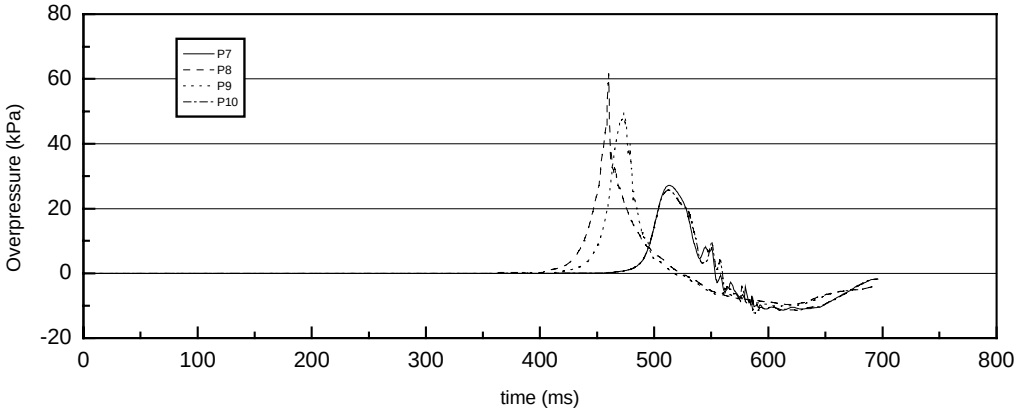

GAMES Chemical Plant: scenario NH05

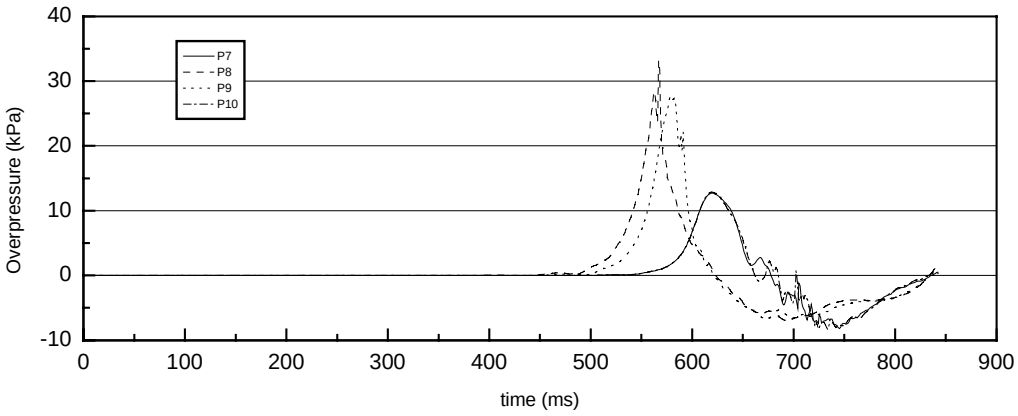

GAMES Chemical Plant: scenario NH06

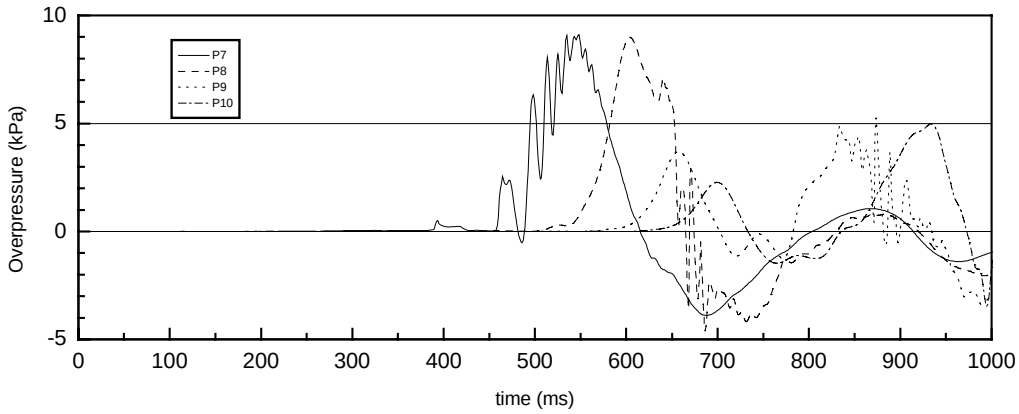

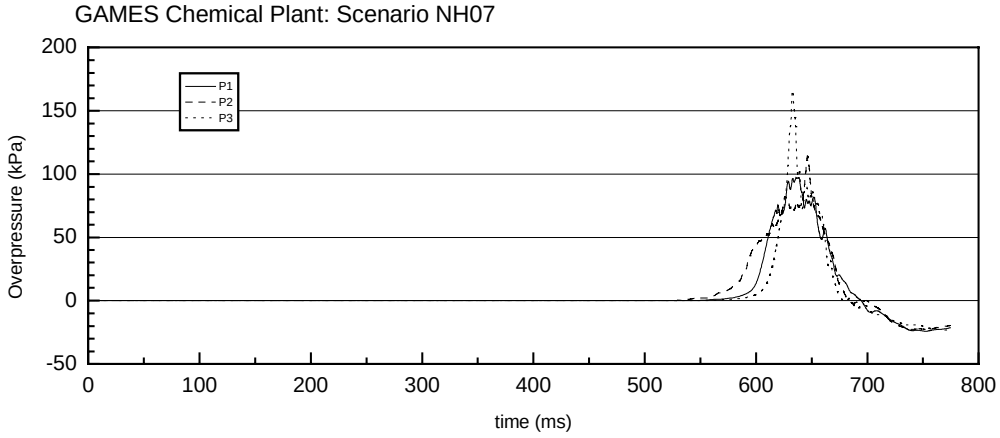
GAMES Chemical Plant: Scenario NH07
Overpressure (kPa)
time (ms)
P1
P2
P3

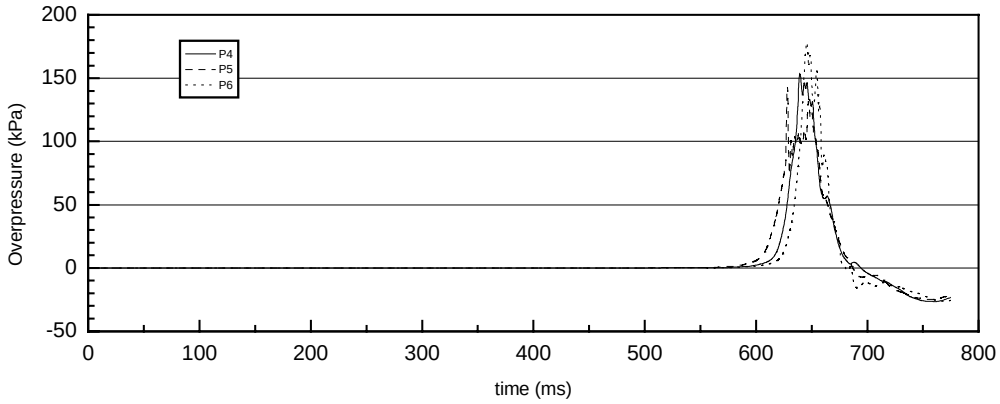
Overpressure (kPa)
time (ms)
P4
P5
P6

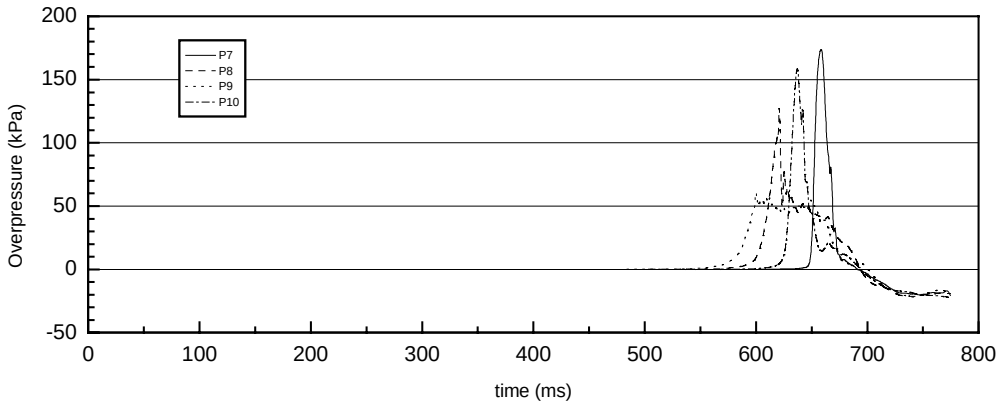
Overpressure (kPa)
time (ms)
P7
P8
P9
P10

GAMES Chemical Plant: scenario NH08

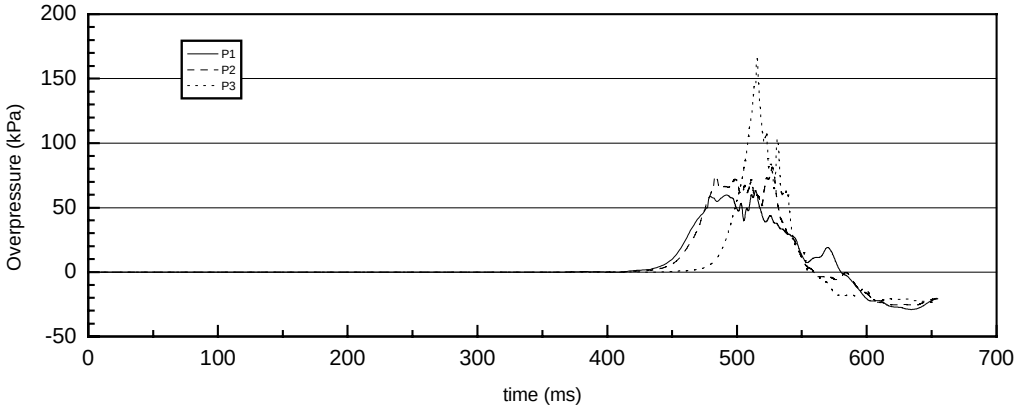

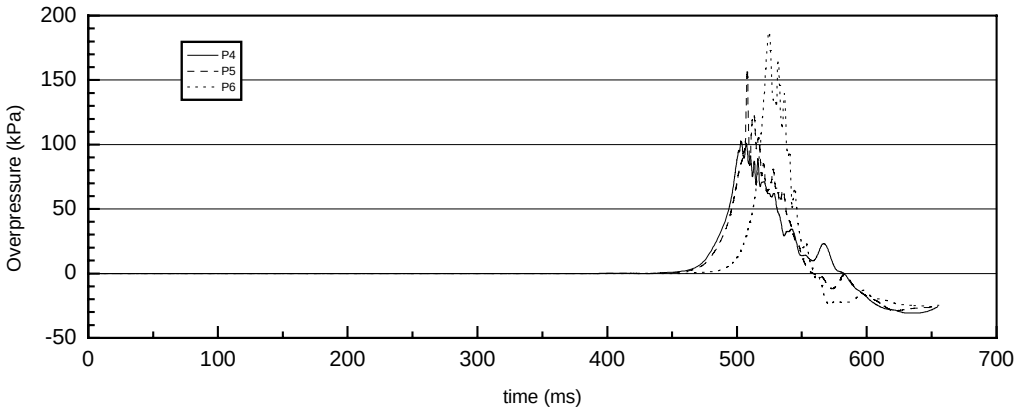

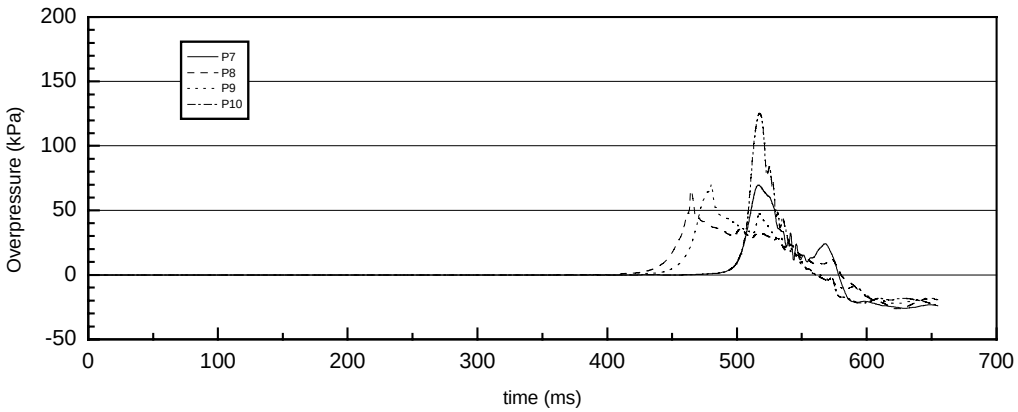

GAMES Chemical Plant: scenario NH09

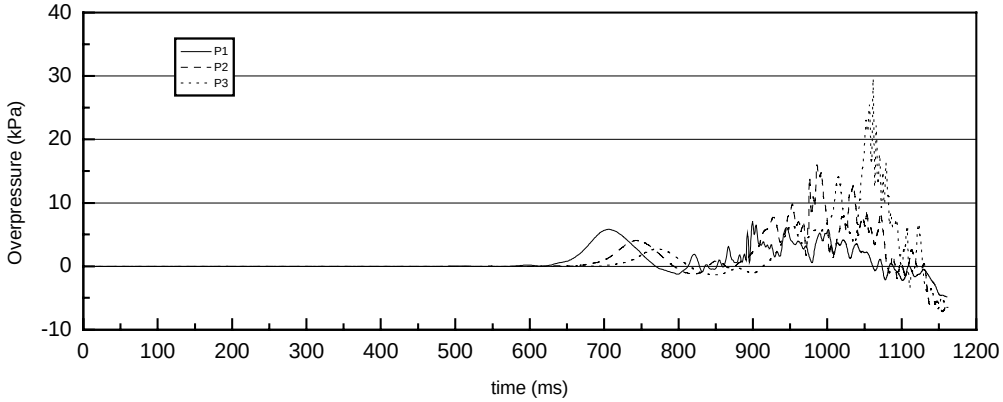

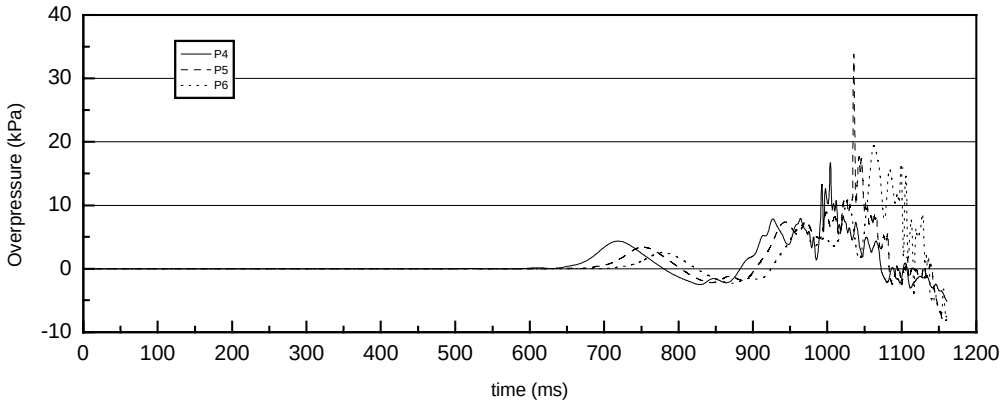

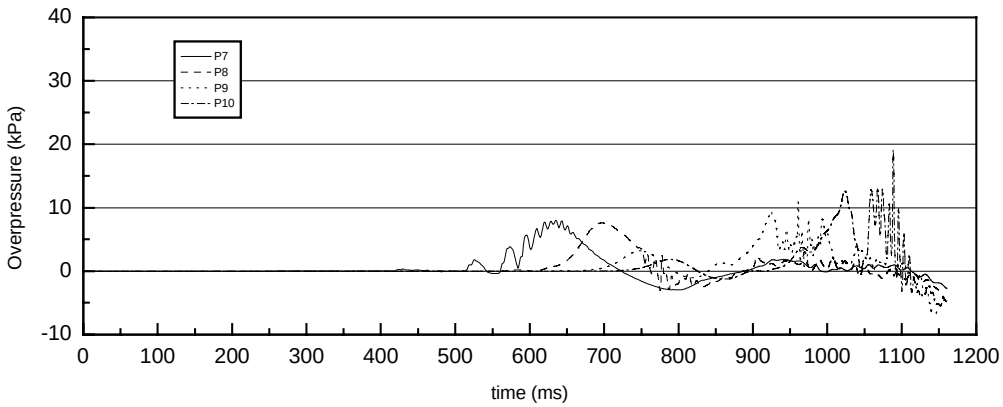

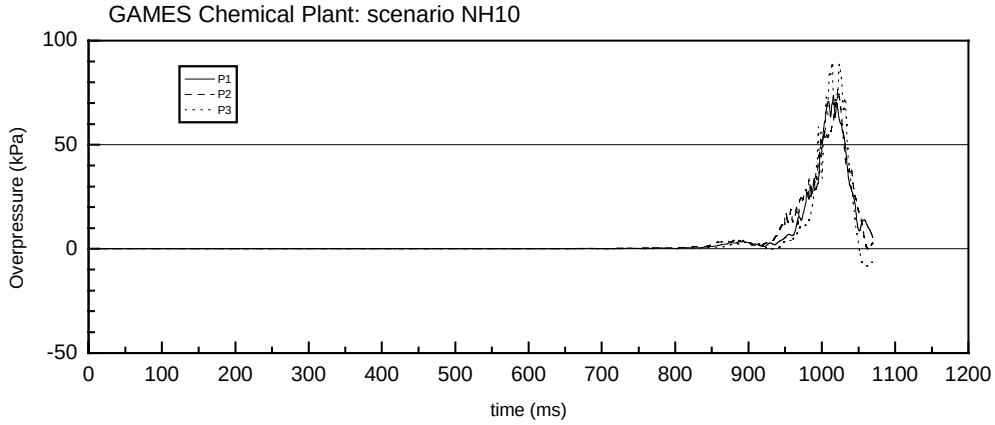
GAMES Chemical Plant: scenario NH10
P1
P2
P3
Overpressure (kPa)
time (ms)

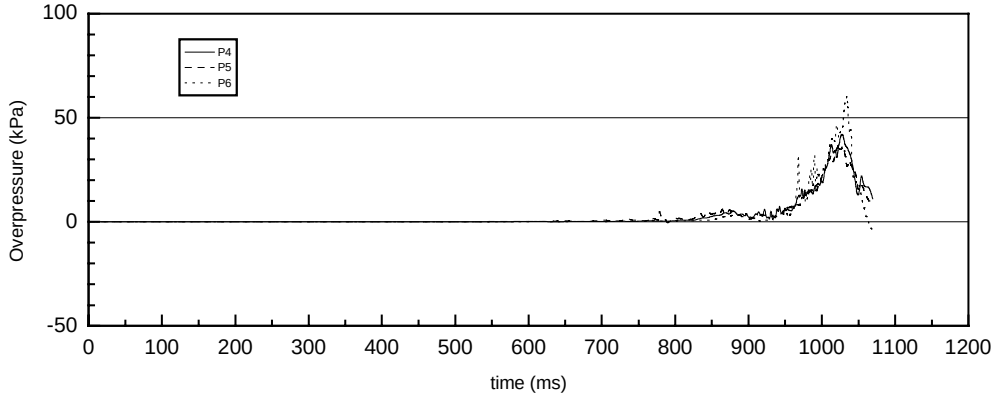
P4
P5
P6
Overpressure (kPa)
time (ms)

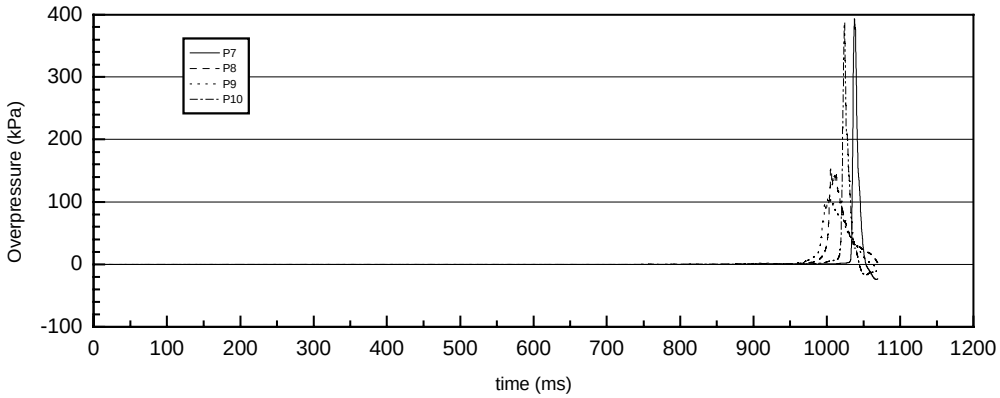
P7
P8
P9
P10
Overpressure (kPa)
time (ms)

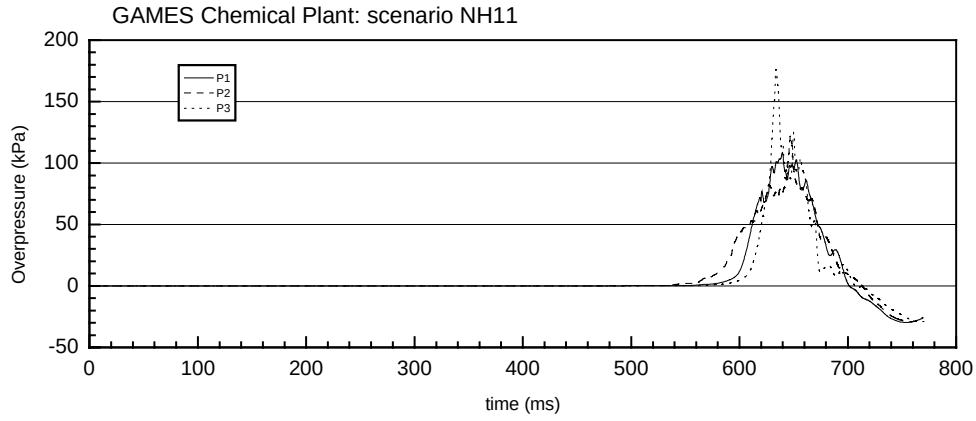
GAMES Chemical Plant: scenario NH11
P1
P2
P3
Overpressure (kPa)
time (ms)

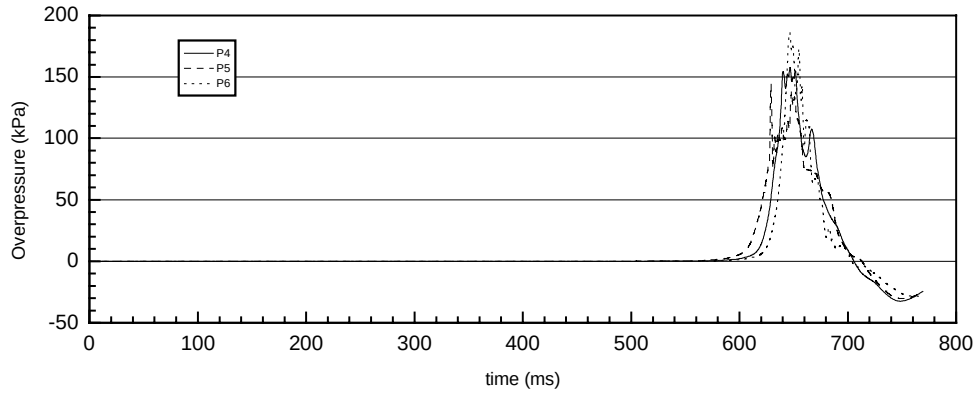
P4
P5
P6
Overpressure (kPa)
time (ms)

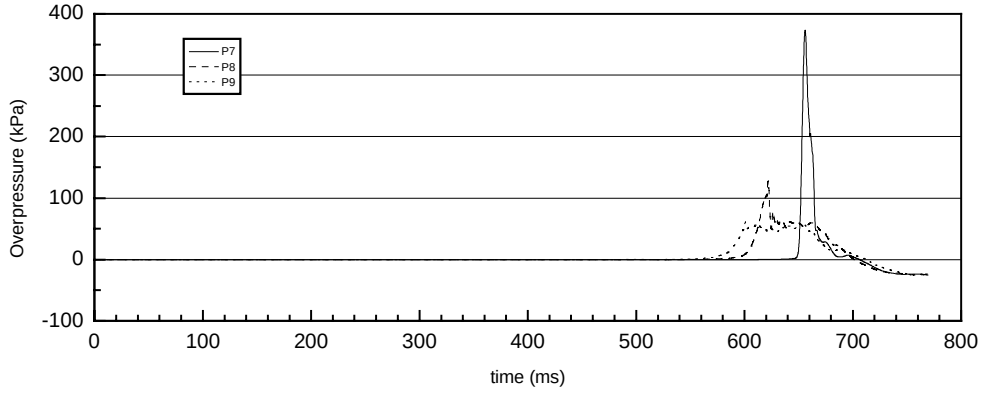
P7
P8
P9
Overpressure (kPa)
time (ms)

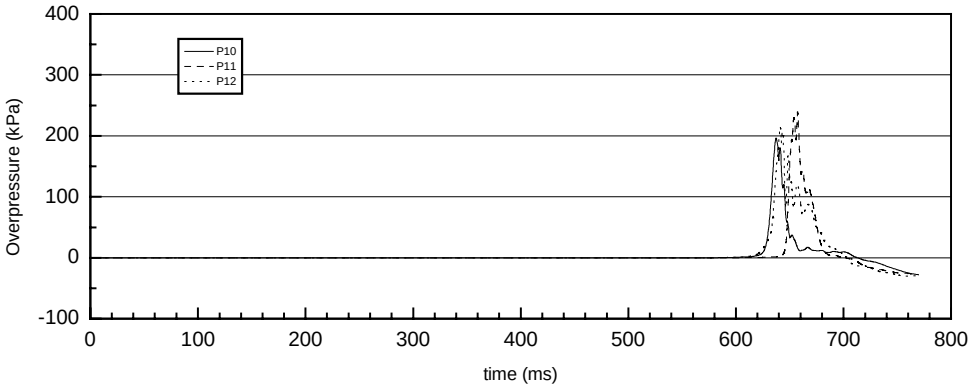

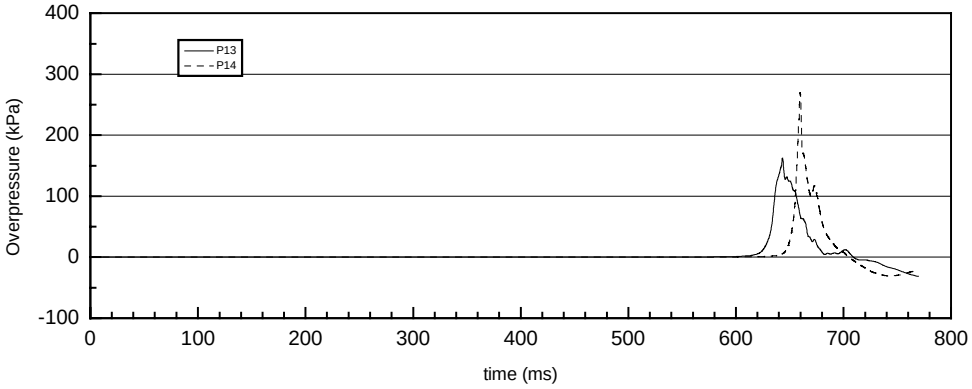

GAMES Chemical Plant: scenario NH12

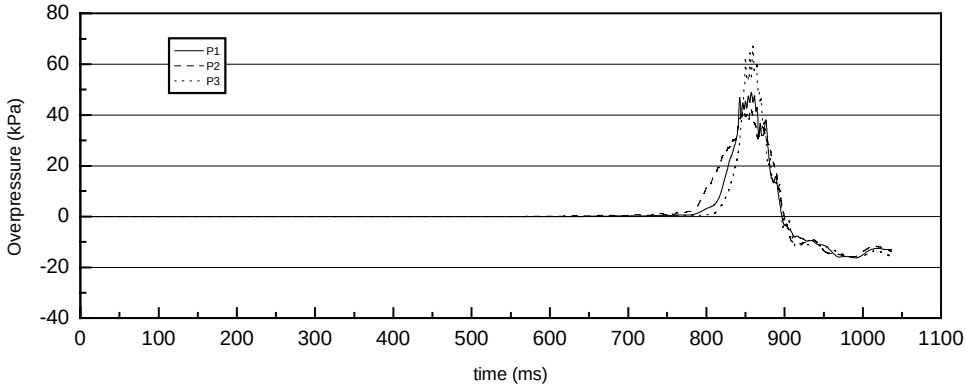

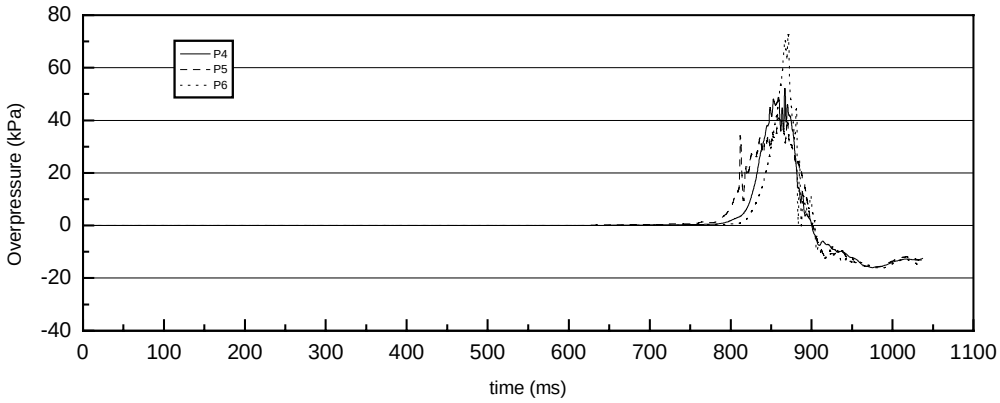

GAMES Chemical Plant: scenario NH13

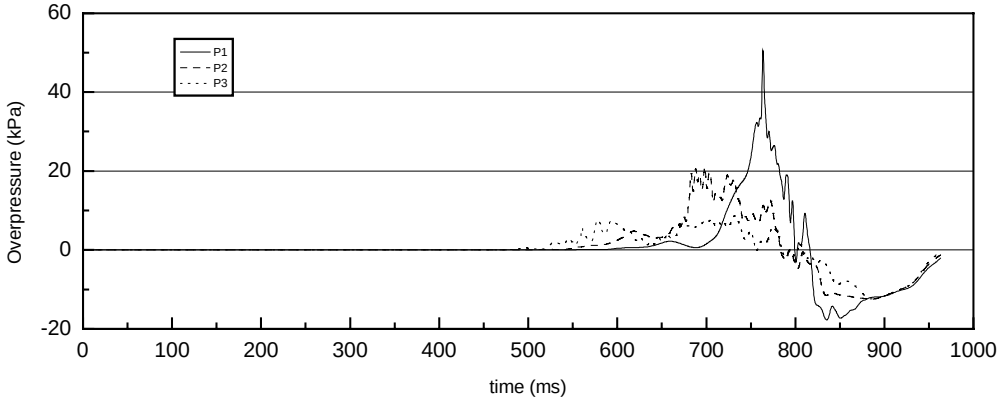

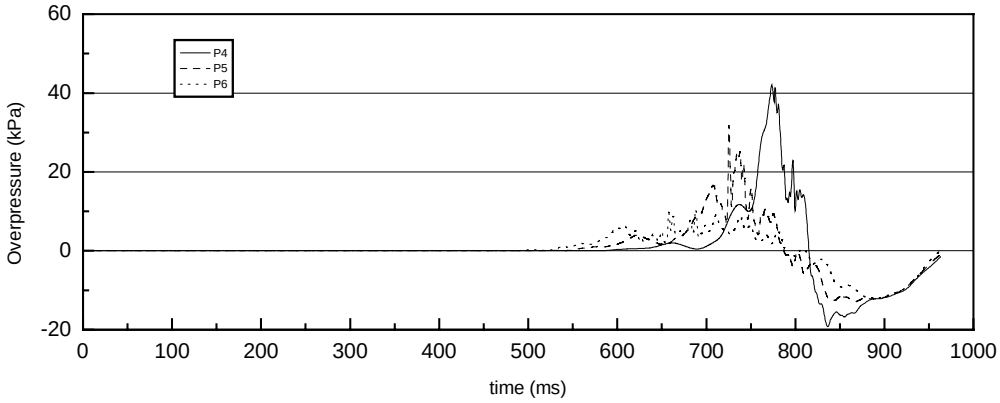

GAMES Chemical Plant: scenario NH14

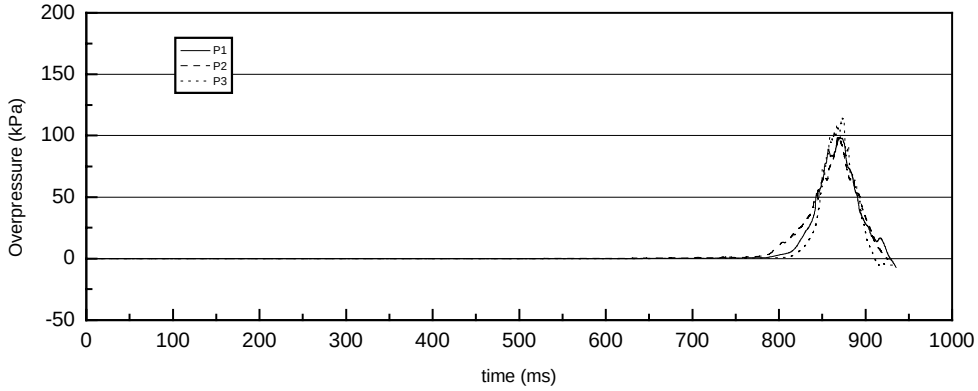

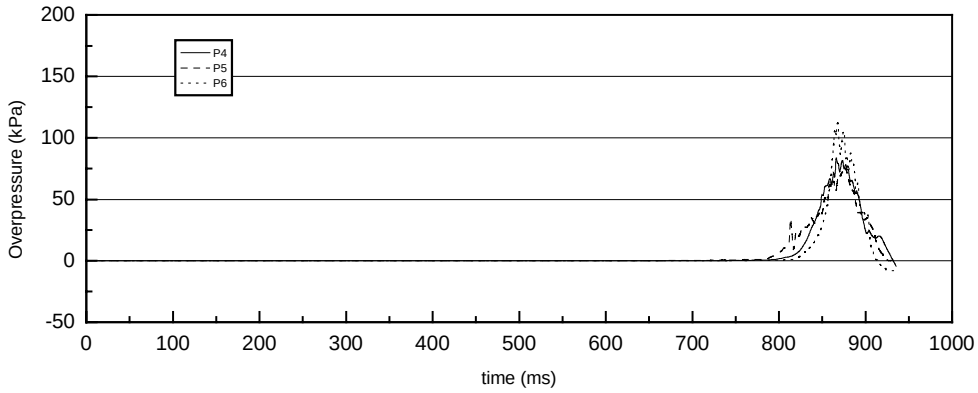

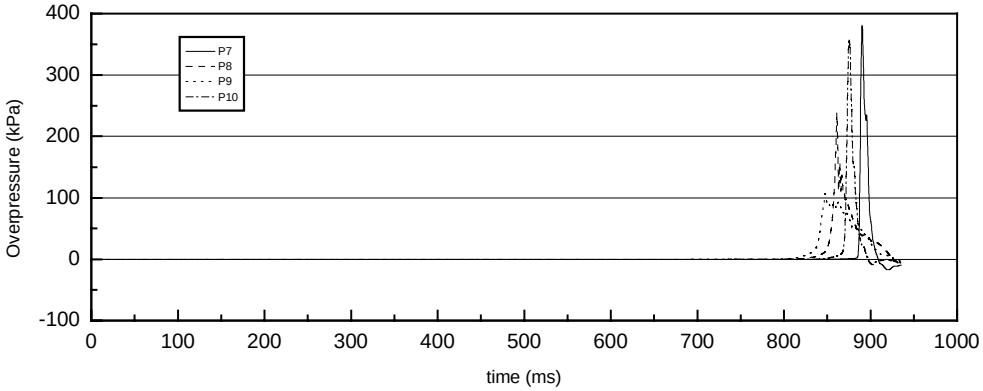

Annex G AutoReaGas pressure histories for the various situations simulated with the LNG Terminal case

GAMES LNG Terminal: scenario OSR-1, IL-1

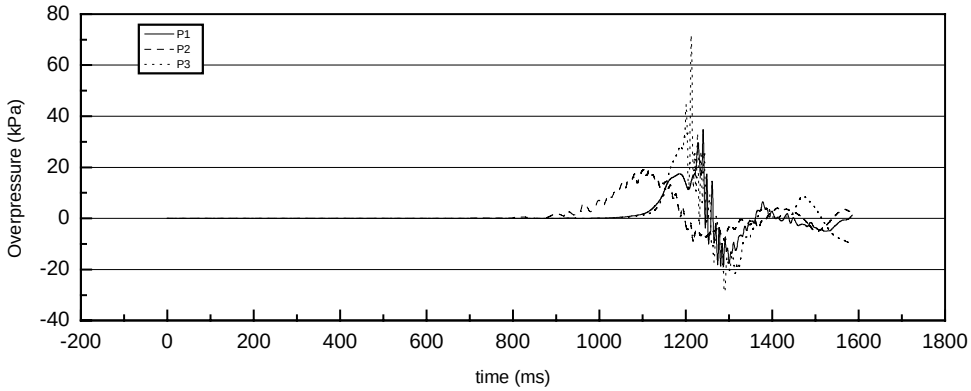

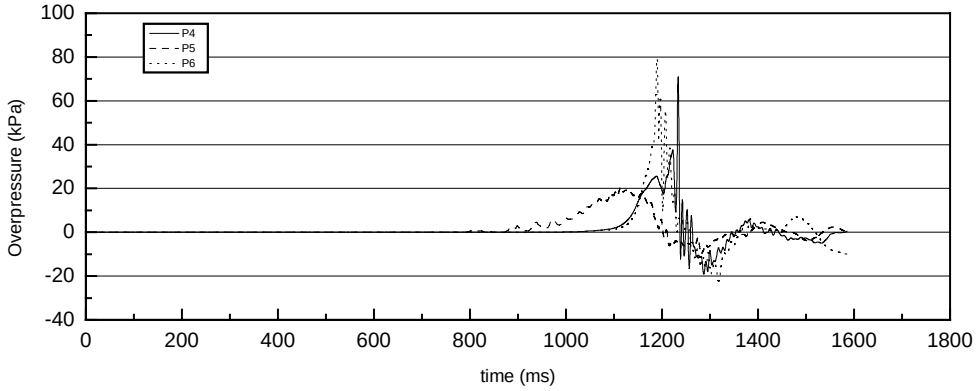

GAMES LNG Terminal: scenario OSR-1, IL-2

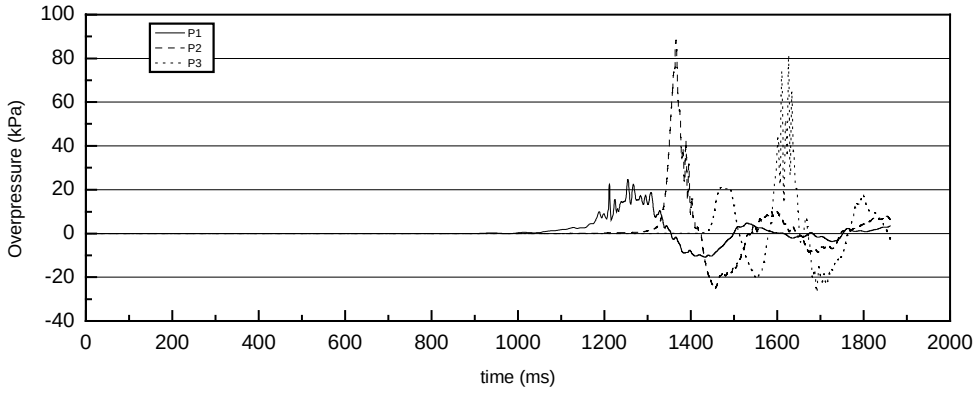

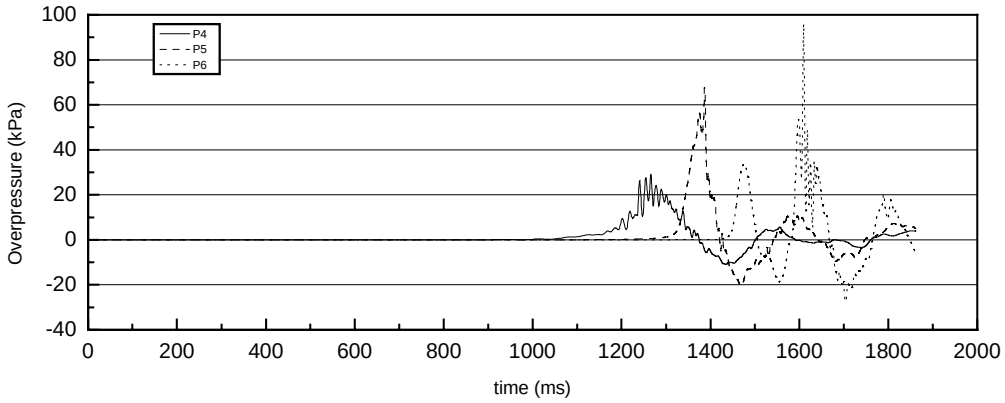

GAMES LNG Terminal: scenario OSR-1,IL-4

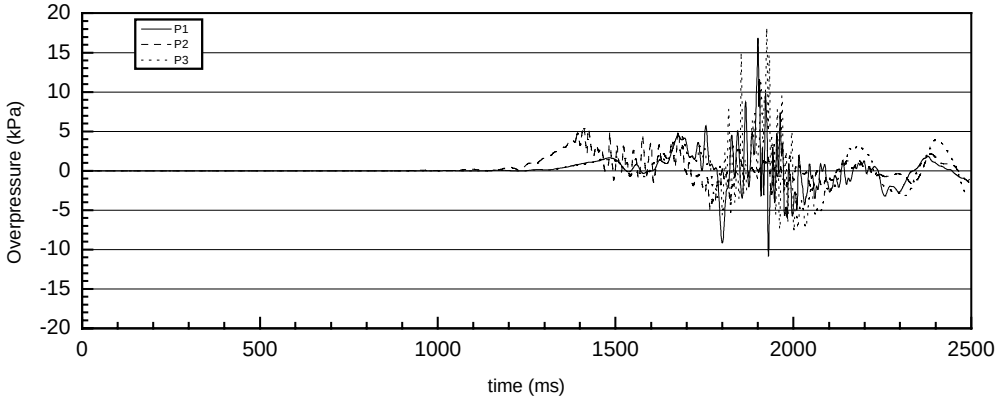

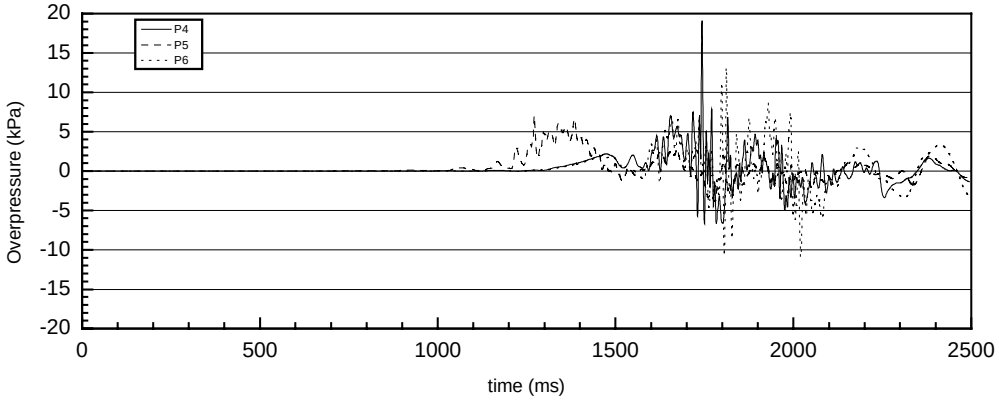

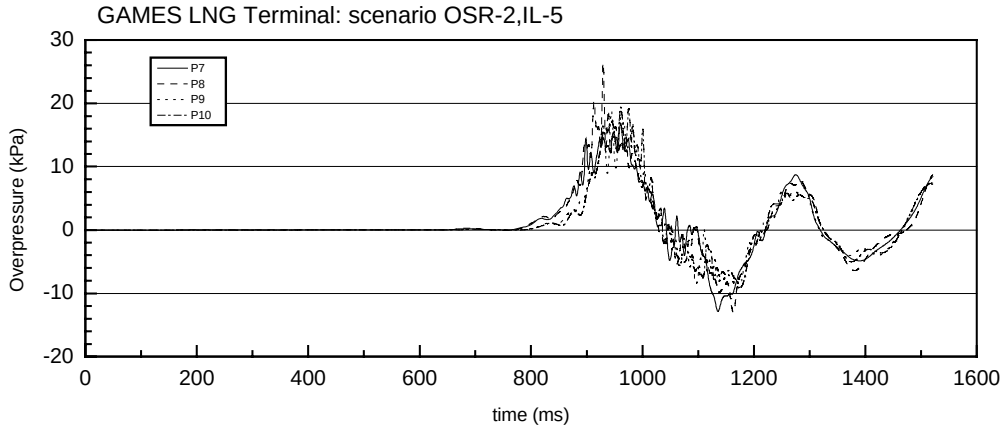
GAMES LNG Terminal: scenario OSR-2,IL-5
P7
P8
P9
P10
Overpressure (kPa)
time (ms)

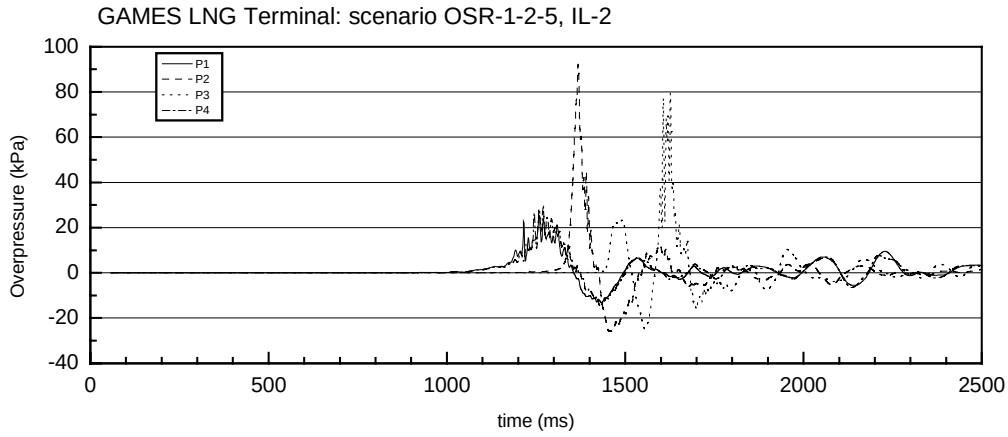
GAMES LNG Terminal: scenario OSR-1-2-5, IL-2
P1
P2
P3
P4
Overpressure (kPa)
time (ms)

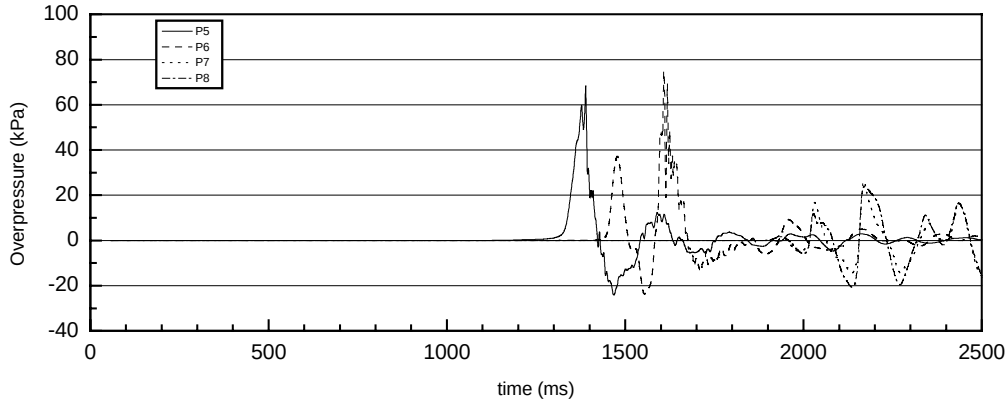
P5
P6
P7
P8
Overpressure (kPa)
time (ms)

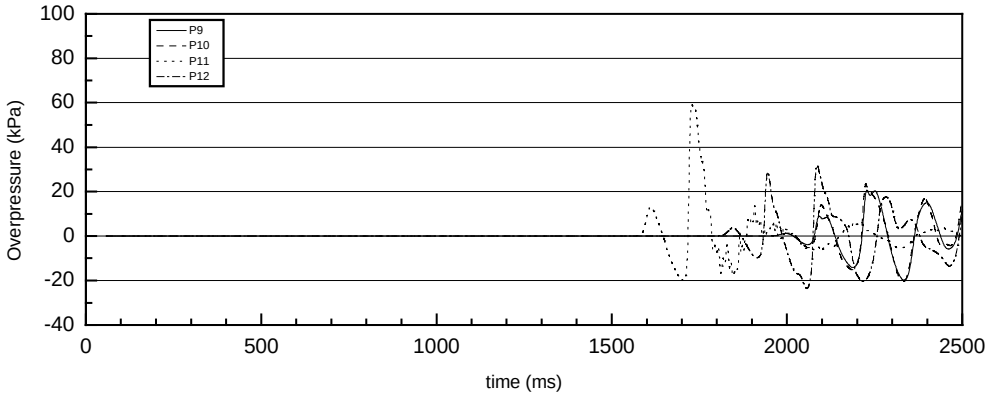

GAMES LNG Terminal: scenario OSR-1-3-6-7-8, IL-3

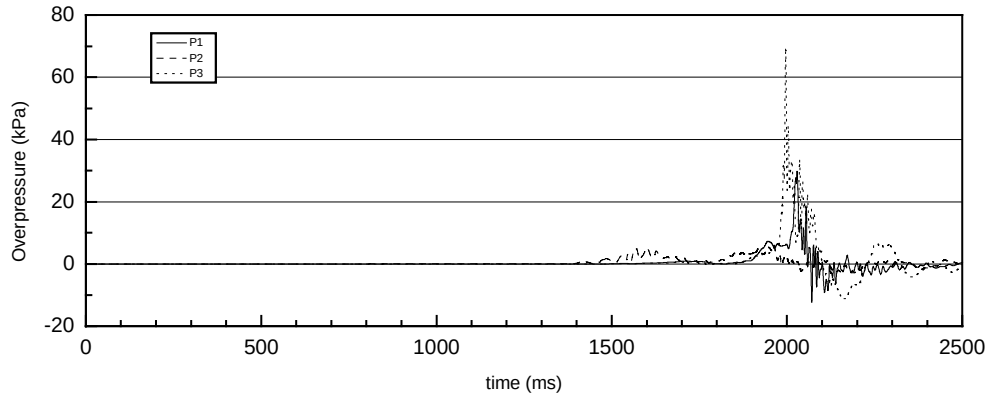

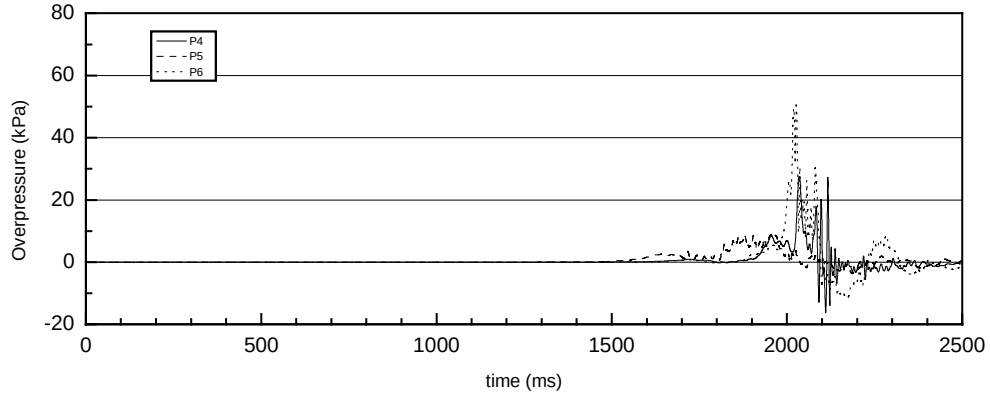

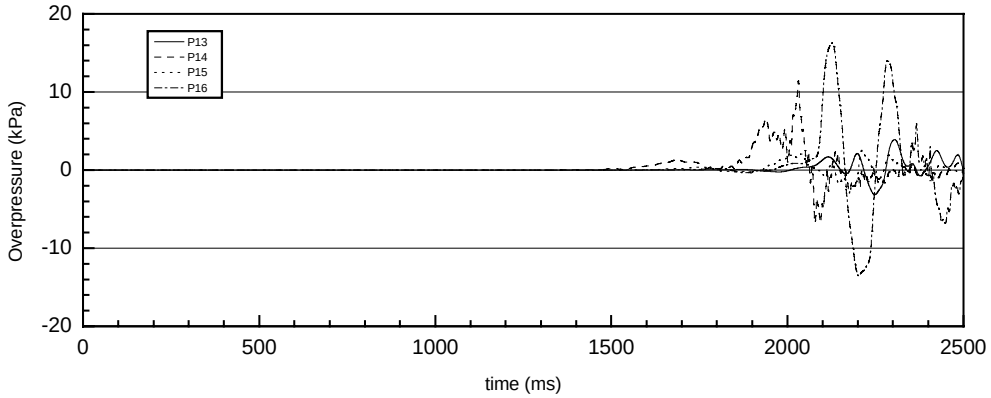

GAMES LNG Terminal: scenario OSR-1-3-6-7-8, IL-4

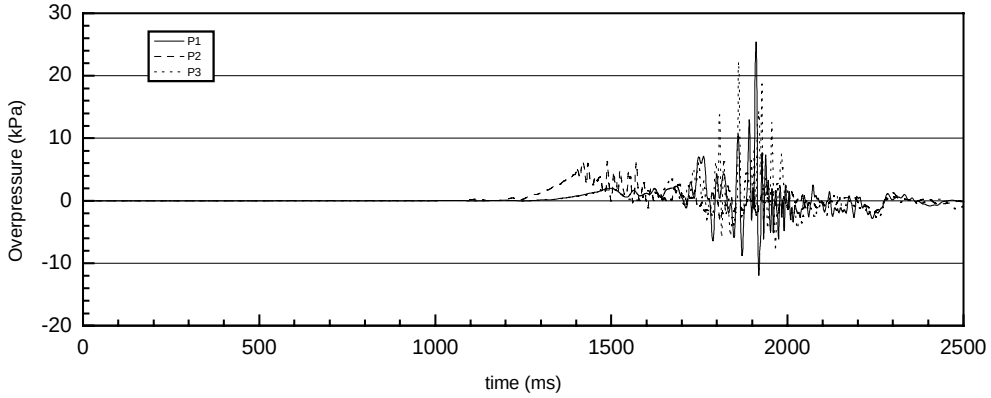

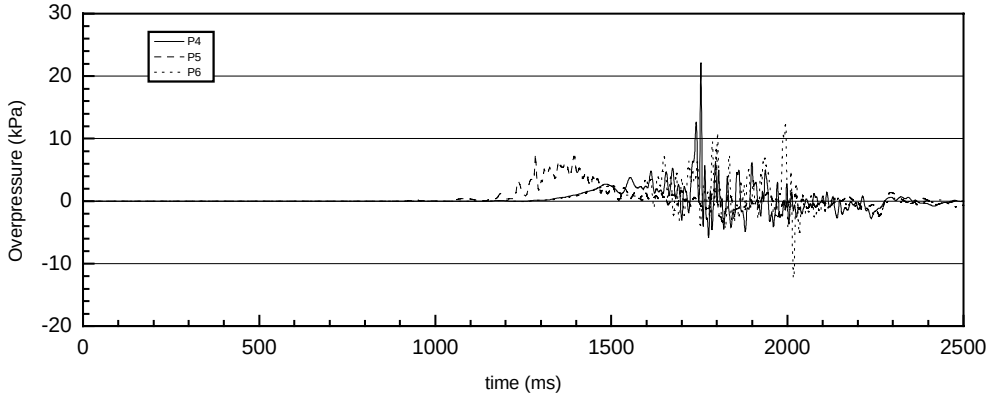

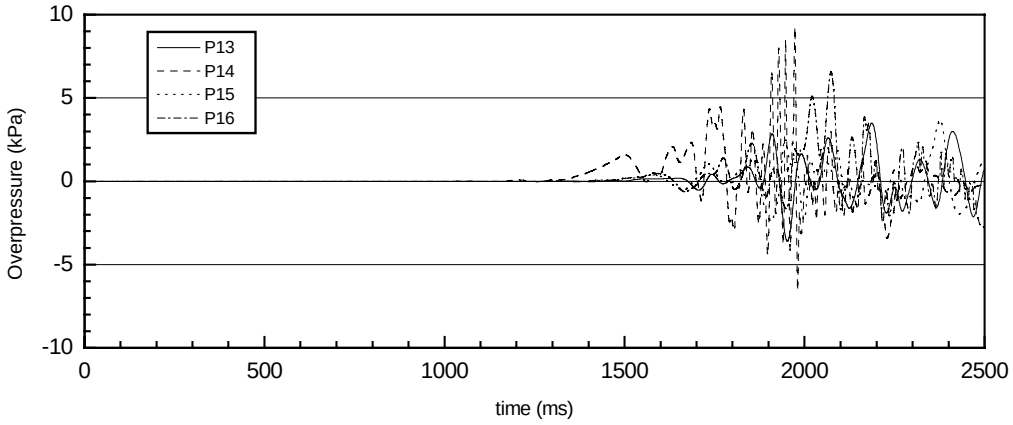

GAMES LNG Terminal): scenario OSR-1-3-6-7-8, IL-7

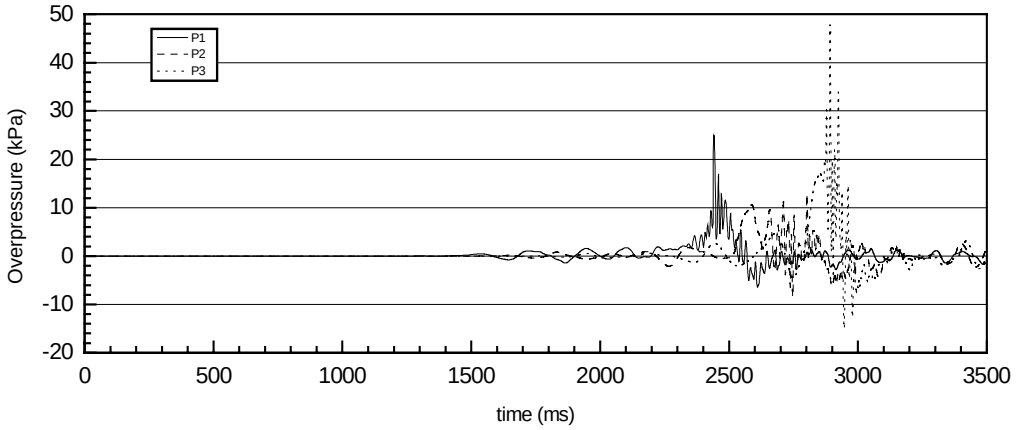

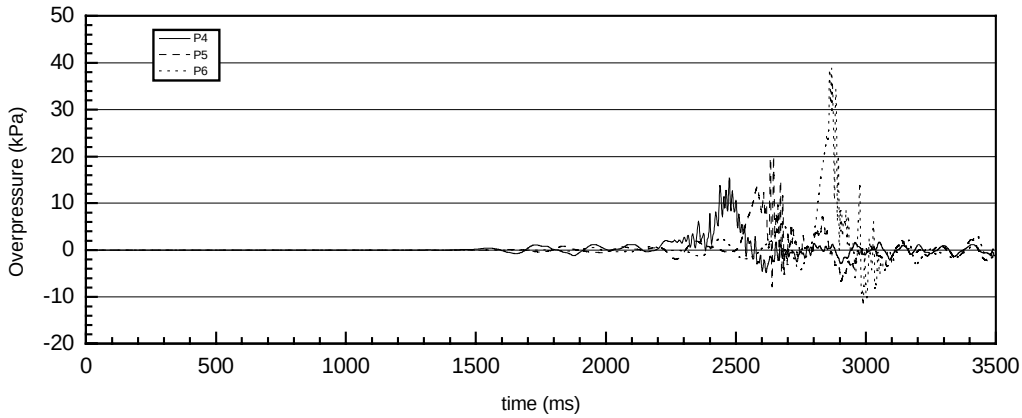

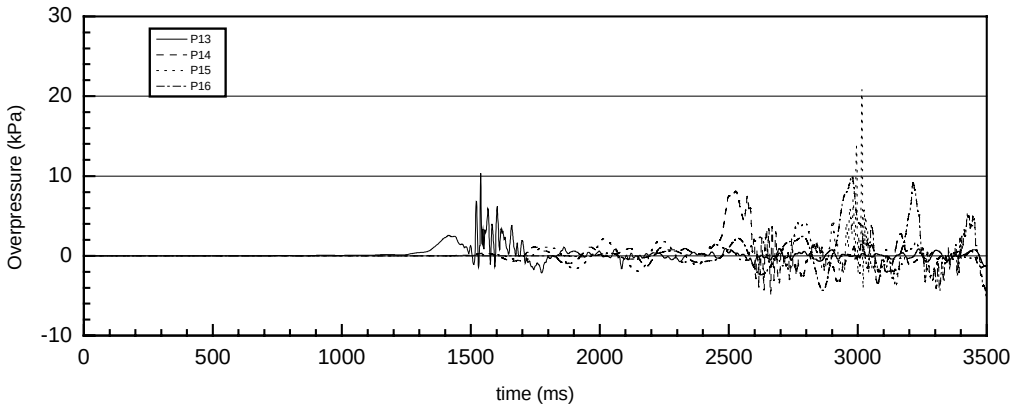
P13
P14
P15
P16
Overpressure (kPa)
30
20
10
0
-10
0
500
1000
1500
2000
2500
3000
3500
time (ms)

SUMMARY: ONGERUBRICEERD

Correlations were derived in the preceding GAME project to quantify the source strength of a vapour cloud explosion required to apply the Multi-Energy Method for the determination of the blast characteristics. The correlations relate a set of parameters describing the obstacle configuration in which the flammable cloud is present and the fuel, to a single value for the overpressure in the exploding vapour cloud.
This project investigates the difficulties and problems encountered while applying the correlations to a number of realistic scenarios. The objective is to provide guidance and recommendations on how to overcome these difficulties and to decide on the actual values to be chosen for the parameters of the correlations in specific situations. The emphasis is on the determination of the parameters: 'Volume Blockage Ratio' and 'Average Obstacle Diameter'.
The main finding is that a safe approach in most situations is to apply the procedure of the new Yellow Book for the determination of the volume of the obstructed region in combination with the hydraulic average obstacle diameter and a flame path length equal to the radius of a hemisphere with a volume equal to the volume of the obstructed region. Lack of experimental data on specific items prevents the generation of more detailed guidance. Some guidance is developed based on a theoretical approach, to assess the influence of the aspect ratio of the obstructed region and to quantify the separation distance between multiple explosion sources. It is recommended to perform an experimental research programme to generate the required data to improve and validate the suggested procedures.

TNO Prins Maurits Laboratory

Report no.: PML 1998-C53

Assignment no(s): 224195374

Date: October 1998

Title: Application of correlations to quantify the source strength of vapour cloud explosions in realistic situations.
Final report for the project: 'GAMES'

Author: W.P.M. Mercx
A.C. van den Berg
D. van Leeuwen

Descriptor(s): Blast effects, Explosions, Clouds (meteorology), Sources, Correlations, Vapors

The classification designation Ongerubriceerd is equivalent to Unclassified.

SUMMARY: ONGERUBRICEERD

Correlations were derived in the preceding GAME project to quantify the source strength of a vapour cloud explosion required to apply the Multi-Energy Method for the determination of the blast characteristics. The correlations relate a set of parameters describing the obstacle configuration in which the flammable cloud is present and the fuel, to a single value for the overpressure in the exploding vapour cloud.
This project investigates the difficulties and problems encountered while applying the correlations to a number of realistic scenarios. The objective is to provide guidance and recommendations on how to overcome these difficulties and to decide on the actual values to be chosen for the parameters of the correlations in specific situations. The emphasis is on the determination of the parameters: 'Volume Blockage Ratio' and 'Average Obstacle Diameter'.
The main finding is that a safe approach in most situations is to apply the procedure of the new Yellow Book for the determination of the volume of the obstructed region in combination with the hydraulic average obstacle diameter and a flame path length equal to the radius of a hemisphere with a volume equal to the volume of the obstructed region. Lack of experimental data on specific items prevents the generation of more detailed guidance. Some guidance is developed based on a theoretical approach, to assess the influence of the aspect ratio of the obstructed region and to quantify the separation distance between multiple explosion sources. It is recommended to perform an experimental research programme to generate the required data to improve and validate the suggested procedures.

TNO Prins Maurits Laboratory

Report no.: PML 1998-C53

Assignment no(s): 224195374

Date: October 1998

Title: Application of correlations to quantify the source strength of vapour cloud explosions in realistic situations.
Final report for the project: 'GAMES'

Author: W.P.M. Mercx
A.C. van den Berg
D. van Leeuwen

Descriptor(s): Blast effects, Explosions, Clouds (meteorology), Sources, Correlations, Vapors

The classification designation Ongerubriceerd is equivalent to Unclassified.